

สารออกฤทธิ์ทางชีวภาพจากไลเคนและราในไลเคนวงศ์ Trypetheliaceae



บทคัดย่อและแฟ้มข้อมูลฉบับเต็มของวิทยานิพนธ์ตั้งแต่ปีการศึกษา 2554 ที่ให้บริการในคลังปัญญาจุฬาฯ (CUIR)
เป็นแฟ้มข้อมูลของนิสิตเจ้าของวิทยานิพนธ์ ที่ส่งผ่านทางบัณฑิตวิทยาลัย

The abstract and full text of theses from the academic year 2011 in Chulalongkorn University Intellectual Repository (CUIR)
are the thesis authors' files submitted through the University Graduate School.

วิทยานิพนธ์นี้เป็นส่วนหนึ่งของการศึกษาตามหลักสูตรปริญญาวิทยาศาสตรดุษฎีบัณฑิต
สาขาวิชาเคมี ภาควิชาเคมี
คณะวิทยาศาสตร์ จุฬาลงกรณ์มหาวิทยาลัย
ปีการศึกษา 2560
ลิขสิทธิ์ของจุฬาลงกรณ์มหาวิทยาลัย

BIOACTIVE COMPOUNDS FROM LICHENS AND MYCOBIONTS IN Trypetheliaceae FAMILY



A Dissertation Submitted in Partial Fulfillment of the Requirements
for the Degree of Doctor of Philosophy Program in Chemistry

Department of Chemistry

Faculty of Science

Chulalongkorn University

Academic Year 2017

Copyright of Chulalongkorn University

5572840523 : MAJOR CHEMISTRY

KEYWORDS: TRYPETHELIACEAE / NAPHTHOQUINONES / LICHEN / MYCOBIONT

SUEKANYA JARUPINTHUSOPHON: BIOACTIVE COMPOUNDS FROM LICHENS AND MYCOBIONTS IN Trypetheliaceae FAMILY. ADVISOR: ASST. PROF. WARINTHORN CHAVASIRI, Ph.D., 87 pp.

Chemical constituents of two lichens *Marcelaria cumingii* and *Trypethelium subeluteriae*, and four cultured mycobionts from *M. cumingii*, *T. platystomum*, *T. eluteriae* and *Trypethelium sp.* (Trypetheliaceae) were explored. Their secondary metabolites were structurally elucidated by spectroscopic methods as xanthones, anthraquinones, naphthoquinones and phenalenones. Lichexanthone, parietin, xanthorin and emodin were disclosed as constituents of lichens *M. cumingii*. Whereas, two anthraquinones: parietin and emodin could be isolated from *T. subeluteriae* together with another anthraquinone, haematommone.

The chemical compositions of four cultured mycobionts were found to totally differ from those from lichen. The phenalenone bipolaride C was derived from *T. platystomum* while two 1,2-naphthoquinones, 8-hydroxytrypethelone methyl ether and 4'-hydroxytrypethelone, were isolated from *Trypethelium sp.* The other five 1,2-naphthoquinones, namely (-)-(2'S,3'S)-4'-hydroxytrypethelone (a new compound), three compounds with new absolute configuration (-)-(2'S)-trypethelone methyl ether, (-)-(2'S)-8-methoxytrypethelone methyl ether, and (-)-(2'S,3'R)-4'-hydroxy-8-methoxytrypethelone methyl ether, along with the known compound, (-)-(2'S)-trypethelone were isolated from *M. cumingii*. Cytotoxicity test revealed that (-)-(2'S)-trypethelone methyl ether exhibited selective inhibition against HCT116 and A549 cell lines with IC₅₀ of 0.32 ± 0.03 and 1.05 ± 0.12 μM, respectively. A compound with new absolute configuration: (+)-(2'R)-bipolaride D, and three known compounds: (+)-(2'R)-sclerodin, trypethelone, and 8-hydroxy-7-methoxytrypethelone were isolated from *T. eluteriae*. The latter revealed potential inhibition of amyloid-β aggregation with IC₅₀ 9.9 μM.

Department: Chemistry Student's Signature

Field of Study: Chemistry Advisor's Signature

Academic Year: 2017

ACKNOWLEDGEMENTS

The author wishes to express highest appreciation to her thesis advisor Assistant Professor Dr. Warinthorn Chavasiri for his valuable instructions, kind supervision, profound assistance, encouragement and suggestions throughout the course of this research. In addition, thanks are extended to Center of Excellence in Natural Products Chemistry for the support of chemical and laboratory facilities.

The greatest thanks are also extended to Associate Professor. Dr. Kaoru Kinoshita for inhibitory activity of A β aggregation, Professor Dr. Thammarat Aree for Single crystal X-ray crystallography, Dr. Kiattisak Lugsanangarm for molecular docking calculations, Miss Prayumat Onsrirawat and Dr. Pongpun Siripong for cytotoxicity, Dr. Thuc-Huy Duong for suggestions, and gratefully thank to Assistant Professor Dr. Ek Sangvichien and Dr. Theerapat Luangsaphabool for their worthy comments, corrections and helps in lichen and mycobiont cultures. Without their assistance, encouragement and invaluable suggestions, this thesis could not have been accomplished. Moreover, thanks are extended to the Graduate School, Chulalongkorn University for research grant.

Finally, a deep affectionate gratitude is acknowledged to her family for their understanding, encouragement and support throughout the course of education. Especially, thanks to her friends for friendship and helps throughout the entire course of study. Without them, the author would never have been able to achieve this goal.

CONTENTS

	Page
THAI ABSTRACT	iv
ENGLISH ABSTRACT	v
ACKNOWLEDGEMENTS	vi
CONTENTS	vii
LIST OF TABLES	x
LIST OF FIGURES	xi
LIST OF ABBREVIATIONS	xiii
CHAPTER I INTRODUCTION.....	1
1.1 Introduction.....	1
1.2 Research background and rationale.....	2
1.3 Objectives	7
CHAPTER II CHEMICAL DIVERSITY OF LICHENS AND CULTURED MYCOBIONTS.....	8
2.1 Introduction.....	8
2.2 Experimental.....	9
2.2.1 General experimental procedures	9
2.2.2 Extraction and isolation.....	9
2.2.3 Cytotoxicity assay	10
2.3 Results and discussion	10
2.3.1 Investigation on chemical diversity of lichen <i>M. cumingii</i>	10
2.3.2 Secondary metabolites of <i>T. subeluteriae</i> , <i>T. platystomum</i> and <i>Trypethelium sp.</i>	14
2.3.2.1 Physical properties and spectroscopic data of isolated compounds	14

	Page
2.4 Conclusion	17
CHAPTER III NAPHTHOQUINONES FROM CULTURED MYCOBIONT OF <i>Marcelaria cumingii</i> (Mont.) AND THEIR CYTOTOXICITY	18
3.1 Introduction	18
3.2 Experimental	19
3.2.1 General experimental procedures	19
3.2.2 Fungal isolation, cultivation and identification.....	19
3.2.3 Extraction and isolation	20
3.2.4 Single crystal X-ray crystallography.....	21
3.2.5 Cytotoxicity assay	21
3.2.6 Molecular docking calculations	22
3.3 Results and discussion	22
3.3.1 Physical and spectroscopic data of isolated compounds.....	22
3.3.2 Single crystal X-ray crystallography data of isolated compounds	23
3.4 Conclusion	34
CHAPTER IV ISOLATION AND ELUCIDATION OF SECONDARY METABOLITES FROM CULTURED MYCOBIONT <i>Trypethelium eluteriae</i> (Spreng.) AND EVALUATION OF ANTI-ALZHEIMER ACTIVITY	35
4.1 Introduction	35
4.2 Experimental	36
4.2.1 General experimental procedures	36
4.2.2 Cultivation	36
4.2.3 Extraction and isolation.....	37
4.2.4 Inhibitory activity of A β aggregation.....	37

	Page
4.3 Results and discussion	38
4.3.1 Physical and spectroscopic data of isolated compounds.....	38
4.4 Conclusion	43
REFERENCES	44
APPENDIX.....	49
VITA.....	87



LIST OF TABLES

Table 2.1 The specimens of <i>M. cumingii</i> and their geographical data.....	11
Table 2.2 The percentage of chemical composition from <i>M. cumingii</i> specimens	13
Table 2.3 ^1H NMR data of 2.2, 2.4, 2.5 δ_{H} (ppm), (multi, <i>J</i> in Hz).....	15
Table 2.4 ^1H NMR data of 2.2, 2.4, 2.5 δ_{H} (ppm), (multi, <i>J</i> in Hz).....	16
Table 2.5 ^1H NMR data of 2.7, 2.8 , δ_{H} (ppm), (multi, <i>J</i> in Hz)	16
Table 3.1 ^1H NMR data of 3.1-3.5 , δ_{H} (ppm), (multi, <i>J</i> in Hz)	25
Table 3.2 ^{13}C NMR data of 3.1-3.5 , δ_{C} (ppm).....	26
Table 3.3 In vitro cytotoxicity of 3.1-3.5 against KB and HeLaS3 cell lines	30
Table 3.4 In vitro cytotoxicity of 3.1 against MRC-5, HT29, HCT116 and A549 cell lines	31
Table 4.1 ^1H NMR data of 4.1, 4.2 , δ_{H} (ppm), (multi, <i>J</i> in Hz).....	39
Table 4.2 ^1H NMR data of 4.3, 4.4 , δ_{H} (ppm), (multi, <i>J</i> in Hz).....	40
Table 4.3 Inhibitory activity of $\text{A}\beta$ aggregation of sample.....	42

LIST OF FIGURES

Figure 1.1 Three main types of lichens.....	1
Figure 1.2 An example of anthraquinone from <i>L. purpurina</i>	2
Figure 1.3 Anthraquinones and xanthonones from <i>T. aeneum</i> and <i>T. aureomaculata</i>	3
Figure 1.4 Anthraquinones from <i>T. cruentum</i>	3
Figure 1.5 Xanthonones and anthraquinones from <i>L. benguelensis</i>	4
Figure 1.6 Xanthorin from <i>L. benguelensis</i>	5
Figure 1.7 1,2-Naphthoquinones from <i>T. eluteriae</i>	5
Figure 1.8 1,2-Naphthoquinones and phenalenone derivatives from <i>Trypethelium sp.</i>	6
Figure 2.1 The study area. Numbers on the map correspond to the study sites given in Appendix S2.1	8
Figure 2.2 Chemical structures of 2.2, 2.4–2.8	14
Figure 3.1 Lichen and cultured mycobiont of <i>M. cumingii</i>	19
Figure 3.2 Chemical structures of 3.1–3.5	24
Figure 3.3 ORTEP plot of 3.1 (20% probability level; atom colors: C, cyan; O, red; H, white)	25
Figure 3.4 ORTEP plot of 3.2 (20% probability level; atom colors: C, cyan; O, red; H, white). Two similar molecules in the asymmetric unit are stabilized by off-centered parallel π stacking interactions	27
Figure 3.5 Selected COSY, HMBC, and NOESY correlations for 3.3 and 3.5	28
Figure 3.6 ORTEP plot of 3.3 (20% probability level; atom colors: C, cyan; O, red; H, white). The 1.5 water molecules are distributed over three sites, acting as space fillers in the crystal lattice; shortest $O_w \cdots O$ (3.5) distance is 3.67 Å.....	29

Figure 3.7 The superimposition of Doxorubicin (orange) and 3.1 (yellow), 3.2 (pink), 3.3 (gray), 3.4 (blue) and 3.5 (red). The figure is depicted by using the Chimera version 1.9 software[49]	32
Figure 3.8 The Comparison of binding mode of Doxorubicin (A) and inhibitor 3.1 (B), 3.2 (C), 3.3 (D), 3.4 (E), and 3.5 (F). All inhibitors are shown as ball and stick while amino acids involved in H-bonding interaction are shown as green stick model. All figures are depicted by using the Chimera version 1.9 software[49].....	32
Figure 3.9 The hydrophobic interaction analysis. Compound 3.1 is shown in purple and 3.2 in gray. The red circles show equivalent amino acids involved for hydrophobic interaction[50]	33
Figure 3.10 The hydrophobic interaction analysis. Compound 3.1 is shown in purple and 3.4 in gray. The red circles show equivalent amino acids involved for hydrophobic interaction[50]	34
Figure 4.1 <i>T. eluteriae</i>	36
Figure 4.2 Chemical structures of 4.1-4.4	38
Figure 4.3 Inhibitory activity of A β aggregation. “Cont.” indicates the control group	42

LIST OF ABBREVIATIONS

HPLC	high performance liquid chromatography
^1H NMR	proton nuclear magnetic resonance
^{13}C NMR	carbon nuclear magnetic resonance
MHz	megahertz
CDCl_3	deuterated chloroform
δ	chemical shift
TLC	thin layer chromatography
UV	ultraviolet detector
nm	nanometer
mm	millimeter
cm	centimeter
v/v	volume percent
mL	millilitre
min	minute
g	grams
%	percent
HRESIMS	High-resolution electrospray ionisation mass spectrometry
Calcd	calculated
$\text{DMSO-}d_6$	deuterated dimethylsulfoxide
IC_{50}	the half maximal inhibitory concentration
μM	micro molar
ppm	part per million
J	coupling constant
Hz	hertz
s	singlet
d	doublet
q	quartet
mg	milligram (s)

$[\alpha]_D^{25}$	specific rotation at 25° with sodium lamp
C	concentration
$\lambda_{\max}(\Delta\varepsilon)$	the maximum intensity of the Cotton effect at λ
CE	cotton effect
Å	angstrom
α	alpha
<i>m</i>	multiplet
MW	molecular weight
β	beta
SD	standard deviation



CHAPTER I

INTRODUCTION

1.1 Introduction

Mycobiont is the fungal partner in lichen, a symbiosis between mycobiont and one or more photobiont(s) which can be green algae or cyanobacteria. This association is beneficial for both partners. Two principal roles of mycobiont in the lichen symbiosis are to protect the photobiont from overexposure to intense sunlight and drying and to absorb mineral nutrients from the fundamental surface or from atmospheric contaminants. The photobiont also has two roles including synthesis of organic nutrients from carbon dioxide and, in the case of cyanobacteria, production of ammonia (and subsequently organic nitrogen compounds) from nitrogen gas by nitrogen fixation. Therefore, through this partnership, the photobionts are protected and able to grow in conditions in which they could not grow alone. They also benefit from the highly efficient uptake of mineral nutrients by the lichen fungi. The fungi, in turn, obtain sugars and in some cases organic nitrogen from the photosynthetic partner, enabling them to grow in environments deficient in organic nutrients. Generally, lichens are classified into three growth morphological forms: crustose, foliose, and fruticose types.[1-3] (Figure 1.1)

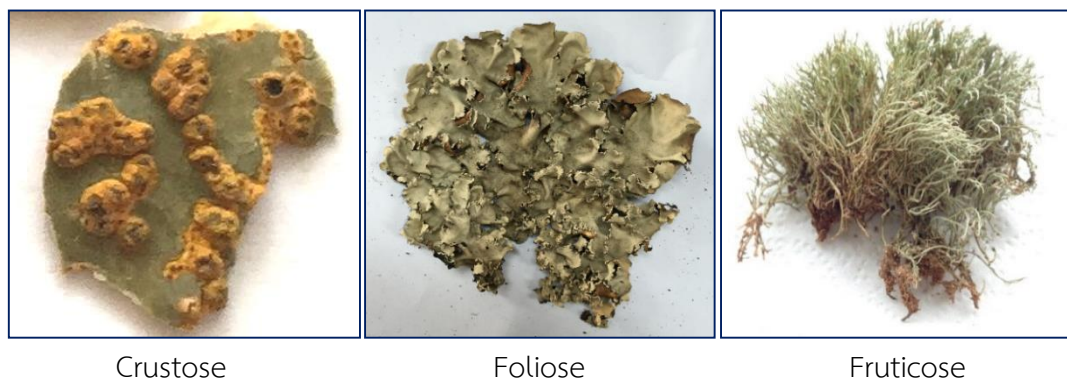
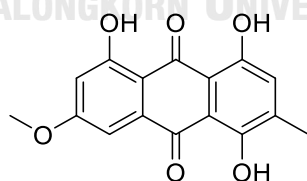


Figure 1.1 Three main types of lichens

The crustose lichens are dominant and various species have been used as ecological and environment detector, source of pigment, and traditional medicine.[4, 5] Trypetheliaceae is a family of crustose lichens, approximately 15 genera and 418 species in 2016.[6, 7] Thailand is located in the tropical region with diverse distribution of lichens. In 2017, the total Thai lichen was reported to be at least 1,292 species[8] and currently, Trypetheliaceae crustose lichen were found in 6 genera (*Astrothelium*, *Campylothelium*, *Laurera*, *Polymeridium*, *Pseudopyrenula*, and *Trypethelium*) and 33 species.[9] In this research, potentially bioactive compounds from three lichens including *Trypethelium subeluteriae* from Tak province, *T. platystomum* from Phitsanulok province, and *Marcelaria cumingii* from Nakhonratchasima province and their mycobionts will be examined. In addition, certain derivatives of isolated compounds will be synthesized and evaluated for their cytotoxic and antioxidant activities.

1.2 Research background and rationale

In Trypetheliaceae, secondary metabolites from several lichens have been isolated and elucidated. In 1969, Stensio and Wachtmeister[10] isolated a red pigment, 1,5,8-trihydroxy-6-methoxy-3-methylantraquinone (**1.1**), from *Laurera purpurina*. The structure was verified by the synthesis from parietin (**1.2**) using Elbs persulfate oxidation. (Figure 1.2)



1,5,8-trihydroxy-6-methoxy-3-methylantraquinone (**1.1**)

Figure 1.2 An example of anthraquinone from *L. purpurina*

Moreover, Santesson[11] examined seven lichens by LC-MS. Parietin (**1.2**), emodin (**1.3**), fallacinalol (**1.4**), and fallacinal (**1.5**) were reported from *T. aeneum* while

parietin (1.2), lichexanthone (1.6), and norlichexanthone (1.7) were found in *T. aureomaculata*. (Figure 1.3)

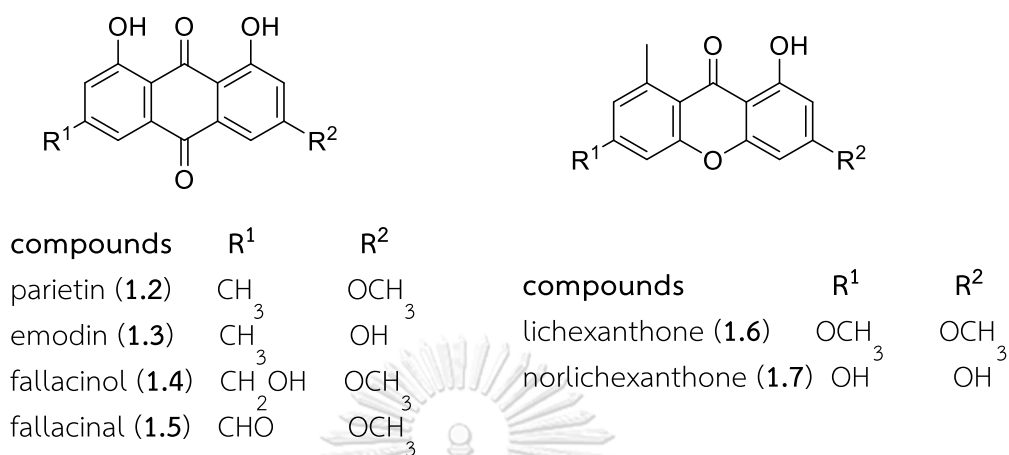


Figure 1.3 Anthraquinones and xanthenes from *T. aeneum* and *T. aureomaculata*

A new red anthraquinone, draculone, was isolated from the corticolous tropical lichen *T. cruentum* together with minor quantities of known anthraquinone pigment haematommone (1.8) by Mathey *et al.*[12] The structure of draculone (1.9) was determined as 2-acetyl-1,3,4,6,8-pentahydroxyanthraquinone by spectroscopic methods. (Figure 1.4)

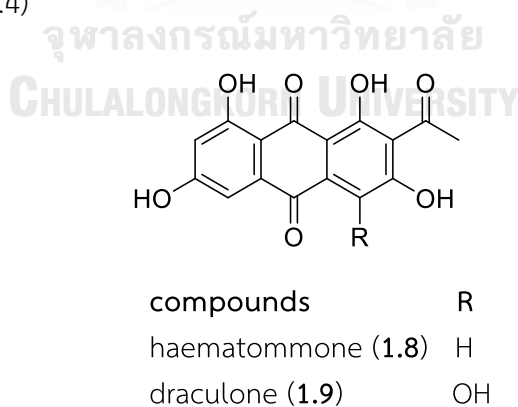


Figure 1.4 Anthraquinones from *T. cruentum*

In a series of publication, Manojlovic *et al.*[13] developed a high performance liquid chromatographic (HPLC) method for the characterization of anthraquinone metabolites in the extracts of lichen *L. benguelensis*. With this method, four anthraquinone derivatives named parietin (1.2), emodin (1.3), fallacinal (1.4), and fallacinal (1.5) were analyzed. The lichen components were characterized by UV spectra and relative HPLC retention times. This was the first report of phytochemical analysis of *L. benguelensis*. This study revealed significant in recognizing some new sources (lichen and its extracts) as a natural emplacement of antioxidants for preservation of food products.

The secondary metabolites of lichen *L. benguelensis* collected from Thailand including parietin (1.2), emodin (1.3), fallacinal (1.4), lichexanthone (1.6), norlichexanthone (1.7), secalonic acid D (1.10), and citreorsein (1.11) were detected by HPLC. (Figure 1.5) The preliminary testing of the chloroform extract showed the highest antioxidant activity.[14]

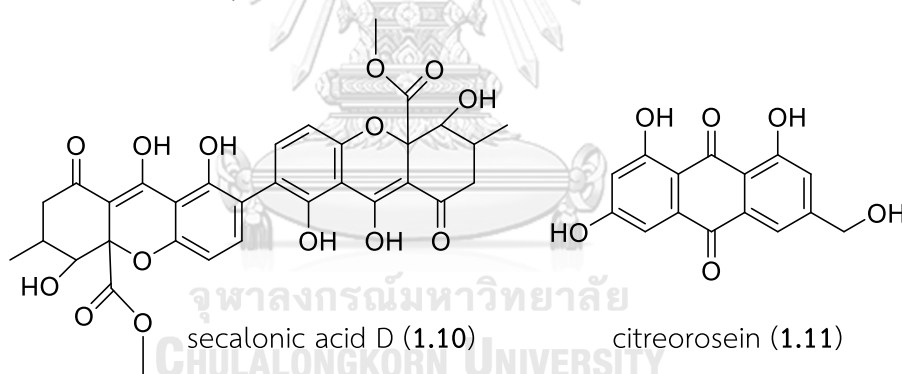
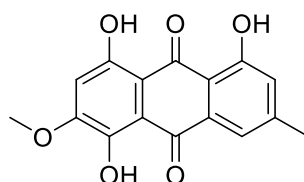


Figure 1.5 Xanthenes and anthraquinones from *L. benguelensis*

The chloroform extracts of lichen *L. benguelensis* were active against bacteria *Staphylococcus aureus*, *Escherichia coli* and *Bacillus subtilis*, and fungi *Candida albicans*, *Mucor mucedo*, and *Trichoderma harzianum*. The antimicrobial activity of *L. benguelensis* was mainly related to the fraction where lichexanthone (1.6) was present. Other chemical constituents were identified as parietin (1.2), emodin (1.3), fallacinal (1.4), citreorsein (1.11), and xanthorin (1.12) by HPLC. (Figure 1.6) These results

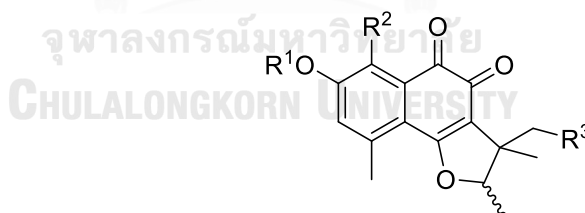
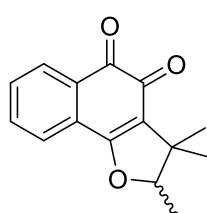
provided scientific basis for the use of the lichen extracts as an accessible source of natural antimicrobial substances in pharmaceutical industries.[15]



xanthorin (1.12)

Figure 1.6 Xanthorin from *L. benguelensis*

Mycobiont, however, has been much less studied. From cultures of the mycobiont of the tropical cortical lichen *T. eluteriae*, Mathey *et al.*[16] reported the isolation of certain 1,2-naphthoquinone antibiotic agents, namely trypethelone (1.14), trypethelone methyl ether (1.15), 8-methoxytrypethelone methyl ether (1.16), and 4'-hydroxy-8-methoxytrypethelone methyl ether (1.17). The substitution pattern of these new derivatives of (+)-dunnione (1.13) was in accord with a polyketide biogenesis of the quinone system. (Figure 1.7)



(+)-dunnione compounds

(1.13) trypethelone (1.14)

trypethelone methyl ether (1.15)

8-methoxytrypethelone methyl ether (1.16)

4'-hydroxy-8-methoxytrypethelone methyl ether (1.17)

R ¹	R ²	R ³
H	H	H
CH ₃	H	H
CH ₃	OCH ₃	H
CH ₃	OCH ₃	OH

Figure 1.7 1,2-Naphthoquinones from *T. eluteriae*

In 2013, the spore-derived mycobionts of the crustose lichen *Trypethelium* sp. collected in Vietnam were cultivated on a malt-yeast extract medium supplemented with 10% sucrose. Takenaka *et al.*[17] investigated their secondary metabolites, resulting in the isolation of a new naphthoquinone named (+)-8-hydroxy-7-methoxytrypethelone (**1.19**) and a new phenalenone derivative named (+)-7,8-dihydro-6-hydroxy-3-methoxy-1,7,7,8-tetramethyl-5H-furo[2',3':5,6]naphtho[1,8-bc]furan-5-one (**1.20**), together with (+)-trypethelone methyl ether (**1.18**) and (+)-sclerodin (**1.21**). (Figure 1.8) Their structures were determined by spectroscopic methods.

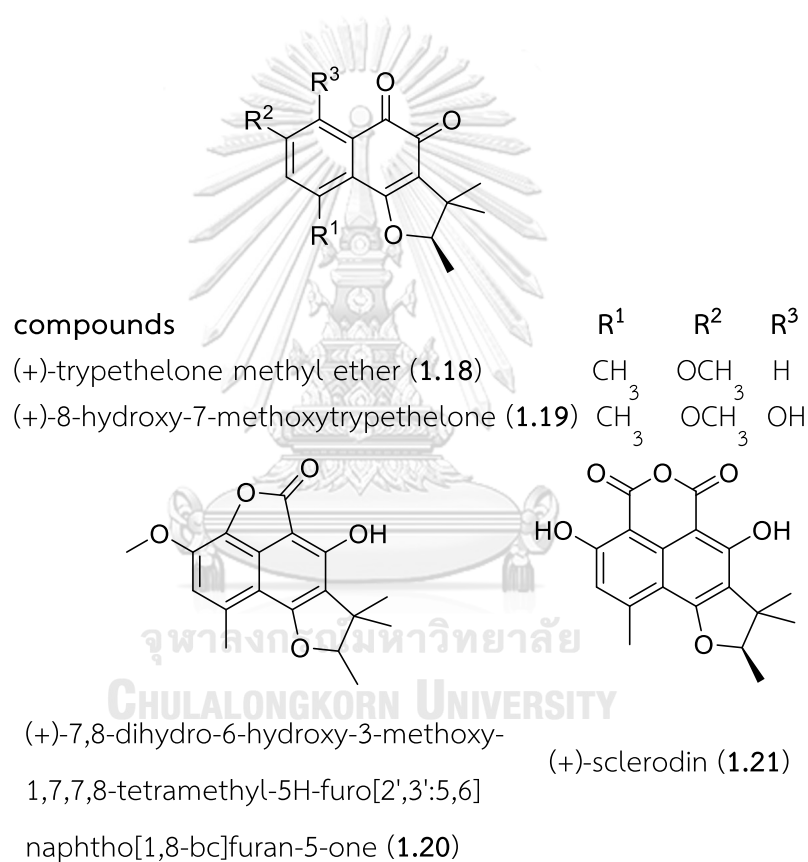


Figure 1.8 1,2-Naphthoquinones and phenalenone derivatives from *Trypethelium* sp.

The biological tests of lichens and mycobionts have shown the frequent appearance of their secondary metabolites with antioxidant, antimicrobial, antiviral, antibiotic, and anticancer *etc.*[18-21] In addition, cytotoxicity in Trypetheliaceae has

not been mentioned till now. Therefore, this research is aimed to search for secondary metabolites with potent biological activities.

1.3 Objectives

The main objectives of this investigation are as follows:

1.3.1 To isolate and characterize compounds from lichens and mycobionts in Trypetheliaceae.

1.3.2 To evaluate the biological activities of isolated compounds.



CHAPTER II

CHEMICAL DIVERSITY OF LICHENS AND CULTURED MYCOBIONTS

2.1 Introduction

In Thailand, the tropical rainforest area comprises of quite varieties of lichens. This diversity causes numerous lichen substances which lead to the discovery of bioactive compounds. Two lichens, *Marcelaria cumingii* and *Trypethelium subeluteriae* were considered for this chemical diversity study. The chemical composition of the lichen in Trypetheliaceae was reported only for Nakhonratchasima province.[13-15] Thus, The plan for this study includes the collection of thirty-four specimens of *M. cumingii* in different geographical areas in Thailand as presented in Figure 2.1. The examination of their chemical compositions was conducted by HPLC.



Figure 2.1 The study area. Numbers on the map correspond to the study sites given in Appendix S2.1

Additionally, the secondary metabolites of lichen *T. subeluteriae* and two cultured mycobionts, *T. platystomum* and *Trypethelium sp.* were comparatively investigated.

2.2 Experimental

2.2.1 General experimental procedures

The NMR spectra were measured on a Bruker Avance III (400 MHz for ^1H NMR and 100 MHz for ^{13}C NMR) and Varian Mercury-400 Plus NMR (400 MHz for ^1H NMR) spectrometers. Chemical shifts are expressed in ppm with reference to the residual protonated solvent signals (CDCl_3 with δ_{H} 7.26, δ_{C} 77.16). TLC was carried out on precoated silica gel 60 F₂₅₄ or Sephadex LH-20 and spots were visualized by UV_{254nm}, UV_{365nm} lamp. Gravity column chromatography was performed with silica gel 60 (0.040–0.063 mm). HPLC C18 column (C18; 25 cm x 4.6 mm, 10 mm), UV spectrophotometric detector, methanol: DI water (85:15, v/v) as solvent. The sample injection volume was 10 mL. The flow rate was 1.0 mL/min.

2.2.2 Extraction and isolation

Thirty-four *M. cumingii* specimens were collected. Specimens were prepared by removing bark section, macerated with acetone and analyzed by HPLC with methanol:DI water (85:15, v/v). *T. subeluteriae*, *T. platystomum* and *Trypethelium sp.* were extracted with acetone at room temperature to yield the crude extract (0.80, 0.19 and 0.92 g, respectively). This crude extract was applied to normal phase silica gel column, eluted with the solvent system of dichloromethane:methanol (100:4) and hexane:ethyl acetate:acetone (4:1.5:0.5 and 2:1.5:0.5).

Two cultured mycobionts, *T. subeluteriae* and *T. platystomum* were identified and cultivated by Dr. Theerapat Luangsuphabool and some specimen were deposited at the Lichen Herbarium, Ramkhamhaeng University.

2.2.3 Cytotoxicity assay

Cytotoxic activities of the isolated compounds were tested using the standard MTT colorimetric method previously described.[22] The preliminary cell lines used in this screening procedure were KB (human epidermoid carcinoma) and HeLaS3 (human cervical carcinoma). The experiments on cytotoxicity were under the responsibility by Ms. Prayumat Onsrisawat and Dr. Pongpun Siripong from the national cancer institute.

2.3 Results and discussion

2.3.1 Investigation on chemical diversity of lichen *M. cumingii*

The investigation was focused on the correlation of lichen chemical content and their diversity. Thirty-four *M. cumingii* specimens were collected from various parts from Thailand, reporting by geographic coordinate system (latitude, longitude) (Table 2.1).

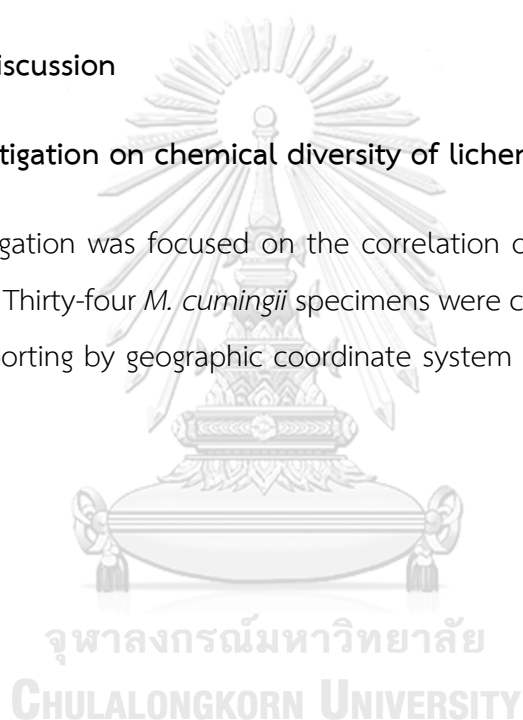


Table 2.1 The specimens of *M. cumingii* and their geographical data

Specimens	Color of lichen		Geographic coordinates			Forest	Sunlight
	Thallus	Perithecia	Latitude	Longitude	Elevation (m)		
CM192	brown	yellow	18°47'27.34"N	98°50'24.79"E	507	hill evergreen	++
DCD3	green	yellow				hill evergreen	+
DCD4	yellow	yellow	19°21'43.90"N	98°55'6.70"E	552	hill evergreen	+++
DCD7	green	yellow				hill evergreen	+
DKT30	green	yellow				hill evergreen	+
DKT36	green	yellow	18°29'42.34"N	99°17'54.77"E	1178	hill evergreen	+
DKT45	green	yellow				hill evergreen	+
DKT95	green	yellow				hill evergreen	+
K11	green	yellow	14°25'44.08"N	101°23'6.42"E	768	mixed deciduous	++
PBR24	green	dark yellow	12°42'58.56"N	99°53'35.74"E	108	mixed deciduous	++
PJK8	orange	yellow	12°31'47.94"N	99°31'56.40"E	159	mixed deciduous	+++
PJK9	orange	yellow				mixed deciduous	+++
PL126	pale	pale	16°50'35.24"N	100°32'4.90"E	149	mixed deciduous	++
RAT43	green	yellow				mixed deciduous	+
RAT50	green	yellow				mixed deciduous	+
RAT57	green	yellow				mixed deciduous	+
RAT60	green	yellow	13°24'26.38"N	99°16'47.89"E	228	mixed deciduous	++
RAT65	green	yellow				mixed deciduous	+
RAT66	green	yellow				mixed deciduous	+
RAT70	green	yellow				mixed deciduous	+
RAT200	green	yellow	13°26'2.28"N	99°16'44.63"E	184	mixed deciduous	+
RAT248	green	yellow				mixed deciduous	+
RAT263	green	yellow				mixed deciduous	+
RAT270	green	yellow	13°31'16.99"N	99°14'1.81"E	273	mixed deciduous	+
RAT346	green	yellow				mixed deciduous	+
RAT359	green	yellow				mixed deciduous	+
RN104	green	pale	9°57'31.52"N	98°38'44.20"E	229	rain	+
SMS	yellow	yellow	12°34'31.41"N	100°56'52.50"E	99	mixed deciduous	+++
SNK8	yellow	yellow				mixed deciduous	+++
SNK36	yellow	yellow	16°57'35.53"N	103°58'4.27"E	294	mixed deciduous	+++
SNK39	yellow	yellow				mixed deciduous	+++
TSL28	brown	yellow	16°31'25.59"N	100°50'7.98"E	932	savanna	+++
UBN13	orange	orange	15° 7'57.96"N	105°25'6.63"E	152	mixed deciduous	+++
UBN158	orange	orange	14°59'58.71"N	105°27'13.29"E	164	mixed deciduous	+++

From HPLC analysis, two significant compounds from *M. cumingii* (Table 2.2, Appendix S2.2) were lichexanthone (**2.1**) and parietin (**2.2**) while xanthorin (**2.3**) and emodin (**2.4**) were obtained in trace amount. This indicated two chemotypes (**2.1**, **2.2**) of this lichen. In northern Thailand, high altitude area, lichen had more chemical content of **2.1** and **2.2**. For instance, DKT45, DCD7 and DCD3 located in Chiang Mai, Northern Thailand (Appendix S2.2) had high content of **2.1** as 74, 68 and 60% and **2.2** 9, 19 and 13%, respectively. On the other hand, RAT65, RAT66 and RAT70 located in Ratchaburi, Western Thailand (Appendix S2.2) reviewed low content of **2.1** as 8, 10 and 18% and **2.2** as 17, 17 and 15%, respectively. These results indicated that the chemical diversity varied depending on geographical area. Chiang Mai, where is the highest elevation with hill evergreen forest has quite cool climate. Because of high altitudes and plenty of water sources the environment is bountiful thus their lichens are bright yellow color with significant amount of chemical composition. While Ratchaburi has lower altitudes with mixed deciduous forest. This forest has condition of falling the leaves at the same time during the dry season. The color of lichens was pale. Their chemical contents were greatly different between those study sites, for example, DKT45 in Chiang Mai had **2.1** as 74%, RAT65 in Ratchaburi as 8%. This is the evident to confirm that the geographical area influenced to the chemical composition. Moreover, their thalli were also much brighter yellow which is the same color of compound **2.1** and **2.2**. Thus the color of lichen thallus referred to their chemical content.

Table 2.2 The percentage of chemical composition from *M. cumingii* specimens

specimens	% content			
	lichexanthone (2.1)	parietin (2.2)	xanthorin (2.3)	emodin (2.4)
CM192	35.63	13.52	2.65	0.14
DCD3	60.40	12.50	0.46	0.16
DCD4	41.02	12.96	1.39	0.00
DCD7	68.05	18.55	0.15	0.03
DKT30	58.20	12.73	1.11	0.00
DKT36	48.62	2.51	0.54	0.00
DKT45	74.03	9.16	1.02	0.00
DKT95	39.37	1.44	0.66	0.00
K11	11.54	10.62	1.09	0.29
PBR24	29.68	19.80	2.24	0.00
PJK8	12.38	29.31	9.69	0.11
PJK9	14.74	26.28	10.33	0.28
PL126	3.32	18.41	2.67	0.00
RAT43	34.13	10.57	2.99	0.00
RAT50	0.23	12.75	0.75	0.00
RAT57	36.19	11.30	1.92	0.00
RAT60	50.96	14.43	1.80	0.00
RAT65	7.53	16.56	8.59	0.00
RAT66	10.01	17.41	6.73	0.00
RAT70	17.57	14.53	3.09	0.00
RAT200	1.15	8.94	2.08	3.64
RAT248	18.04	13.50	4.77	0.00
RAT263	13.55	19.71	3.64	0.00
RAT270	2.01	35.32	9.90	0.00
RAT346	1.02	3.25	0.15	0.00
RAT359	4.56	17.25	0.76	0.00
RN104	5.62	19.42	3.25	0.00
SMS	15.62	23.18	0.90	0.00
SNK8	35.68	13.40	1.64	0.00
SNK36	8.89	21.56	1.84	0.23
SNK39	19.35	22.00	4.30	0.91
TSL28	43.40	10.28	0.57	0.00
UBN13	8.71	33.76	6.72	0.00
UBN158	23.75	15.07	10.22	0.00

2.3.2 Secondary metabolites of *T. subeluteriae*, *T. platystomum* and *Trypethelium* sp.

2.3.2.1 Physical properties and spectroscopic data of isolated compounds

parietin (**2.2**): yellow crystalline solid; ^1H NMR (CDCl_3) see Table 2.4.

emodin (**2.4**): yellow crystalline solid; ^1H NMR (acetone- d_6) see Table 2.4.

haematommone (**2.5**): yellow amorphous solid; ^1H NMR (acetone- d_6) see Table 2.4.

bipolaride C (**2.6**): dark violet amorphous solid; ^1H NMR (CDCl_3) see Table 2.5.

8-hydroxytrypethelone methyl ether (**2.7**): dark violet crystalline solid; ^1H NMR (CDCl_3) see Table 2.6.

4'-hydroxytrypethelone (**2.8**): violet crystalline solid; ^1H NMR (acetone- d_6) see Table 2.6.

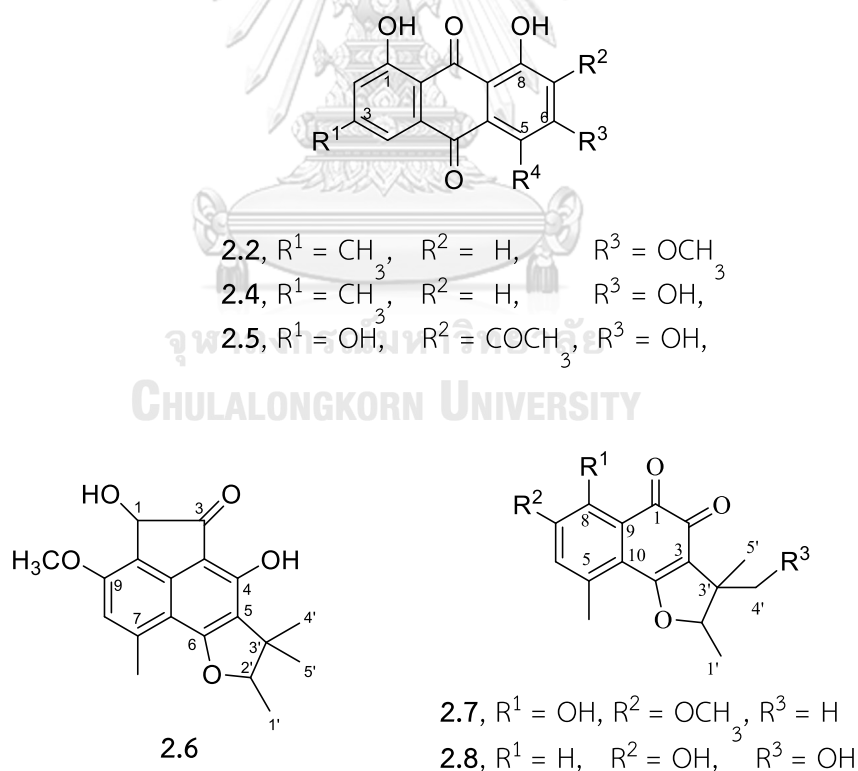


Figure 2.2 Chemical structures of **2.2**, **2.4**–**2.8**

The lichen *T. subeluteriae* produced three major compounds namely parietin (**2.2**), emodin (**2.4**) and haematommone (**2.5**) (Figure 2.2). The structures of these compounds were elucidated and compared with previous reports.[12, 16, 17, 23] (Table 2.3) Compound **2.2** was subjected to cytotoxic activity against KB and HeLaS3 cell lines, the result showed cytotoxic activity with IC₅₀ of 64.17 ± 36.44 and 92.47 ± 2.79 μM, respectively.

Table 2.3 ¹H NMR data of **2.2**, **2.4**, **2.5** δ_H (ppm), (multi, *J* in Hz)

position	2.2 ^a	2.4 ^b	2.5 ^b
2	7.01 (s)	7.15 (s)	6.79 (s)
4	7.62 (s)	7.58 (s)	7.09 (s)
5	7.36 (d, 2.8)	7.26 (d, 2.4)	7.31 (s)
7	6.69 (d, 2.8)	6.67 (d, 2.4)	
1-OH	12.32 (s)	12.20 (s)	12.86 (s)
3-CH ₃	2.45 (s)	2.47 (s)	12.14 (s)
6-OCH ₃	3.94 (s)		
7-COCH ₃			2.38 (s)
8-OH	12.13 (s)	12.08 (s)	

Spectra were recorded in ^a CDCl₃, ^b acetone-*d*₆.

In addition, bipolaride C (**2.6**) (Figure 2.2) isolated from cultured mycobionts *T. platystomum* and 8-hydroxytryptethelone methyl ether (**2.7**), 4'-hydroxytryptethelone (**2.8**) from *Trypethelium sp.* were isolated and characterized by NMR spectroscopic data and comparing with the data reported in literature.[17, 24-26] (Tables 2.4 and 2.5)

Table 2.4 ^1H NMR data of **2.2**, **2.4**, **2.5** δ_{H} (ppm), (multi, J in Hz)

position	2.6^a
1	5.12 (s)
8	6.71 (s)
1'	1.44 (d, 7.2)
2'	4.60 (q, 6.8)
4'	1.43 (s)
5'	1.68 (s)
4-OH	13.16 (s)
7-CH ₃	2.54 (s)
9-OCH ₃	3.94 (s)

Spectrum was recorded in ^a CDCl₃.

Table 2.5 ^1H NMR data of **2.7**, **2.8**, δ_{H} (ppm), (multi, J in Hz)

position	2.7^a	2.8^b
6	6.71 (s)	6.99 (d, 1.6)
8		7.37 (d, 2.4)
1'	1.44 (d, 6.8)	1.51 (d, 6.8)
2'	4.61 (q, 6.4)	5.10 (q, 6.8)
4'	1.43 (s)	3.83 (m)
		3.58 (m)
5'	1.25 (s)	1.26 (s)
5-CH ₃	2.54 (s)	2.59 (s)
7-OCH ₃	3.94 (s)	
7-OH		9.51
8-OH	13.15 (s)	

Spectra were recorded in ^a CDCl₃, ^b acetone-*d*₆.

2.4 Conclusion

Chemical content of *M. cumingii* dealt with the altitudes and environment. The bountiful of air, water and low temperature caused more amount of lichexanthone (2.1) and parietin (2.2). These compounds can be designated as chemotypes for *M. cumingii*.

Lichens and cultured mycobionts produced different secondary metabolites. Lichen *T. subeluteriae* produced mainly anthraquinones: parietin (2.2), emodin (2.4) and haematommone (2.5). While cultured mycobionts *T. platystomum* and *Trypethelium* sp. produced phenalenone derivatives: bipolaride C (2.6), and 1,2-naphthoquinones: 8-hydroxytrypethelone methyl ether (2.7) and 4'-hydroxytrypethelone (2.8), respectively.



CHAPTER III

NAPHTHOQUINONES FROM CULTURED MYCOBIONT OF *Marcelaria cumingii* (Mont.) AND THEIR CYTOTOXICITY

3.1 Introduction

M. cumingii from Nakhonratchasima was quite dominant because of its deep yellow thallus (Figure 3.1). The secondary metabolites were reported to comprise of anthraquinones and xanthonenes.[13-15] However, the cultured mycobiont of *M. cumingii* had different color as dark red and there was no report on the chemical constituents of cultured mycobiont of *M. cumingii*. In addition to their natural role, the secondary metabolites exhibited a variety of biological activities such as, antibiotic, antimycobacterial, antimutagenic, antioxidant, antiviral, antipyretic, analgesic and have been used for treatment of various conditions in traditional medicine, especially, a significant of potentially useful cytotoxic activity.[27-32] Based on this research interests in cytotoxicity of the metabolites from cultured mycobionts, this investigation will involve the isolated isolation and examination of potentially cytotoxic activity of the secondary metabolites.

Classification

Kingdom	Fungi
Phylum	Ascomycota
Class	Eurotiomycetes
Order	Pyrenulales
Family	Trypetheliaceae
Genus	<i>Marcelaria</i>
Specific epithet	<i>cumingii</i>

Synonym

Trypethelium cumingii Mont., *J. Bot.*: 5 (1845)

Bathelium cumingii (Mont.) Trevis., *Flora (Regensburg)* 44: 21 (1861)

Laurera cumingii (Mont.) Zahlbr., *Catalogus Lichenum Universalis* 1: 503 (1922)



Figure 3.1 Lichen and cultured mycobiont of *M. cumingii*

3.2 Experimental

3.2.1 General experimental procedures

The NMR spectra were measured on a Bruker Avance III (400 MHz for ^1H NMR and 100 MHz for ^{13}C NMR) and Varian Mercury-400 Plus NMR (400 MHz for ^1H NMR and 100 MHz for ^{13}C NMR) spectrometers with TMS as internal standard. Chemical shifts are expressed in ppm with reference to the residual protonated solvent signals (chloroform- d_1 with δ_{H} 7.26, δ_{C} 77.16, dimethylsulfoxide- d_6 with δ_{H} 2.50 and δ_{C} 39.52 and acetone- d_6 with δ_{H} 2.05 and δ_{C} 29.84). The HRESIMS were recorded on a HRESIMS Bruker microTOF. TLC was carried out on precoated silica gel 60 F₂₅₄ or Sephadex LH-20 and spots were visualized by UV_{254nm}, UV_{365nm} lamp. Gravity column chromatography was performed with silica gel 60 (0.040–0.063 mm). Solvent used for isolation are *n*-hexane, dichloromethane, ethyl acetate, acetone, and methanol.

3.2.2 Fungal isolation, cultivation and identification

Specimen of *M. cumingii* was collected from tree bark at Pak Chong district, Nakhon Ratchasima, Thailand (700 m alt.), in December 2007. The mycobiont of *M.*

cumingii was successfully isolated from perithecia of lichen thallus by the ascospore discharge technique[33] and was cultivated in 90 mm Petri dishes containing Malt-Yeast-Extract agar (MYA) at room temperature (30-32°C) for 9 weeks. The voucher specimen was identified by Dr. Theerapat Luangsaphabool and was deposited at the Lichen Herbarium, Ramkhamhaeng University (voucher No. RAMK027993). The fungal culture is maintained in the lichen research unit at Ramkhamhaeng University, Thailand. The molecular data were analyzed to confirm for species identification. The genomic DNA was extracted from the mycobiont culture using CTAB precipitation protocol.[34] The nuclear large subunit ribosomal DNA (nuLSU) and mitochondrial small subunit ribosomal DNA (mtSSU) loci were amplified using primer pairs LR0R/LR3[35] and mrSSU1/MSU7,[36, 37] respectively. PCR conditions and DNA sequencing followed protocols previously described.[38] The nuLSU and mtSSU sequences were deposited in DDBJ (accession number LC223104 and LC223105) and confirmed similarity sequences to *M. cumingii* (KM453789; 99%) and (LC034284; 99%), respectively.

3.2.3 Extraction and isolation

The fungal biomass and media were separately extracted. The mycobiont colonies were extracted with methanol at room temperature to yield the crude extract (0.45 g). This crude extract was applied to a normal phase silica gel column, eluted with the solvent system of dichloromethane-methanol (100:4) to afford five fractions **C1** (50.2 mg), **C2** (41.3 mg), **C3** (101.8 mg), **C4** (98.4 mg), and **C5** (30.1 mg). Fraction **C1** was applied to silica gel column, eluted with dichloromethane:methanol (100:4) to give two fractions, **C1.1** (21.2 mg) and **C1.2** (15.8 mg). Purifying fraction **C1.1** by crystallizing in methanol yield **3.1** (4.9 mg). Fraction **C1.2** was chromatographed, eluted with hexane:ethyl acetate:acetone (4:1.5:0.5) to afford **3.2** (2.9 mg). Fraction **C3** was subjected to column chromatography, eluted with hexane:ethyl acetate:acetone (2:1.5:0.5) to afford **3.5** (1.1 mg) and **3.4** (3.0 mg). Fraction **C5** was washed three times by dichloromethane (each 5 mL) to obtain the precipitate **C5.1** (10.1 mg), which was dissolved in methanol, then purified by column chromatography to yield **3.3** (4.1 mg).

3.2.4 Single crystal X-ray crystallography

With the help of a Bruker X8 PROSPECTOR KAPPA CCD diffractometer equipped with an μS X-ray microfocus source operated at 45 kV, 0.65 mA, producing an intense monochromatic $\text{CuK}\alpha$ radiation ($\lambda = 1.54178 \text{ \AA}$), the diffraction data of **3.1**, **3.2**, and **3.3** were collected at 296(2) K to atomic resolution of 0.83 \AA and completeness of 96–99%. Data processing covering integration, reduction together with correction of the absorption effects, and subsequent merging were carried out using SAINT, SADABS, and XPREP, respectively in the APEX2 program suite.[39] The three structures were solved by intrinsic phasing method with SHELXTL XT,[40] expanded using the difference Fourier technique, and were refined anisotropically by full matrix least-squares on F^2 with SHELXTL XLMP.[41] All H-atom positions were placed geometrically and treated using a riding model: C–H = 0.93 \AA , $U_{\text{iso}} = 1.2U_{\text{eq}}(\text{C})(\text{aromatic})$; C–H = 0.96 \AA , $U_{\text{iso}} = 1.5U_{\text{eq}}(\text{C})(\text{methyl})$; C–H = 0.98 \AA , $U_{\text{iso}} = 1.2U_{\text{eq}}(\text{C})(\text{methine})$; and O–H = 0.82 \AA , $U_{\text{iso}} = 1.5U_{\text{eq}}(\text{hydroxyl})$. In **3.3**, a cluster of disordered water sites was found as trace impurities of crystallization solvent (ethanol); the water H-atoms could not be determined. Absolute configurations of the three compounds were established by anomalous dispersion (Fleck parameters (x)[42] close to zero). Crystal data of compounds **3.1**, **3.2**, and **3.3** (CIFs) are given in Supporting Information and have been deposited with the Cambridge Crystallographic Data Centre (CCDC 1507772–1507774). They can be obtained free of charge via http://www.ccdc.cam.ac.uk/data_request/cif.

3.2.5 Cytotoxicity assay

Cytotoxic activities of isolated compounds were tested using the standard MTT colorimetric method previously described.[22] The preliminary cell lines used in this screening procedure were KB (human epidermoid carcinoma) and HeLaS3 (human cervical carcinoma). The significant compound was chosen for further observation against cancer cell lines: HT29 (human colon adenocarcinoma), HCT116 (human colon carcinoma), A549 (human lung carcinoma) and doxorubicin was used as standard antibiotic antitumor agent with normal cells: rhesus monkey kidney cells (Vero) and human diploid fibroblast cell (MRC-5). The experiments on cytotoxicity were under the

responsibility by Ms. Prayumat Onsrisawat and Dr. Pongpun Siripong from the national cancer institute.

3.2.6 Molecular docking calculations

Protein and inhibitors preparation: The protein structure of topoisomerase II was retrieved from the Protein Data Bank (pdb code: 1AB4).[43] The crystallographic water molecules were deleted and the hydrogen atoms were added to protein by using AutodockTool 1.5.6.[44] The inhibitors were constructed and geometry optimizations with PM6 level of theory by using MOPAC2009.[45, 46]

Molecular docking calculations: The atomic potential grid box for molecular docking was constructed with the grid size of 126 126 126 point. The distance spacing between each point is 0.375 Å. Subsequently, the Doxorubicin and all five inhibitor were docked into the protein by using Autodock 4.2.6 program.[44] The Lamarckian Genetic Algorithm was employ and the charge as Gasteiger was employed to all inhibitors. The calculations of each inhibitor were set to 500 cycles while the other parameters were set as default. The most population of each posed was selected for further molecular binding analyses.

3.3 Results and discussion

3.3.1 Physical and spectroscopic data of isolated compounds

(-)-tryptethelone methyl ether (3.1): dark violet-red crystalline solid (4.9 mg); $[\alpha]_D^{25}$ -7 (c 0.13 mg/mL, acetone); CD (c 0.5 mg/mL, MeOH), $\lambda_{\max}(\Delta\epsilon)$ 492 nm (-1.1); ^1H and ^{13}C NMR (CDCl_3) see Tables 3.1 and 3.2; HRESIMS m/z 309.1108 $[\text{M}+\text{Na}]^+$ (calcd for $\text{C}_{17}\text{H}_{18}\text{NaO}_4$, m/z 309.1103).

(-)-8-methoxytryptethelone methyl ether (3.2): violet-red crystalline solid (2.9 mg); $[\alpha]_D^{25}$ -38 (c 0.50 mg/mL, acetone); CD (c 0.5 mg/mL, MeOH), $\lambda_{\max}(\Delta\epsilon)$ 492 nm (-

0.8); ^1H and ^{13}C NMR (CDCl_3) see Tables 3.1 and 3.2; HRESIMS m/z 339.1213 $[\text{M}+\text{Na}]^+$ (calcd for $\text{C}_{18}\text{H}_{20}\text{NaO}_5$, m/z 339.1208).

(-)-4'-hydroxytryptelone (**3.3**): Violet crystalline solid (4.1 mg); $[\alpha]_{\text{D}}^{25}$ -23 (c 0.47, Acetone); CD (c 0.5 mg/mL, MeOH), $\lambda_{\text{max}}(\Delta\epsilon)$ 490 nm (-0.3); ^1H and ^{13}C NMR ($\text{DMSO-}d_6$) see Tables 3.1 and 3.2; HRESIMS m/z 311.0900 $[\text{M}+\text{Na}]^+$ (calcd for $\text{C}_{16}\text{H}_{16}\text{NaO}_5$, m/z 311.0895).

(-)-tryptelone (**3.4**): Violet amorphous solid (3.0 mg); $[\alpha]_{\text{D}}^{25}$ -9 (c 0.22, acetone); CD (c 0.5 mg/mL, MeOH), $\lambda_{\text{max}}(\Delta\epsilon)$ 490 nm (-0.9); ^1H and ^{13}C NMR ($\text{DMSO-}d_6$) see Tables 3.1 and 3.2; HRESIMS m/z 295.0949 $[\text{M}+\text{Na}]^+$ (calcd for $\text{C}_{16}\text{H}_{16}\text{NaO}_4$, m/z 295.0946).

(-)-4'-hydroxy-8-methoxytryptelone methyl ether (**3.5**): Orange amorphous solid (1.1 mg); $[\alpha]_{\text{D}}^{25}$ -17 (c 0.70 mg/mL, acetone); CD (c 0.5 mg/mL, MeOH), $\lambda_{\text{max}}(\Delta\epsilon)$ 462 nm (-0.3); ^1H and ^{13}C NMR (CDCl_3) see Tables 3.1 and 3.2; HRESIMS m/z 355.1159 $[\text{M}+\text{Na}]^+$ (calcd for $\text{C}_{18}\text{H}_{20}\text{NaO}_6$, m/z 355.1158).

3.3.2 Single crystal X-ray crystallography data of isolated compounds

Crystal data of (-)-tryptelone methyl ether (3.1): $\text{C}_{17}\text{H}_{18}\text{O}_4$, MW = 286.31, violet-red rod-like crystal: $0.16 \times 0.30 \times 0.50 \text{ mm}^3$, monoclinic space group $P2_1$ (no. 4), $a = 9.6486(3) \text{ \AA}$, $b = 6.9084(2) \text{ \AA}$, $c = 10.6500(3) \text{ \AA}$, $\beta = 95.722(1)^\circ$, $V = 706.35(4) \text{ \AA}^3$, $Z = 2$, $D_x = 1.346 \text{ g cm}^{-3}$, $\mu(\text{Cu-K}\alpha) = 0.780 \text{ mm}^{-1}$, $F(000) = 304$. Collected/unique/observed reflections: 5577/4439/2172 ($R_{\text{int}} = 0.0472$). Final $R_1(F^2) = 0.0588$, $wR_2(F^2) = 0.1661$ and $S = 1.099$ for 2172 reflections with $F^2 > 2\sigma(F^2)$. $x = 0.02(14)$.

Crystal data of (-)-8-methoxytryptelone methyl ether (3.2): $\text{C}_{18}\text{H}_{20}\text{O}_5$, MW = 316.34, violet-red rod-like crystal: $0.28 \times 0.28 \times 0.48 \text{ mm}^3$, monoclinic space group $C2$ (no. 5), $a = 11.5518(4) \text{ \AA}$, $b = 14.9946(6) \text{ \AA}$, $c = 18.9702(7) \text{ \AA}$, $\beta = 91.246(1)^\circ$, $V = 3285.1(2) \text{ \AA}^3$, $Z = 8$, $D_x = 1.279 \text{ g cm}^{-3}$, $\mu(\text{Cu-K}\alpha) = 0.767 \text{ mm}^{-1}$, $F(000) = 1344$. Collected/unique/observed reflections: 12122/5830/4439 ($R_{\text{int}} = 0.0344$). Final $R_1(F^2) = 0.0740$, $wR_2(F^2) = 0.2098$ and $S = 1.109$ for 4439 reflections with $F^2 > 2\sigma(F^2)$. $x = 0.02(11)$.

Crystal data of (-)-4'-hydroxytryptethelone (**3.3**): $C_{16}H_{16}O_5 \cdot 1.5H_2O$, $MW = 312.29$, violet rod-like crystal: $0.08 \times 0.10 \times 0.36 \text{ mm}^3$, monoclinic space group $P2_1$ (no. 4), $a = 10.0141(3) \text{ \AA}$, $b = 7.1737(2) \text{ \AA}$, $c = 11.8901(4) \text{ \AA}$, $\beta = 109.290(1)^\circ$, $V = 806.21(4) \text{ \AA}^3$, $Z = 2$, $D_x = 1.286 \text{ g cm}^{-3}$, $\mu(\text{Cu-K}\alpha) = 0.850 \text{ mm}^{-1}$, $F(000) = 328$. Collected/unique/observed reflections: 6270/2868/1994 ($R_{\text{int}} = 0.0676$). Final $R_1(F^2) = 0.0937$, $wR_2(F^2) = 0.2342$ and $S = 1.025$ for 1994 reflections with $F^2 > 2\sigma(F^2)$. $x = 0.0(2)$.

The methanol extract of cultured mycobiont *M. cumingii* was separated by column chromatography yielding a new compound, three compounds with new absolute configuration together with (-)-tryptethelone (**3.4**) as presented in Figure 3.2. Four new compounds were elucidated as follows.

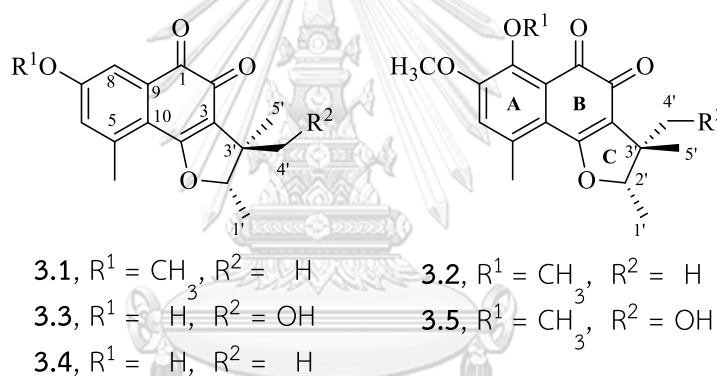


Figure 3.2 Chemical structures of **3.1–3.5**

Compound **3.1** was isolated as a dark violet-red crystalline solid. The HRESIMS of the solidated positive-ion peak $[\text{M}+\text{Na}]^+$ at m/z 309.1108 established the molecular formula of $C_{17}H_{18}O_4$. Comparison of the NMR data of **3.1** and known naphthoquinones[12, 17, 47] indicated the similarity in the structures (Tables 3.1 and 3.2). To define the absolute configuration of C-2', the circular dichroism (CD), the optical rotation as well as single crystal X-ray analysis was applied. Elsabai *et al.*[48] reported the characteristic Cotton effect (CE) of mycobiont-derived naphthoquinone scaffold at $\lambda_{\text{max}}(\Delta\epsilon)$ 480 nm (-1.8) and confirmed their (-)-tryptethelone with 2'S configuration by single crystal X-ray analysis. Accordingly, a negative CE at $\lambda_{\text{max}}(\Delta\epsilon)$ 490 nm (-0.9) of (-

-)-tryptethelone (**3.4**) assigned the 2'S configuration, further supported by the levorotatory specific rotation. In case of **3.1**, its negative CE at $\lambda_{\max}(\Delta\epsilon)$ 492 nm (-1.1) in accordance with a levorotatory specific rotation can be described with the reference (-)-tryptethelone, indicating the 2'S configuration of **3.1**. Accordingly, **3.1** was defined as (-)-2'S-tryptethelone methyl ether. The absolute configuration of **3.1** was unequivocally evidenced by single crystal X-ray crystallography (Figure 3.3).

Table 3.1 ^1H NMR data of 3.1-3.5, δ_{H} (ppm), (multi, J in Hz)

position	3.1 ^a	3.2 ^a	3.3 ^b	3.4 ^b	3.5 ^a
6	6.87 (<i>d</i> , 2.4)	6.80 (<i>s</i>)	6.88 (<i>d</i> , 2.0)	6.88 (<i>d</i> , 2.0)	6.82 (<i>s</i>)
8	7.49 (<i>d</i> , 2.8)		7.22 (<i>d</i> , 2.8)	7.21 (<i>d</i> , 2.8)	
1'	1.45 (<i>d</i> , 6.4)	1.43 (<i>d</i> , 6.8)	1.38 (<i>d</i> , 6.8)	1.39 (<i>d</i> , 6.4)	1.50 (<i>d</i> , 6.8)
2'	4.62 (<i>q</i> , 6.4)	4.58 (<i>q</i> , 6.4)	5.02 (<i>q</i> , 6.8)	4.66 (<i>q</i> , 6.4)	4.68 (<i>q</i> , 6.4)
4'	1.25 (<i>s</i>)	1.23 (<i>s</i>)	3.67 (<i>d</i> , 9.2)	1.32 (<i>s</i>)	3.67 (<i>d</i> , 10.4)
			3.49 (<i>m</i>)		3.64 (<i>d</i> , 10.4)
5'	1.43 (<i>s</i>)	1.41 (<i>s</i>)	1.13 (<i>s</i>)	1.14 (<i>s</i>)	1.25 (<i>s</i>)
5-CH ₃	2.58 (<i>s</i>)	2.58 (<i>s</i>)	2.49 (<i>s</i>)	2.50 (<i>s</i>)	2.60 (<i>s</i>)
7-OCH ₃	3.88 (<i>s</i>)	3.91 (<i>s</i>)			3.93 (<i>s</i>)
8-OCH ₃		3.87 (<i>s</i>)			3.88 (<i>s</i>)

Spectra were recorded in ^a CDCl₃, ^b DMSO-*d*₆.

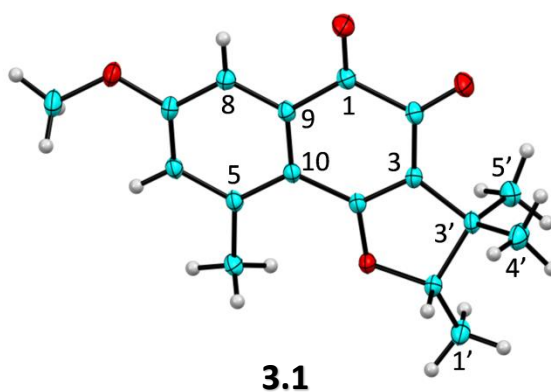


Figure 3.3 ORTEP plot of **3.1** (20% probability level; atom colors: C, cyan; O, red; H, white)

Table 3.2 ^{13}C NMR data of **3.1-3.5**, δ_{c} (ppm)

position	3.1 ^a	3.2 ^a	3.3 ^b	3.4 ^b	3.5 ^a
1	183.2	182.7	181.7	181.5	181.8
2	176.4	176.0	174.5	174.3	176.2
3	123.0	121.9	123.2	120.5	121.6
4	172.5	170.9	171.8	170.9	173.4
5	141.4	135.6	140.0	140.3	117.6
6	124.2	119.9	123.4	123.6	119.8
7	162.5	151.6	160.3	160.2	157.3
8	114.4	156.3	115.1	115.1	152.1
9	135.1	125.6	133.8	133.8	120.8
10	119.5	118.2	116.2	116.3	136.4
1'	15.8	14.8	15.3	14.5	14.9
2'	93.1	92.3	88.0	91.8	88.3
3'	44.0	43.0	48.2	42.3	49.3
4'	21.0	20.4	15.7 ^c	20.0	68.1 ^c
5'	26.7	25.9	65.3 ^c	25.2	16.1 ^c
5-CH ₃	23.3	22.7	21.6	21.5	23.1
7-OCH ₃	56.7	56.1			56.3
8-OCH ₃		61.3			61.5

Spectra were recorded in ^a CDCl₃, ^b DMSO-*d*₆, ^c see Figure 3.2.

Compound **3.2** was isolated as a violet-red crystalline solid. The molecular formula of **3.2** was determined as C₁₈H₂₀O₅ by [M+Na]⁺ ion at m/z 339.1213 in HRESIMS, which has an additional methoxy group than **3.1**. Detailed NMR comparison of **3.2** with 8-methoxytryptelone methyl ether[16] suggested their same planar structures. As the result of **3.2** had the negative CE at $\lambda_{\text{max}}(\Delta\epsilon)$ 492 nm (-0.8), thus **3.2** was defined as (-)-2'S-8-methoxytryptelone methyl ether having a 2'S configuration, which was confirmed by single crystal X-ray crystallography (Figure 3.4). Mathey *et al.*[16] reported the CD data of 8-methoxytryptelone methyl ether, having a strong positive CE at

$\lambda_{\max}(\Delta\epsilon)$ 480 nm (1.34) but its absolute configuration was not assigned. With more data of **3.2**, that opposite CE indicated that their compound was the enantiomer of **3.2**, having the 2'*R* configuration.

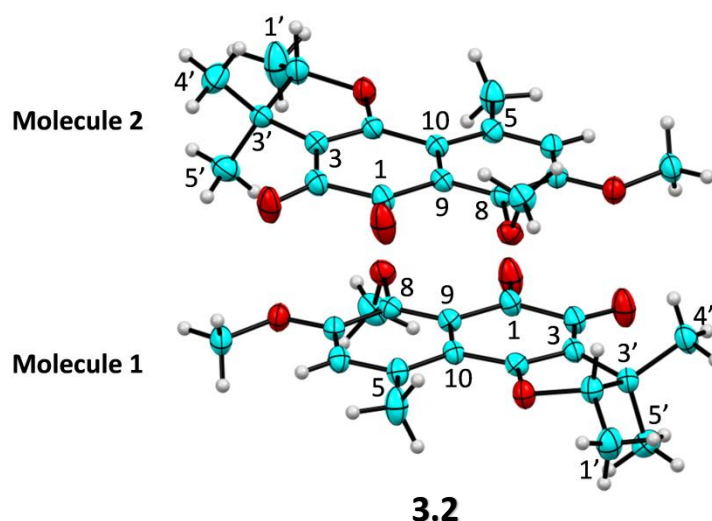


Figure 3.4 ORTEP plot of **3.2** (20% probability level; atom colors: C, cyan; O, red; H, white). Two similar molecules in the asymmetric unit are stabilized by off-centered parallel π stacking interactions

Compound **3.3** was isolated as a violet crystalline solid. Its molecular formula was determined as $C_{16}H_{16}O_5$ from the HRESIMS at m/z 311.0900 $[M+Na]^+$. The 1H NMR spectrum of **3.3** showed two meta coupling aromatic protons, one hydroxymethylene, one oxygenated methine and three methyl groups. The ^{13}C NMR spectrum exhibited 16 carbon signals including two carbonyl groups, two aromatic methines, seven quaternary carbons, two of which were oxygenated in the range of 151-171 ppm, one oxymethylene carbon, one oxymethine carbon, and three methyl groups. These findings indicated that **3.1**, **3.3**, and **3.4** had the same scaffold. The difference between **3.3** and **3.4** was the presence of the hydroxymethylene group instead of the methyl at C-3'. HMBC cross peaks of H_2-4' to C-3 and H_3-5' to C-2', C-3', C-4', and C-3 confirmed the aforementioned finding (Figure 3.5). The strong NOESY correlation between H_2-4'

and H-2' indicated their syn orientation. Likewise, the two moieties H₃-1' and H₃-5' were syn-facial. The negative CE at $\lambda_{\max}(\Delta\epsilon)$ 490 nm (-0.3) in accordance with single crystal X-ray diffraction analysis (Figure 3.6) determined unambiguously the stereochemistry of **3.3**. Accordingly, **3.3** was defined as (-)-(2'S,3'S)-4'-hydroxytryptelone.

Compound **3.4** was obtained as a violet amorphous solid. The HRESIMS at m/z 311.0900 [M+Na]⁺, the NMR spectroscopic data (Table 3.1 and 3.2), $[\alpha]_D^{25}$ -9 and $\lambda_{\max}(\Delta\epsilon)$ 490 nm (-0.9) of **3.4** indicated to a known compound (-)-2'S-tryptelone.

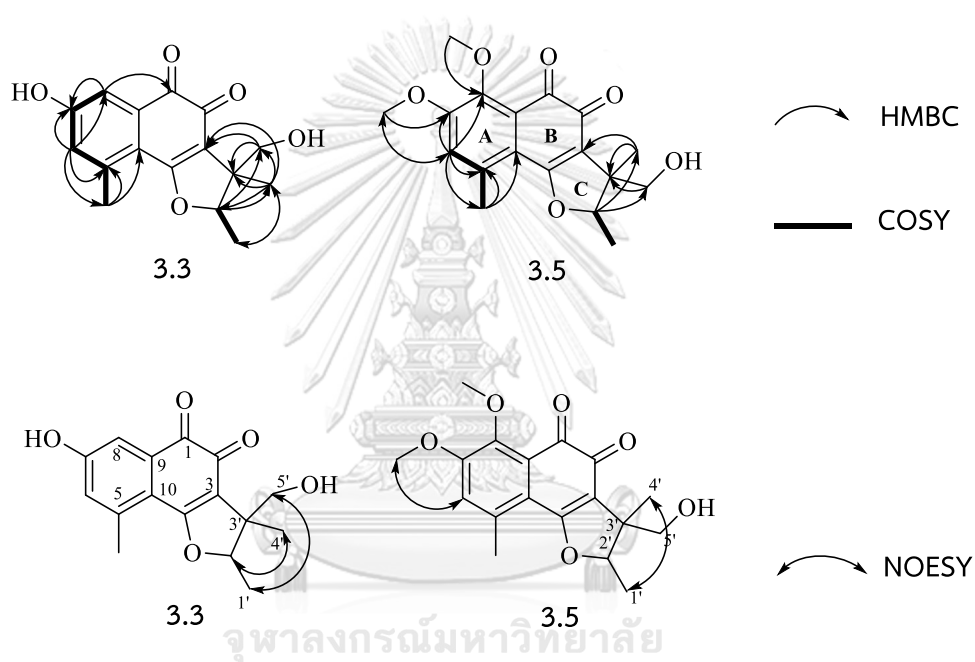


Figure 3.5 Selected COSY, HMBC, and NOESY correlations for **3.3** and **3.5**

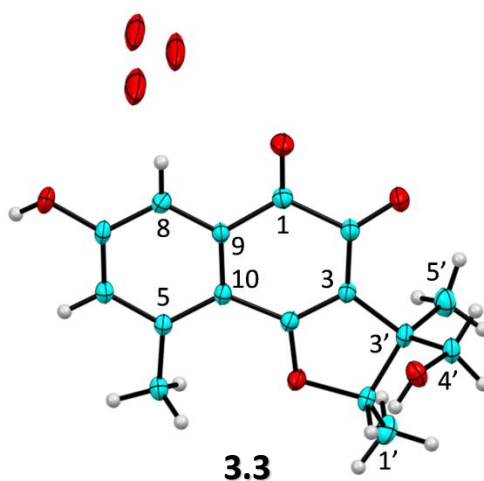


Figure 3.6 ORTEP plot of **3.3** (20% probability level; atom colors: C, cyan; O, red; H, white). The 1.5 water molecules are distributed over three sites, acting as space fillers in the crystal lattice; shortest $O_w \cdots O$ (**3.5**) distance is 3.67 Å

Compound **3.5** was isolated as an orange amorphous solid and its molecular formula was determined as $C_{18}H_{20}O_6$ through the solidated ion peak at m/z 355.1159 $[M+Na]^+$ in the HRESIMS spectrum. Detailed NMR comparison of **3.5** and **3.2** indicated that they shared the same A- and C- rings. The only difference was the replacement of the methyl group by the hydroxymethylene group in the C-ring. The 1H chemical shifts of $H_{3-1'}$, $H_{2-4'}$, and $H_{3-5'}$ of **3.5** were identical with those of 4'-hydroxy-8-methoxytryptelone methyl ether reported previously,[16] revealing that both of them had the same relative configuration in C-ring and shared the same planar structure. Nevertheless, the absolute configurations of C-2' and C-3' of formerly known 4'-hydroxy-8-methoxytryptelone methyl ether have not assigned yet. The negative CE of **3.5** defined its 2'S configuration but unveiled the C-3' configuration. To determine the latter, NMR data of $H_{2-2'}$, $H_{2-4'}$, and $H_{3-5'}$ of **3.5** were compared with corresponding data of **3.3** (Figure 3.5). Noteworthy, in case of **3.3**, the chemical shift of $H_{2-2'}$ (δ_H 5.02, q , 6.8 Hz) was downfield shifted as compared to those of **3.1**, **3.2**, **3.4** and **3.5** (δ_H 4.58-4.68) when proton $H_{2-2'}$ and the hydroxymethylene $H_{2-4'}$ was syn-facial. In contrast, the upfield chemical shift of $H_{2-2'}$ (δ_H 4.68, q , 6.4 Hz) in **3.5** was similar to that of previously known compound,[16] implying the *trans* orientation of $H_{2-2'}$ and $H_{2-4'}$.

4'. The 3'R configuration of **3.5** was thus proposed. Accordingly, **3.5** was elucidated as (-)-(2'S,3'R)-4'-hydroxy-8-methoxytryptelone methyl ether (Figure 3.2).

Human cancer-derived cell lines are the most widely used as fundamental models in laboratories to study cytotoxicity and to test hypotheses of anticancer agents to improve the therapeutic efficacy of cancer treatment. Each of cancer cell line do not have equal value as general model. Therefore, the success of new assessed cytotoxicity depend on screening procedure against cancer cell lines

All isolated compounds were preliminary evaluated for cytotoxic activity against KB and HeLaS3 cell lines, **3.1** displayed significant cytotoxic activity with IC_{50} of 9.87 ± 0.80 and $5.15 \pm 0.87 \mu\text{M}$, respectively (Table 3.3). Accordingly, **3.1** was set to be tested further. Compound **3.1** exhibited cytotoxicity against HCT116 and A549 with IC_{50} of 0.32 ± 0.03 and $1.05 \pm 0.12 \mu\text{M}$, respectively (Table 3.4). As compared **3.1** to doxorubicin, **3.1** and doxorubicin were toxic against normal cell (Vero) on the same range with IC_{50} of 1.87 ± 0.22 , $2.06 \pm 0.31 \mu\text{M}$, respectively (Table 3.4). While **3.1** was more non-toxic to MRC-5 than doxorubicin with IC_{50} of 14.28 ± 2.33 , $2.74 \pm 0.23 \mu\text{M}$, respectively.

Table 3. 3 *In vitro* cytotoxicity of **3.1–3.5** against KB and HeLaS3 cell lines

Compound	IC_{50} (μM) ^a	
	KB	HeLaS3
3.1	9.87 ± 0.80	5.15 ± 0.87
3.2	41.29 ± 3.12	20.09 ± 1.08
3.3	53.78 ± 1.06	51.33 ± 1.84
3.4	34.80 ± 2.59	36.04 ± 2.12
3.5	>100	>100
Doxorubicin	0.12 ± 0.05	0.06 ± 0.03

^a $IC_{50} \leq 10$ = good activity, $10 < IC_{50} \leq 30$ = moderate activity, $IC_{50} > 100$ = Inactive.

Table 3.4 *In vitro* cytotoxicity of **3.1** against MRC-5, HT29, HCT116 and A549 cell lines

Cells	IC ₅₀ (μM) ^a	
	Compound 3.1	Doxorubicin
Vero	1.87 ± 0.22	2.06 ± 0.31
MRC-5	14.28 ± 2.33	2.74 ± 0.23
HT29	6.13 ± 0.15	0.30 ± 0.06
HCT116	0.32 ± 0.03	<0.1
A549	1.05 ± 0.12	0.24 ± 0.05

^a IC₅₀ ≤ 10 = good activity, 10 < IC₅₀ ≤ 30 = moderate activity, IC₅₀ > 100 = Inactive.

Computational chemistry was applied for understanding structure activity relationship (SAR). Figure 3.7 showed the comparison of molecular binding pose between Doxorubicin and all inhibitors. All compounds bound at the same site and lay on the protein surface. The binding region was found to be similar to that reported by Kongkathip.[22] Doxorubicin shows the most active compound against KB and HeLaS3. This is in accordance with the docking result which shows that it formed hydrogen bond (H-bond) with Arg99 (2.05 Å), Met101 (2.18 and 2.25 Å), Val103 (1.75 Å), Gly105 (1.68 Å), Ile130 (2.83 Å), and Asp515 (1.86 Å). Compound **3.1** exhibited lower activity than Doxorubicin. It still formed the H-bond with Ile130 with the distance of 1.99 Å. Moreover, oxygen atom of carbonyl group at C-1 formed H-bond with NH (backbone) of Lys129 at 1.92 Å, see Figure 3.8.

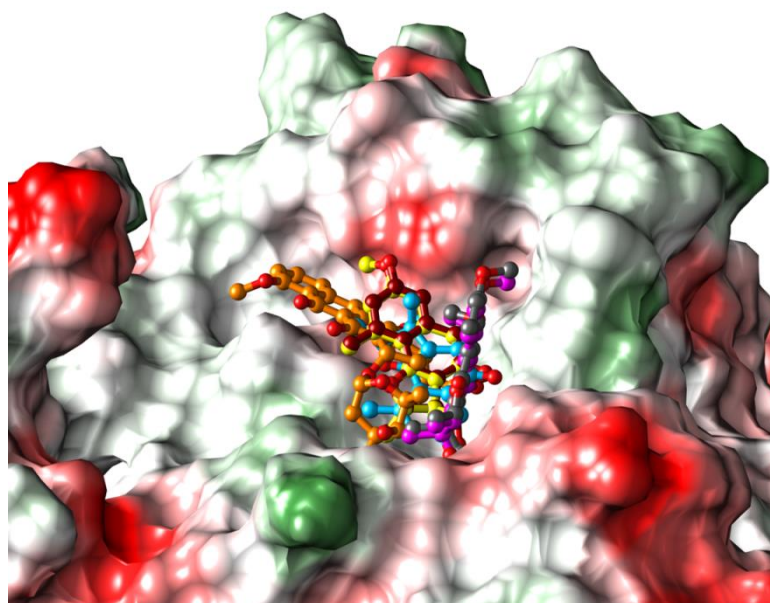


Figure 3.7 The superimposition of Doxorubicin (orange) and **3.1** (yellow), **3.2** (pink), **3.3** (gray), **3.4** (blue) and **3.5** (red). The figure is depicted by using the Chimera version 1.9 software[49]

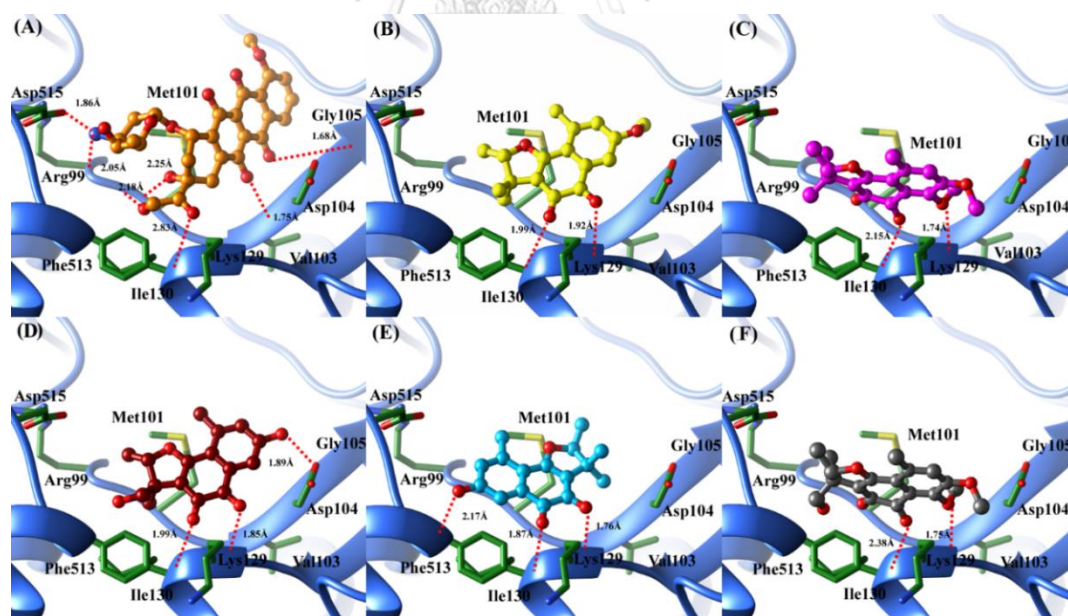


Figure 3.8 The Comparison of binding mode of Doxorubicin (A) and inhibitor **3.1** (B), **3.2** (C), **3.3** (D), **3.4** (E), and **3.5** (F). All inhibitors are shown as ball and stick while amino acids involved in H-bonding interaction are shown as green stick model. All figures are depicted by using the Chimera version 1.9 software[49]

Compounds **3.1** and **3.2** were different in the presence of methoxy substituent at position C-8 and their biological activity **3.1** and **3.2** formed equivalent hydrophobic interactions with Tyr100, Asp104, Ala128, and Phe513 and only **3.1** formed the hydrophobic interaction with Arg99, Met101 and Gly105. (Figure 3.9) The absence of methoxy substituent at C-8 caused the molecule deeper occupied and formed hydrophobic interactions with those amino acids.

The effect of methoxy substituent at C-7 was evaluated due to its activity against KB higher than **3.4** with a hydroxyl substituent. The comparison of molecular binding of **3.1** and **3.4** revealed that the methoxy substituent at C-7 of **3.1** formed hydrophobic interaction with Gly105 and the methyl substituent at C-5 formed hydrophobic interaction with Arg99, while **3.4** lacked this interaction. This is due to the smaller molecular volume of **3.4** in which the molecule can flip on the large pocket. The other three methyl substituents at C-2' and C-3' of **3.1** formed hydrophobic interactions with amino acid side chain of Tyr100, Met101 and Phe513. (Figure 3.10)

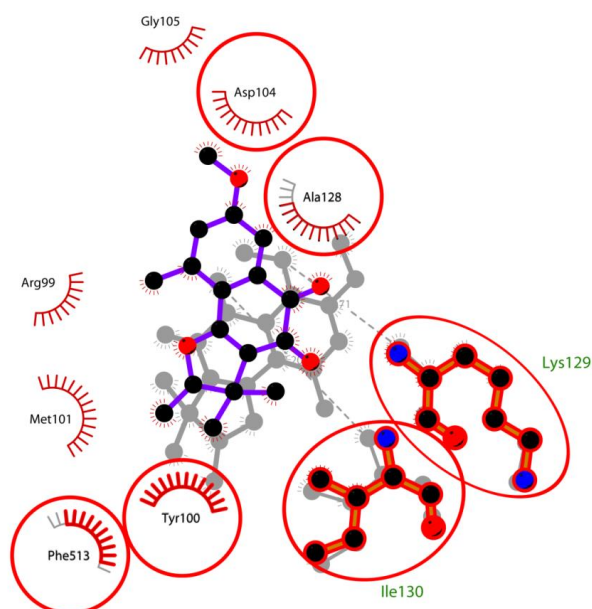


Figure 3.9 The hydrophobic interaction analysis. Compound **3.1** is shown in purple and **3.2** in gray. The red circles show equivalent amino acids involved for hydrophobic interaction[50]

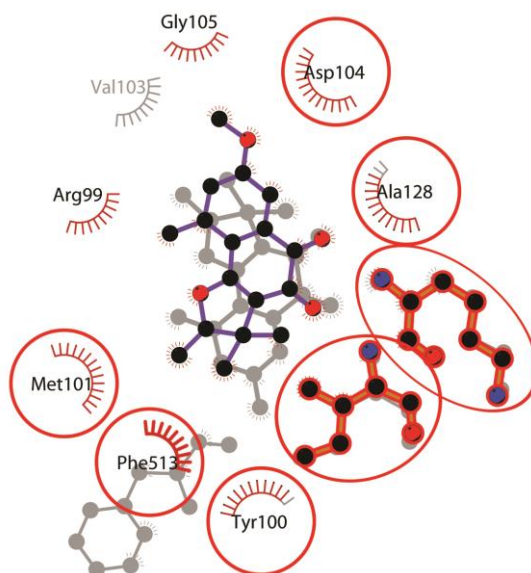


Figure 3.10 The hydrophobic interaction analysis. Compound **3.1** is shown in purple and **3.4** in gray. The red circles show equivalent amino acids involved for hydrophobic interaction[50]

3.4 Conclusion

A new compound, (-)-(2'S,3'S)-4-hydroxytryptethelone (**3.3**), three compounds with new absolute configuration (-)-2'S-tryptethelone methyl ether (**3.1**), (-)-2'S-8-methoxytryptethelone methyl ether (**3.2**), and (-)-(2'S,3'R)-4'-hydroxy-8-methoxytryptethelone methyl ether (**3.5**), along with the known compound, (-)-2'S-tryptethelone (**3.4**) were isolated from the cultured mycobiont of *M. cumingii*. Compound **3.1** showed selective inhibition against HeLaS3 and KB cell lines with IC_{50} of 5.15 ± 0.87 and $9.87 \pm 0.80 \mu\text{M}$, respectively. This compound also showed potent cytotoxicity towards HCT116 and A549 cell lines with IC_{50} of 0.32 ± 0.03 and $1.05 \pm 0.12 \mu\text{M}$, respectively.

CHAPTER IV
ISOLATION AND ELUCIDATION OF SECONDARY METABOLITES FROM CULTURED
MYCOBIONT *Trypethelium eluteriae* (Spreng.) AND EVALUATION OF ANTI-
ALZHEIMER ACTIVITY

4.1 Introduction

Trypethelium eluteriae is a crustose lichen (Figure 4.1) with bright yellow thallus belonging to the family Trypetheliaceae within the class Dothideomycetes. Their secondary metabolites [11, 12] from lichen include anthraquinones, xanthenes and pigments are most common substances. On the contrary, the cultured mycobiont *T. eluteriae* produced completely different compounds such as 1,2-naphthoquinones and phenalenones. [16, 17] Thus, this research aims to search for bioactive compounds with cytotoxicity activity. The report on amyloid-beta ($A\beta$) levels has been implicated in development of cancer and related on esophageal, colorectal, lung and hepatic cancers. $A\beta$ is the component of amyloid-beta peptide, aggregates in the brains of patients with Alzheimer's disease. Some reports suggest that flexible soluble oligomers of $A\beta$ molecules cause the development of Alzheimer's disease. Moreover, this cultured mycobiont has less studied in comparison with lichens, and no report on this activity. Therefore, those provide an insight for further investigation with potent *anti*-Alzheimer activity. [51-53]

Classification

Kingdom	Fungi
Phylum	Ascomycota
Class	Dothideomycetes
Order	Trypetheliales
Family	Trypetheliaceae
Genus	<i>Trypethelium</i>
Specific epithet	<i>eluteriae</i>

Synonym *Pseudopyrenula eluteriae* (Spreng.) Vain., *Botanical Magazine Tokyo* 35: 76 (1921)



Figure 4.1 *T. eluteriae*

4.2 Experimental

4.2.1 General experimental procedures

The NMR spectra were measured on a JEOL (400 MHz for ^1H NMR) spectrometers with TMS as internal standard. Chemical shifts are expressed in ppm with reference to the residual protonated solvent signals (chloroform- d_1 with δ_{H} 7.26). TLC was carried out on precoated silica gel plates (Merck Kieselgel 60 GF254, 0.25 nm thickness and spots were visualized by UV_{254nm}, UV_{365nm} lamp. Gravity column chromatography was performed with silica gel 60 (0.063–0.2 mm). Solvent used for isolation are *n*-hexane, chloroform, ethyl acetate, and methanol.

4.2.2 Cultivation

The ascospores of *T. eluteriae* mycobiont was successfully isolated from perithecia of lichen thallus by ascospore discharge technique and was observed on Water Agar (WA) for ascospore germination. The germinated spores were transferred to new Petri dish containing Malt-Yeast-Extract agar (Difco). The fungal culture is maintained in the lichen research unit at Ramkhamhaeng University, Thailand. The

mycobiont strain of *T. eluteriae* was cultivated on solid MYA in 80 Petri dishes and incubated at room temperature (30-32°C) for 9 weeks.

4.2.3 Extraction and isolation

The fungal biomass and mediawere separately extracted. The mycobiont colonies were extracted with acetone at room temperature to yield the crude extract (0.69 g). This crude extract was applied to normal phase silica gel column, eluted with the solvent system of chloroform:methanol (100:4) to afford 7 fractions **T1** (21 mg), **T2** (9 mg), **T3** (20 mg), **T4** (105 mg), **T5** (22 mg), **T6** (39 mg), and **T7** (212 mg). Fraction **T3** was applied to silica gel column, eluted with 100% chloroform, hexane:ethyl acetate (1:1), and purified by crystallizing in chloroform to give **4.1** (1.7 mg). Fraction **T4** was chromatographed, eluted with hexane:ethyl acetate (1:1), chloroform:methanol (100:1 – 100:4), then purified by preparative HPLC with chloroform:methanol (200:1) to afford compounds **4.2** (1.0 mg), **4.3** (0.5 mg), and **4.4** (3.0 mg).

4.2.4 Inhibitory activity of A β aggregation

The aggregation of Amyloid beta (A β) was evaluated using a slight modification of the thioflavin-T (Th-T) method developed by Naiki *et al.*[54] A β peptide was dissolved at 250 μ M in 0.02% NH₄OH. Sample solution (10 μ L) was diluted with 80 μ L of 50 mM sodium phosphate containing 100 mM NaCl at pH 7.4, then 10 μ L of peptide solution was added. All procedures were performed on ice. The mixture (25 μ M A β peptide and test sample in phosphate buffer solution) was incubated at 37 °C for 24 h, then diluted with 300 μ L 5 μ M Th-T in 50 mM Gly-NaOH, pH 8.5. The solution was transferred to black bottom 96-well plates at 100 μ L per well and then gently vortexed for 30 min. Fluorescence intensity was measured at excitation and emission wavelengths of 440 nm and 485 nm using a Synergy HTX Multi-Mode Reader. The aggregation of A β was calculated by comparing the fluorescence intensity of each sample with that of a control (A β and DMSO containing no test sample). Myricetin was used as a positive control and the final concentration of all samples was 10, 20 and 40 μ M, respectively. The experiment proceeded under the supervision of Associate Professor. Dr. Kaoru Kinoshita.

4.3 Results and discussion

4.3.1 Physical and spectroscopic data of isolated compounds

(+)-*sclerodin* (**4.1**): yellow crystalline solid (1.7 mg); $[\alpha]_D^{25} +48$ (c 1.34), CD (c 0.1 mg/mL, MeOH), $\lambda_{max}(\Delta\epsilon)$ 350 nm (+0.4), 296 nm (+0.7), $^1\text{H NMR}$ (CDCl_3) see Table 4.1.

(+)-*bipolaride D* (**4.2**): orange crystalline solid (1.0 mg); $[\alpha]_D^{25} +87$ (c 0.07), CD (c 0.02 mg/mL, MeOH), $\lambda_{max}(\Delta\epsilon)$ 350 nm (+1.4), 296 nm (+2.0), $^1\text{H NMR}$ (CDCl_3) see Table 4.1.

trypethelone (**4.3**): violet amorphous solid (0.5 mg); $^1\text{H NMR}$ (CDCl_3) see Table 4.2.

8-hydroxy-7-methoxytrypethelone (**4.4**): dark red crystalline solid (3.0 mg); $^1\text{H NMR}$ (CDCl_3) see Table 4.2.

Phenalenone and naphthoquinones derivatives were isolated from the acetone extract of this cultured mycobiont, including (+)-*sclerodin* (**4.1**), (+)-*bipolaride D* (**4.2**), *trypethelone* (**4.3**) and *8-hydroxy-7-methoxytrypethelone* (**4.4**) as shown in Figure 4.2.

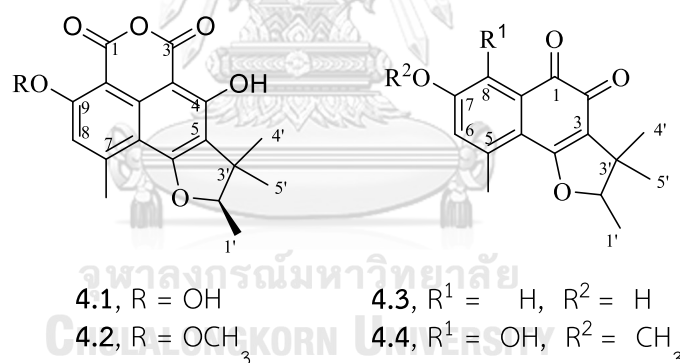


Figure 4.2 Chemical structures of **4.1-4.4**

Secondary metabolites from *T. eluteriae* mycobiont were elucidated with $^1\text{H NMR}$ spectroscopic method and circular dichroism (CD) spectra depended on their amount and confirmed by comparison of their NMR spectroscopic data with previously literatures as follows.

Compound **4.1** was obtained as a yellow crystalline solid. The $^1\text{H NMR}$ spectrum (Table 4.1) consisted of signal for an aromatic proton at δ_{H} 6.85 (1H, *d*, $J = 0.9$ Hz, H-8); four methyl groups at δ_{H} 1.49 (3H, *d*, $J = 6.6$ Hz, H-1'), 1.54 (3H, *s*, H-4'),

1.31 (3H, *s*, H-5'), 2.82 (3H, *d*, $J = 0.9$ Hz, 7-CH₃); one oxygenated methine at δ_{H} 4.70 (1H, *q*, $J = 6.6$ Hz, H-2') and two hydroxyl protons at δ_{H} 11.63 (1H, *s*, 4-OH), 11.43 (1H, *s*, 9-OH). Based on the ¹H NMR spectrum of (–)-sclerodin,[55] showing the same planar structure. As the result of **4.1** had $[\alpha]_{\text{D}}^{25} +48$ as dextrorotatory compound compared with $[\alpha]_{\text{D}}^{25} -72.6$ of (–)-sclerodin and confirmed the positive CE at $\lambda_{\text{max}}(\Delta\varepsilon)$ 350 nm (+0.4), 296 nm (+0.7), indicating the 2'*R* configuration of **4.1**. Therefore, **4.1** was assigned as (+)2'*R*-sclerodin.¹⁶

Table 4.1 ¹H NMR data of **4.1**, **4.2**, δ_{H} (ppm), (multi, J in Hz)

position	4.1 ^a	4.2 ^a
8	6.85 (<i>d</i> , 0.9)	6.90 (<i>s</i>)
1'	1.49 (<i>d</i> , 6.6)	1.49 (<i>d</i> , 6.6)
2'	4.70 (<i>q</i> , 6.6)	4.70 (<i>q</i> , 6.6)
4'	1.54 (<i>s</i>)	1.54 (<i>s</i>)
5'	1.31 (<i>s</i>)	1.31 (<i>s</i>)
7-CH ₃	2.82 (<i>d</i> , 0.9)	2.88 (<i>s</i>)
4-OH	11.63 (<i>s</i>)	12.28 (<i>s</i>)
9-OH	11.43 (<i>s</i>)	
9-OCH ₃		4.13 (<i>s</i>)

Spectra were recorded in ^a CDCl₃

Table 4.2 ^1H NMR data of 4.3, 4.4, δ_{H} (ppm), (multi, J in Hz)

position	4.3 ^a	4.4 ^a
6	6.87 (<i>d</i> , 2.3)	6.71 (<i>s</i>)
8	7.46 (<i>d</i> , 2.5)	
1'	1.45 (<i>d</i> , 6.6)	1.44 (<i>d</i> , 6.9)
2'	4.63 (<i>q</i> , 6.6)	4.61 (<i>q</i> , 6.6)
4'	1.44 (<i>s</i>)	1.44 (<i>s</i>)
5'	1.25 (<i>s</i>)	1.25 (<i>s</i>)
5-CH ₃	2.57 (<i>s</i>)	2.55 (<i>s</i>)
7-OCH ₃		3.95 (<i>s</i>)
8-OH		13.16 (<i>s</i>)

Spectra were recorded in ^a CDCl₃

Compound **4.2** was isolated as orange crystalline solid. The ^1H NMR spectrum (Table 4.1) showed the signal almost the same with that of **4.1** except an additional methoxy group instead of a hydroxyl group as follows: an aromatic proton at δ_{H} 6.90 (1H, *s*, H-8); four methyl groups at δ_{H} 1.49 (3H, *d*, $J = 6.6$ Hz, H-1'), 1.54 (3H, *s*, H-4'), 1.31 (3H, *s*, H-5'), 2.88 (3H, *s*, 7-CH₃); one oxygenated methine at δ_{H} 4.70 (1H, *q*, $J = 6.6$ Hz, H-2'); one hydroxyl proton at δ_{H} 12.28 (1H, *s*, 4-OH) and a methoxy group at δ_{H} 4.13 (3H, *s*, 9-OCH₃). Accordingly, **4.2** had $[\alpha]_{\text{D}}^{25} +87$ as dextrorotatory specific rotation with a positive CE at $\lambda_{\text{max}}(\Delta\epsilon)$ 350 nm (+0.4), 296 nm (+2.0) and compared with (-)-bipolaride D⁴² that reported $[\alpha]_{\text{D}}^{25} -55$, resulting as 2'*R* configuration of **4.2**. Thus, **4.2** was indicated as the (+)2'*R*-bipolaride D.

Trypethelone (**4.3**), a well-known compound was obtained as violet amorphous solid. **4.3** was assigned by its NMR spectroscopic data, comparison with literatures.[48, 56]

Compound **4.4** was isolated as a dark red crystalline solid. Based on the ^1H NMR spectrum (Table 4.2), the signal was observed an aromatic proton at δ_{H} 6.71 (1H, *s*, H-6); four methyl groups at δ_{H} 1.44 (3H, *d*, $J = 6.9$ Hz, H-1'), 1.44 (3H, *s*, H-4'), 1.25 (3H, *s*, H-5'), 2.55 (3H, *s*, 5-CH₃); one oxygenated methine at δ_{H} 4.61 (1H, *q*, $J = 6.6$ Hz, H-2');

one hydroxyl proton at δ_{H} 13.16 (1H, s, 8-OH) and a methoxy group at δ_{H} 3.95 (3H, s, 7-OCH₃). In addition **4.4** was elucidated by comparison with (+)-8-hydroxy-7-methoxytryptelone,[17] indicating as 8-hydroxy-7-methoxytryptelone.

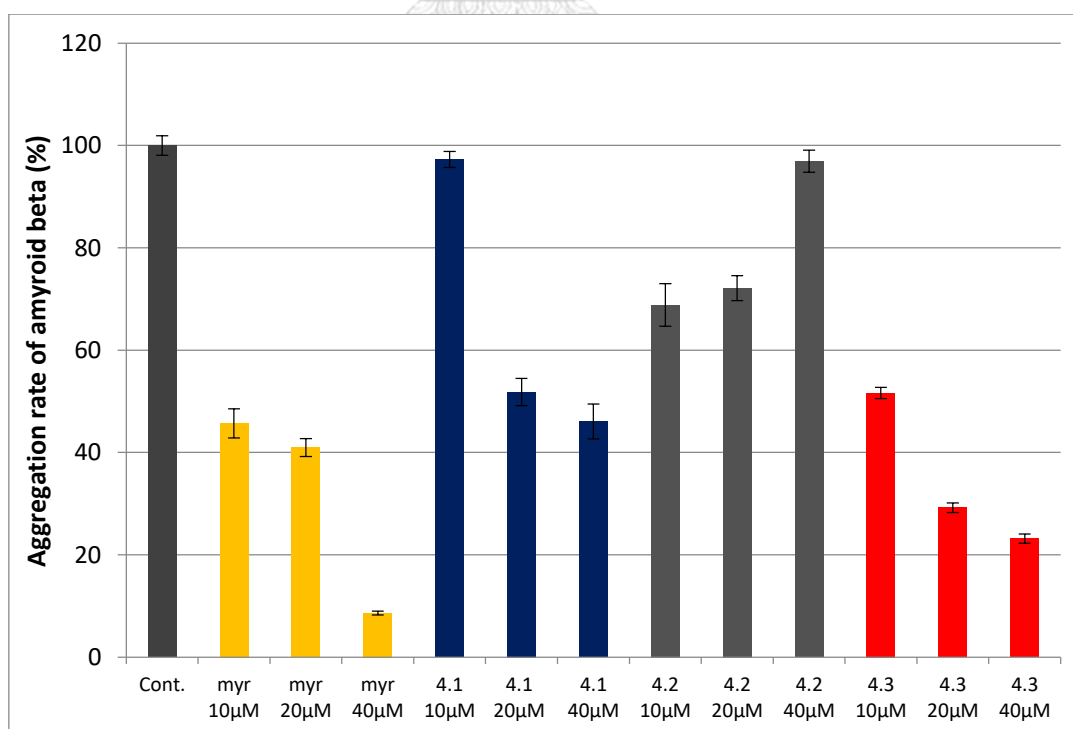
Alzheimer's disease destroys brain function, especially in the hippocampus, and is a social problem worldwide. A major pathogenesis of AD is related to the accumulation of amyloid beta (A β) peptides, resulting in neuronal cell death in the brain.

The inhibitory activities of A β aggregation by **4.1**, **4.2** and **4.4** were examined using the Th-T method. The degree of A β aggregation (the concentration of all samples was 10, 20 and 40 μM , respectively) caused by myricetin (myr), **4.1** and **4.4** was shown in Table 4.3. Data are expressed as the degree of A β aggregation compared with the control as mean \pm SD (n = 3). These results are shown in Figure 4.3.

As the results, **4.1** and **4.4** showed inhibitory effect of A β aggregation with IC₅₀ 30.4, and 9.9 μM , respectively compared with myricetin (positive control). The accumulation of A β peptide is related to the Alzheimer's disease, which is widely considered to be the major toxic agent. Thus **4.4** has potent against the occurring of plaques which relate to the generation of neurofibrillary tangles causing neural damage.

Table 4.3 Inhibitory activity of A β aggregation of sample

sample	Aggregation rate of amyloid beta (%)	SD
Cont.	100	1.92
myr 10 μ M	45.70	2.83
myr 20 μ M	40.97	1.74
myr 40 μ M	8.62	0.39
4.1 10 μ M	97.28	1.57
4.1 20 μ M	51.81	2.66
4.1 40 μ M	46.05	3.41
4.2 10 μ M	68.83	4.15
4.2 20 μ M	72.12	2.42
4.2 40 μ M	96.91	2.15
4.4 10 μ M	51.66	1.10
4.4 20 μ M	29.20	0.92
4 40 μ M	23.18	0.92

Figure 4.3 Inhibitory activity of A β aggregation. "Cont." indicates the control group

(25 μM $\text{A}\beta$ treated with no samples). “myr” indicates the group in which 10, 20, 40 μM $\text{A}\beta$ treated with myricetin. “**4.1, 4.2, 4.4**” indicates the group in which 10, 20, 40 μM $\text{A}\beta$ treated with each sample. Results are shown as mean \pm SD (n = 3)

4.4 Conclusion

A compound with new absolute configuration: (+)-bipolaride D (**4.2**), and three known compounds: (+)-sclerodin (**4.1**), tryptethelone (**4.3**), and 8-hydroxy-7-methoxytryptethelone (**4.4**) were isolated from cultured mycobiont *T. eluteriae*. Compound **4.4** revealed potential activity against β -amyloid aggregation with IC_{50} 9.9 μM .



REFERENCES

- [1] Huneck, S. New results on the chemistry of lichen substances. Prog. Chem. Org. Nat. Prod. 81 (2001): 1-276.
- [2] Huneck, S. The Significance of Lichens and Their Metabolites. Naturwissenschaften 86(12) (1999): 559-570.
- [3] Huneck, S. and Yoshimura, I. Identification of Lichen Substances. in Huneck, S. and Yoshimura, I. (eds.), Identification of Lichen Substances, pp. 11-123. Berlin, Heidelberg: Springer Berlin Heidelberg, 1996.
- [4] Ranković, B. Lichen Secondary Metabolites: Bioactive Properties and Pharmaceutical Potential. Springer International Publishing, 2014.
- [5] Brodo, I.M., et al. Lichens of North America. Yale University Press, 2001.
- [6] Aptroot, A. and LÜcking, R. A revisionary synopsis of the Trypetheliaceae (Ascomycota: Trypetheliales). The Lichenologist 48(6) (2016): 763-982.
- [7] Nelsen, M.P., et al. Elucidating phylogenetic relationships and genus-level classification within the fungal family Trypetheliaceae (Ascomycota: Dothideomycetes). Taxon 63(5) (2014): 974-992.
- [8] Buaruang, K., et al. A new checklist of lichenized fungi occurring in Thailand. MycKeys 23 (2017): 1-91.
- [9] Vongshewarat, K. Study on Taxonomy and Ecology of the Lichens Family Trypetheliaceae in Thailand. M.Sc. Thesis. Department of Biology, Ramkhamhaeng University, Bangkok, 2000.
- [10] Stensiö, K.E. and Wachtmeister, C.A. 1,5-8-trihydroxy-6-methoxy-3-methylantraquinone from *Laurera purpurina* (Nyl.) Zahlbr. Acta chemica Scandinavica 23(1) (1969): 144-148.
- [11] Santesson, J. Some occurrences of the anthraquinone parietin in lichens. Phytochemistry 9(7) (1970): 1565-1567.
- [12] Mathey, A., Spiteller, P., and Steglich, W. Draculone, a new anthraquinone pigment from the tropical lichen *Melanotheca cruenta*. Z Naturforsch C 57(7-8) (2002): 565-7.

- [13] Manojlovic, N.T., Markovic, Z.S., Gritsanapan, W., and Boonpragob, K. High-performance liquid chromatographic analysis of anthraquinone compounds in the *Laurera benguelensis*. Russ. J. Phys. Chem. A 83(9) (2009): 1554-1557.
- [14] Manojlovic, N.T., Vasiljevic, P.J., Gritsanapan, W., Supabphol, R., and Manojlovic, I. Phytochemical and antioxidant studies of *Laurera benguelensis* growing in Thailand. Biol. Res. 43(2) (2010): 169-176.
- [15] Manojlovic, N.T., Vasiljevic, P.J., and Markovic, Z.S. Antimicrobial activity of extracts and various fractions of chloroform extract from the lichen *Laurera benguelensis*. J. Biol. Res.-Thessalon 13 (2010): 27-34.
- [16] Mathey, A., Steffan, B., and Steglich, W. 1,2-Naphthochinon-Derivate aus Kulturen des Mycosymbionten der Flechte *Trypethelium eluteriae* (Trypetheliaceae). Liebigs Ann. Chem. (1980): 779-785.
- [17] Takenaka, Y., Naito, Y., Le, D.H., Hamada, N., and Tanahashi, T. Naphthoquinones and phenalenone derivatives from the cultured lichen mycobionts of *Trypethelium sp.* Heterocycles 87(9) (2013): 1897-1902.
- [18] Cohen, P.A., Hudson, J.B., and Towers, G.H. Antiviral activities of anthraquinones, bianthrone and hypericin derivatives from lichens. Experientia 52(2) (1996): 180-3.
- [19] Rankovic, B., Rankovic, D., and Maric, D. Antioxidant and antimicrobial activity of some lichen species. Mikrobiologija 79(6) (2010): 812-8.
- [20] Nguyen, K.H., Chollet-Krugler, M., Gouault, N., and Tomasi, S. UV-protectant metabolites from lichens and their symbiotic partners. Nat Prod Rep 30(12) (2013): 1490-508.
- [21] Shrestha, G. and Clair, L. Lichens: A promising source of antibiotic and anticancer drugs. Vol. 12, 2013.
- [22] Kongkathip, N., et al. Potent antitumor activity of synthetic 1,2-Naphthoquinones and 1,4-Naphthoquinones. Bioorg. Med. Chem. 11(14) (2003): 3179-3191.
- [23] Guo, S., Feng, B., Zhu, R., Ma, J., and Wang, W. Preparative isolation of three anthraquinones from *Rumex japonicus* by high-speed counter-current chromatography. Molecules 16 (2011): 1201-1210.

- [24] Intaraudom, C., et al. Phenalenone derivatives and the unusual tricyclic sesterterpene acid from the marine fungus *Lophiostoma bipolare* BCC25910. Phytochemistry 120 (2015): 19-27.
- [25] Tanahashi, T., Takenaka, Y., Ikuta, Y., Tani, K., Nagakura, N., and Hamada, N. Xanthonones from the cultured lichen mycobionts of *Pyrenula japonica* and *Pyrenula pseudobufonia*. Phytochemistry 52(3) (1999): 401-405.
- [26] Takenaka, Y., Tanahashi, T., Nagakura, N., Itoh, A., and Hamada, N. Three isocoumarins and a benzofuran from the cultured lichen mycobionts of *Pyrenula* sp. Phytochemistry 65(23) (2004): 3119-3123.
- [27] Lin, S.-Y., et al. Emodin induces apoptosis of human tongue squamous cancer SCC-4 cells through reactive oxygen species and mitochondria-dependent pathways. Anticancer Res. 29(1) (2009): 327-335.
- [28] Jo, G., et al. A compound isolated from *Rumex japonicus* induces early growth response gene-1 expression. J. Korean Soc. Appl. Biol. Chem. 54(4) (2011): 637-643.
- [29] Boustie, J., Tomasi, S., and Grube, M. Bioactive lichen metabolites: Alpine habitats as an untapped source. Phytochem. Rev. 10(3) (2011): 287-307.
- [30] Brandao, L.F.G., et al. Cytotoxic evaluation of phenolic compounds from lichens against melanoma cells. Chem. Pharm. Bull. 61(2) (2013): 176-183.
- [31] Le Pogam, P. and Boustie, J. Xanthonones of lichen source: a 2016 update. Molecules 21(3) (2016): 21/1-21/30.
- [32] Takenaka, Y., Mizushima, Y., Hamada, N., and Tanahashi, T. A cytotoxic pyranonaphthoquinone from cultured lichen mycobionts of *Haematomma* sp. Heterocycles 94(9) (2017): 1728-1735.
- [33] Sangvichien, E., Hawksworth, D.L., and Whalley, A.J.S. Ascospore discharge, germination and culture of fungal partners of tropical lichens, including the use of a novel culture technique. IMA fungus (2) (2011): 143-153.
- [34] Cubero, O.F. and Crespo, A. Isolation of Nucleic Acids From Lichens. Protocols in Lichenology, Culturing, Biochemistry, Ecophysiology and Use in Biomonitoring, ed. Kranner, I.C., Beckett, R.P., and Varma, A.K.: Springer, Berlin, Heidelberg, 2002.

- [35] Vilgalys, R. and Hester, M. Rapid genetic identification and mapping of enzymatically amplified ribosomal DNA from several *Cryptococcus* species. J. Bacteriol 172(8) (1990): 4238-4246.
- [36] Zoller, S., Scheidegger, C., and Sperisen, C. Pcr Primers for the Amplification of Mitochondrial Small Subunit Ribosomal DNA of Lichen-forming Ascomycetes. lichenologist 31 (1999): 511-516.
- [37] Zhou, S. and Stanosz, G.R. Primers for amplification of mt SSU rDNA, and a phylogenetic study of Botryosphaeria and associated anamorphic fungi. Mycol. Res. 105(9) (2001): 1033-1044.
- [38] Luangsuphabool, T., Lumbsch, H.T., Aptroot, A., Piapukiew, J., and Sangvichien, E. Five new species and one new record of *Astrothelium* (Trypetheliaceae, Ascomycota) from Thailand. lichenologist 48 (2016): 727-737.
- [39] Bruker. APEX2 Version 2014.9-0. Madison. WI: Bruker AXS Inc., 2014.
- [40] Bruker. SHELXTL XT, Program for crystal structure solution, v. 2014/4. Madison. WI: Bruker AXS Inc., 2014.
- [41] Bruker. SHELXTL XLMP, Program for crystal structure refinement – Multi-CPU, v. 2014/7. Madison. WI: Bruker AXS Inc., 2014.
- [42] Parsons, S., Flack, H.D., and Wagner, T. Use of intensity quotients and differences in absolute structure refinement. Acta Crystallogr., Sect. B: Struct. Sci., Cryst. Eng. Mater. 69(3) (2013): 249-259.
- [43] Morais Cabral, J.H., Jackson, A.P., Smith, C.V., Shikotra, N., Maxwell, A., and Liddington, R.C. Crystal structure of the breakage-reunion domain of DNA gyrase. Nature (London) 388(6645) (1997): 903-906.
- [44] Morris, G.M., et al. AutoDock and AutoDockTools: Automated docking with selective receptor flexibility. J. Comput. Chem. 30(16) (2009): 2785-2791.
- [45] Stewart, J.J.P. Stewart Computational Chemistry. Colorado Springs, 2009.
- [46] Bikadi, Z. and Hazai, E. Application of the PM6 semi-empirical method to modeling proteins enhances docking accuracy of AutoDock. J.Cheminform 1 (2009): 15.

- [47] Sun, L.Y., Liu, Z.L., Zhang, T., Niu, S.B., and Zhao, Z.T. Three antibacterial naphthoquinone analogues from cultured mycobiont of lichen *Astrothelium* sp. Chin. Chem. Lett. 21(7) (2010): 842-845.
- [48] Elsebai, M.F., et al. HLE-inhibitory alkaloids with a polyketide skeleton from the marine-derived fungus *Coniothyrium cereale*. J. Nat. Prod. 74(10) (2011): 2282-2285.
- [49] Pettersen, E.F., et al. UCSF Chimera-A visualization system for exploratory research and analysis. J. Comput. Chem. 25(13) (2004): 1605-1612.
- [50] Laskowski, R.A. and Swindells, M.B. LigPlot+: Multiple Ligand-Protein Interaction Diagrams for Drug Discovery. J. Chem. Inf. Model. 51(10) (2011): 2778-2786.
- [51] Jin, W.-S., et al. Plasma Amyloid-Beta Levels in Patients with Different Types of Cancer. Neurotoxicity Research 31(2) (2017): 283-288.
- [52] Yang, H.J., et al. Fermenting soybeans with *Bacillus licheniformis* potentiates their capacity to improve cognitive function and glucose homeostasis in diabetic rats with experimental Alzheimer's type dementia. Eur. J. Nutr. 54(1) (2015): 77-88.
- [53] Luo, H., et al. Biruloquinone, an acetylcholinesterase inhibitor produced by lichen-forming fungus *Cladonia macilenta*. J. Microbiol. Biotechnol. 23(2) (2013): 161-166.
- [54] Naiki, H. and Gejyo, F. Kinetic analysis of amyloid fibril formation. Methods Enzymol. 309(Amyloid, Prions, and Other Protein Aggregates) (1999): 305-318.
- [55] Ayer, W.A., Hoyano, Y., Soledade Pedras, M., and Van Altena, I. Metabolites produced by the *Scleroderris canker* fungus, *Gremmeniella abietina*. Part 1. Can. J. Chem. 64(8) (1986): 1585-9.
- [56] Ayer, W.A., Kamada, M., and Ma, Y.T. Sclerodin and related compounds from a plant disease causing fungus. *Scleroderris* yellow. Can. J. Chem. 67(12) (1989): 2089-94.



APPENDIX

จุฬาลงกรณ์มหาวิทยาลัย
CHULALONGKORN UNIVERSITY

CONTENT OF SUPPORING INFORMATION

Chapter II Chemical diversity of lichens and cultured mycobionts

No.	Content	Page
S2.1	Specimens and study sites data	53
S2.2	HPLC chromatograms of <i>M. cumingii</i>	59
S2.3	¹ H NMR spectrum of 2.2 in CDCl ₃	60
S2.4	Mass spectrum of 2.4 (ESI)	60
S2.5	¹ H NMR spectrum of 2.4 in Acetone- <i>d</i> ₆	61
S2.6	¹ H NMR spectrum of 2.5 in Acetone- <i>d</i> ₆	61
S2.7	¹ H NMR spectrum of 2.6 in CDCl ₃	62
S2.8	¹ H NMR spectrum of 2.7 in CDCl ₃	62
S2.9	¹³ C NMR spectrum of 2.7 in CDCl ₃	63
S2.10	¹ H NMR spectrum of 2.8 in Acetone- <i>d</i> ₆	63

Chapter II Naphthoquinones from cultured mycobiont of *Marcelaria cumingii* (Mont.) and their cytotoxicity

No.	Content	Page
S3.1	HRESIMS spectrum of 3.1	64
S3.2	¹ H NMR spectrum of 3.1 in CDCl ₃	65
S3.3	¹³ C NMR spectrum of 3.1 in CDCl ₃	65
S3.4	COSY spectrum of 3.1 in CDCl ₃	66
S3.5	HSQC spectrum of 3.1 in CDCl ₃	66
S3.6	HMBC spectrum of 3.1 in CDCl ₃	67
S3.7	HRESIMS spectrum of 3.2	68
S3.8	¹ H NMR spectrum of 3.2 in CDCl ₃	69
S3.9	¹³ C NMR spectrum of 3.2 in CDCl ₃	69
S3.10	COSY spectrum of 3.2 in CDCl ₃	70
S3.11	HSQC spectrum of 3.2 in CDCl ₃	70
S3.12	HMBC spectrum of 3.2 in CDCl ₃	71

S3.13	NOESY spectrum of 3.2 in CDCl ₃	71
S3.14	HRESIMS spectrum of 3.3	72
S3.15	¹ H NMR spectrum of 3.3 in DMSO- <i>d</i> ₆	73
S3.16	¹³ C NMR spectrum of 3.3 in DMSO- <i>d</i> ₆	73
S3.17	HSQC spectrum of 3.3 in DMSO- <i>d</i> ₆	74
S3.18	HMBC spectrum of 3.3 in DMSO- <i>d</i> ₆	74
S3.19	¹ H NMR spectrum of 3.3 in Acetone- <i>d</i> ₆	75
S3.20	NOESY spectrum of 3.3 in Acetone- <i>d</i> ₆	75
S3.21	HRESIMS spectrum of 3.4	76
S3.22	¹ H NMR spectrum of 3.4 in DMSO- <i>d</i> ₆	77
S3.23	¹³ C, NMR spectrum of 3.4 in DMSO- <i>d</i> ₆	77
S3.24	HRESIMS spectrum of 3.5	78
S3.25	¹ H NMR spectrum of 3.5 in CDCl ₃	79
S3.26	¹³ C NMR spectrum of 3.5 in CDCl ₃	79
S3.27	COSY spectrum of 3.5 in CDCl ₃	80
S3.28	HSQC spectrum of 3.5 in CDCl ₃	80
S3.29	HMBC spectrum of 3.5 in CDCl ₃	81
S3.30	NOESY spectrum of 3.5 in CDCl ₃	81
S3.31	CD spectrum (methanol) of 3.1	82
S3.32	CD spectrum (methanol) of 3.2	82
S3.33	CD spectrum (methanol) of 3.3	83
S3.34	CD spectrum (methanol) of 3.4	83
S3.35	CD spectrum (methanol) of 3.5	84

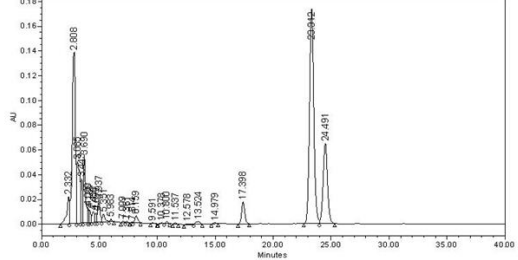
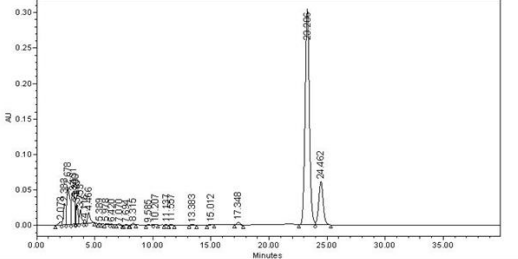
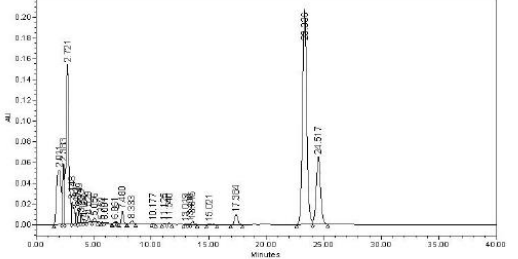
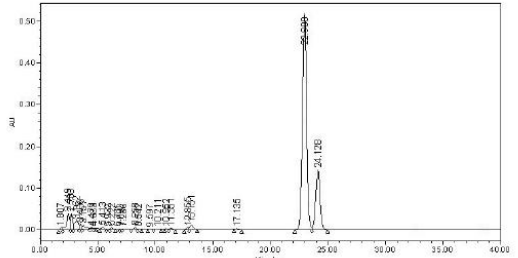
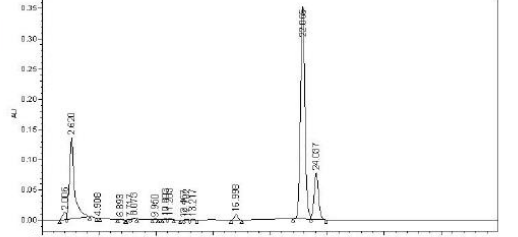
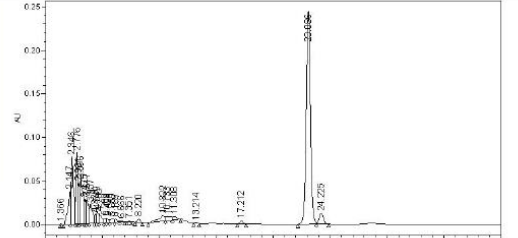
Chapter IV Isolation and elucidation of secondary metabolites from cultured mycobiont *Trypethelium eluteriae* (Spreng.) and evaluation of *anti*-Alzheimer activity

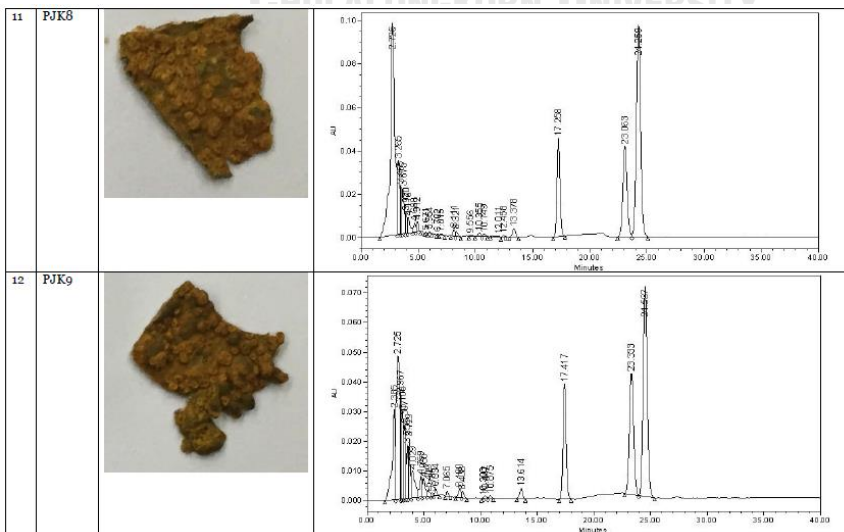
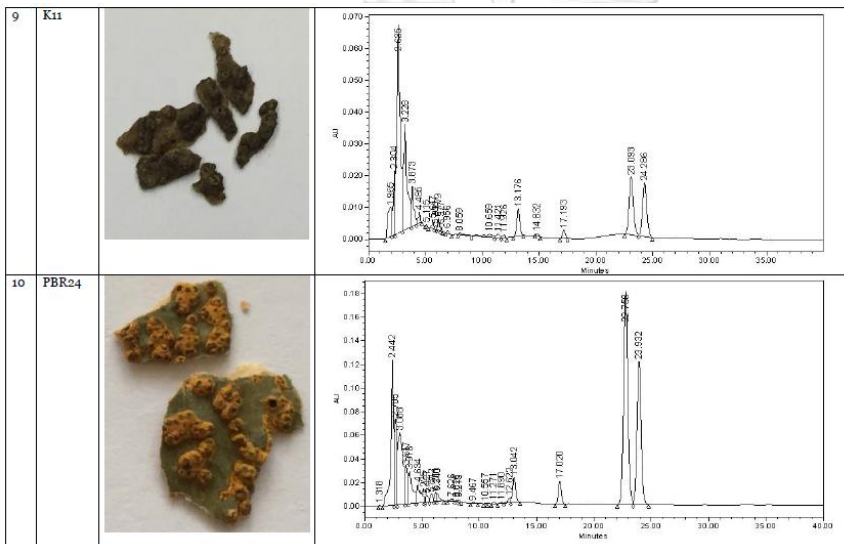
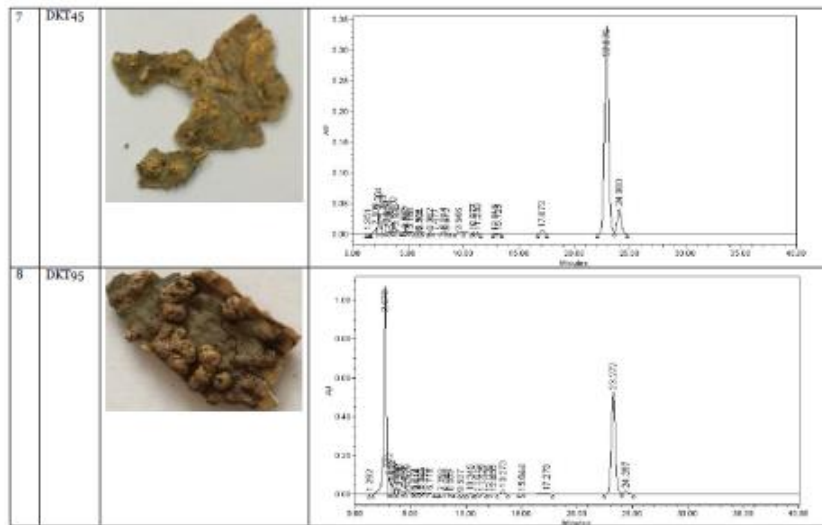
No.	Content	Page
S4.1	^1H NMR spectrum of 4.1 in CDCl_3	84
S4.2	^1H NMR spectrum of 4.2 in CDCl_3	85
S4.3	^1H NMR spectrum of 4.3 in CDCl_3	85
S4.4	^1H NMR spectrum of 4.4 in CDCl_3	86

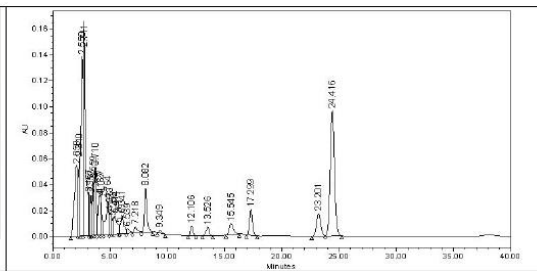
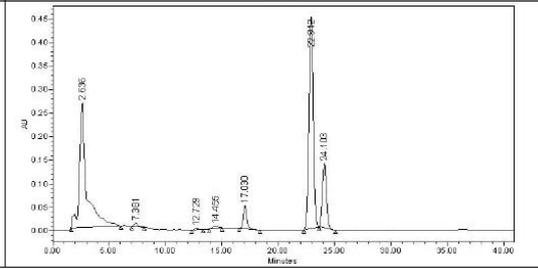
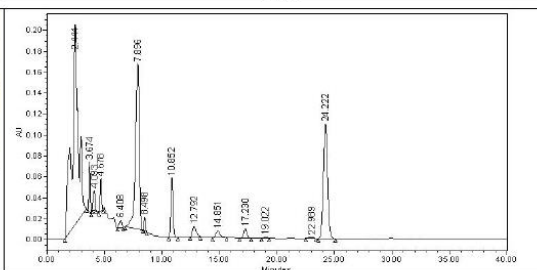
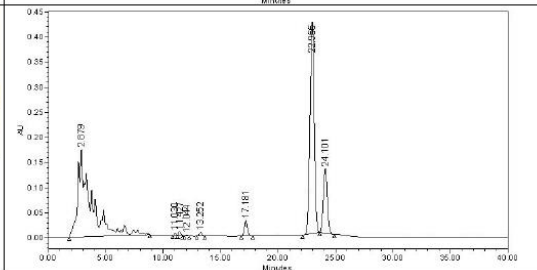
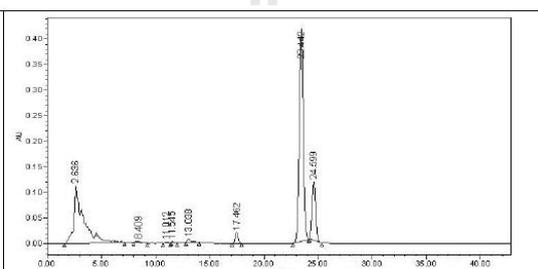
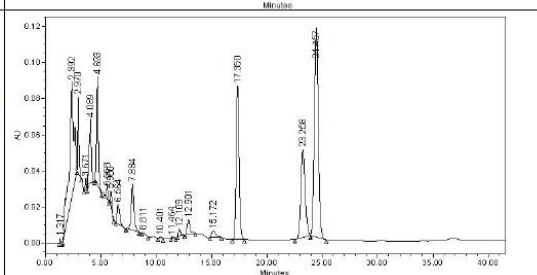


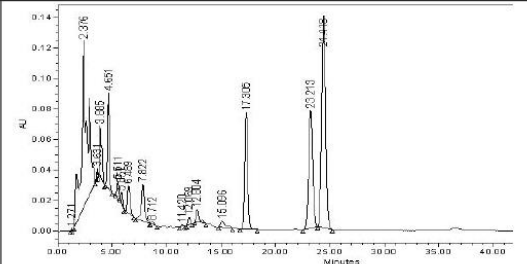
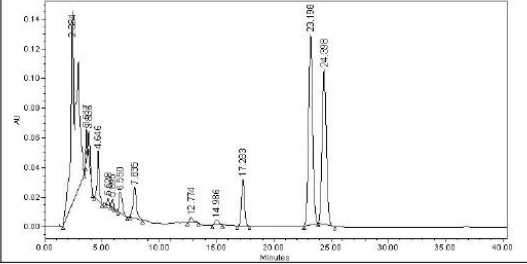
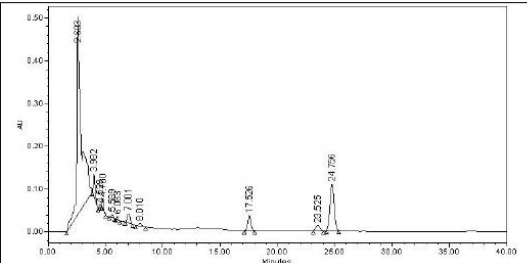
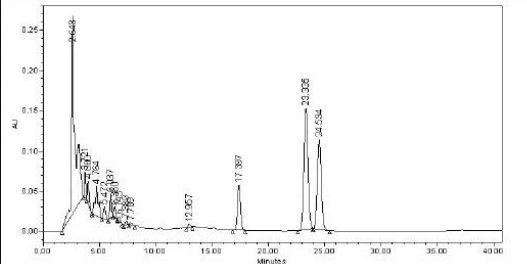
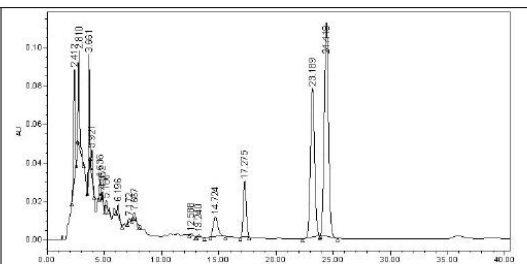
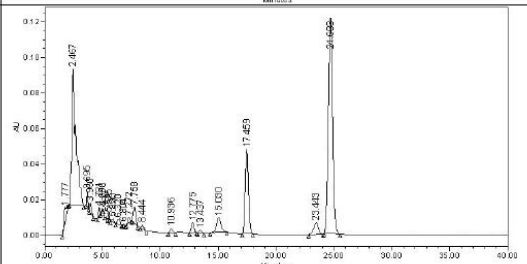
Specimens	Study sites
CM192	Hang Dong, Chiang Mai
DCD3	Doi Chiang Dao, Chiang Mai
DCD4	
DCD7	
DKT30	Doi KhuTan, Lamphun
DKT36	
DKT45	
DKT95	
K11	Khao Yai National Park, Nakhonratchasima
PBR24	Cha-am, Phetchaburi
PJK8	Hua Hin, Prachup Khiri Khan
PJK9	
PL126	Wang Thong, Phitsanulok
RAT43	Queen Sirikit Forest Park, Ratchaburi
RAT50	
RAT57	
RAT60	
RAT65	
RAT66	
RAT70	
RAT200	Suan Phueng, Ratchaburi
RAT248	
RAT263	Natural Science Park, Ratchaburi
RAT270	
RAT346	
RAT359	
RN104	Ngao Waterfall National Park, Ranong
SMS	Samaesan Island, Chon Buri
SNK8	Nam Phung ,Sakon Nakhon
SNK36	
SNK39	
TSL28	Thung Salaeng Luang National Park, Phitsanulok
UBN13	Chong Mek, Sirindhorn, Ubon Ratchathani
UBN158	Non Ko, Sirindhorn, Ubon Ratchathani

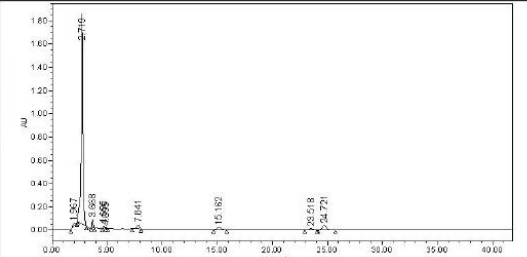
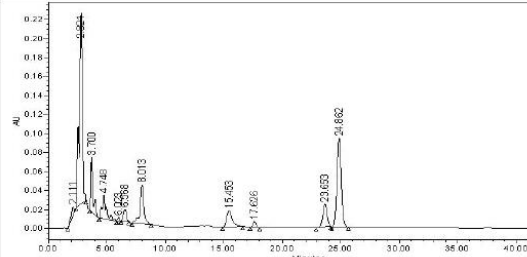
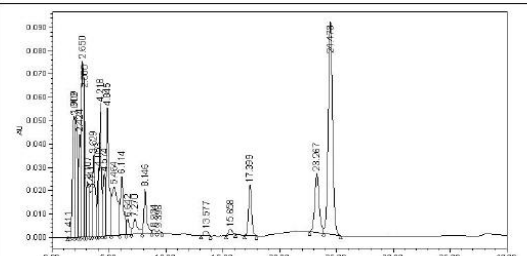
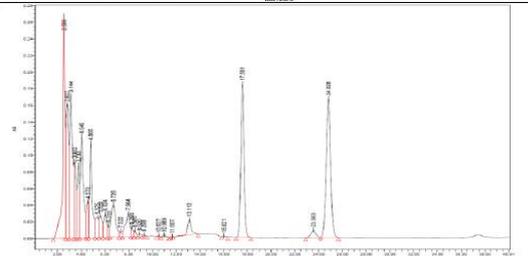
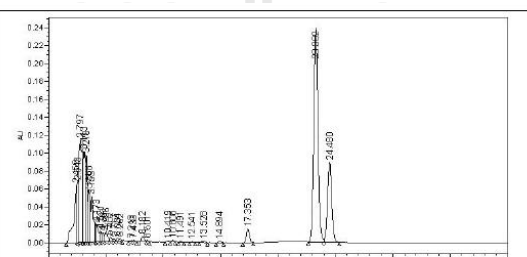
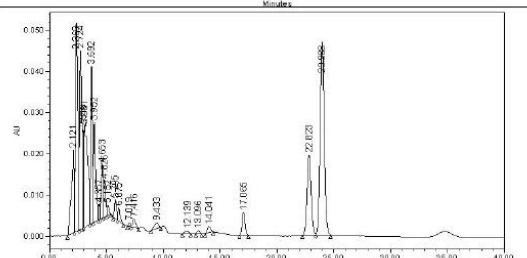
S2.1 Specimens and study sites data

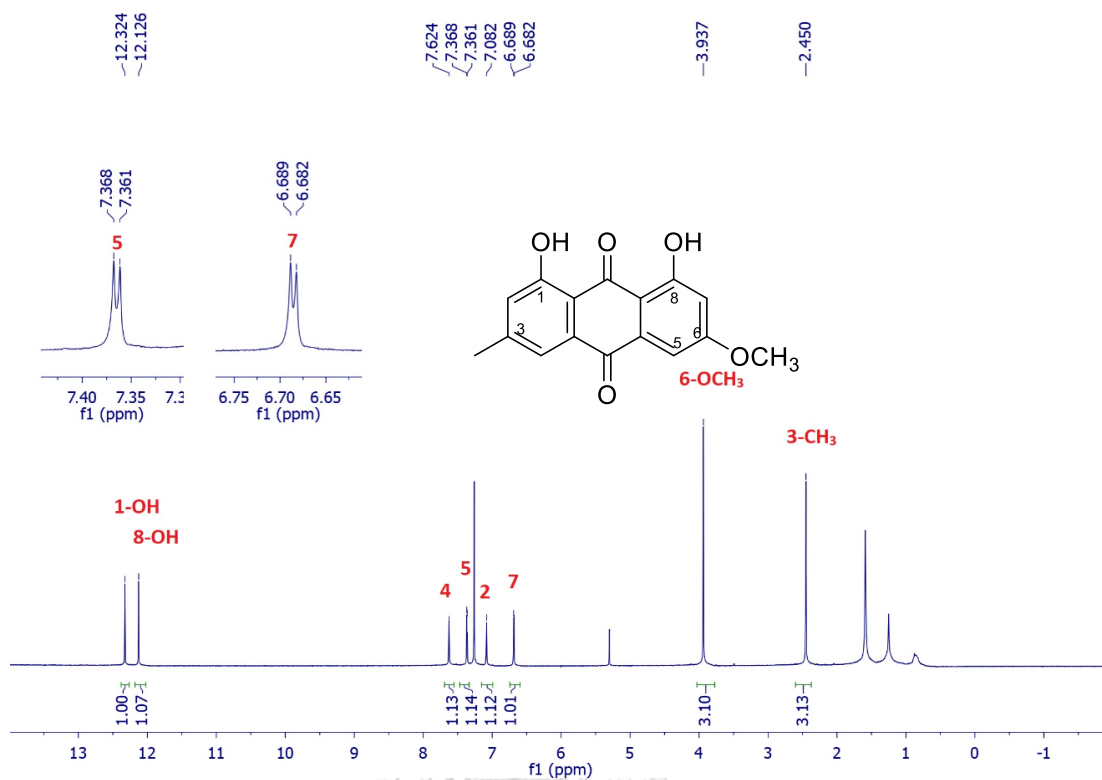
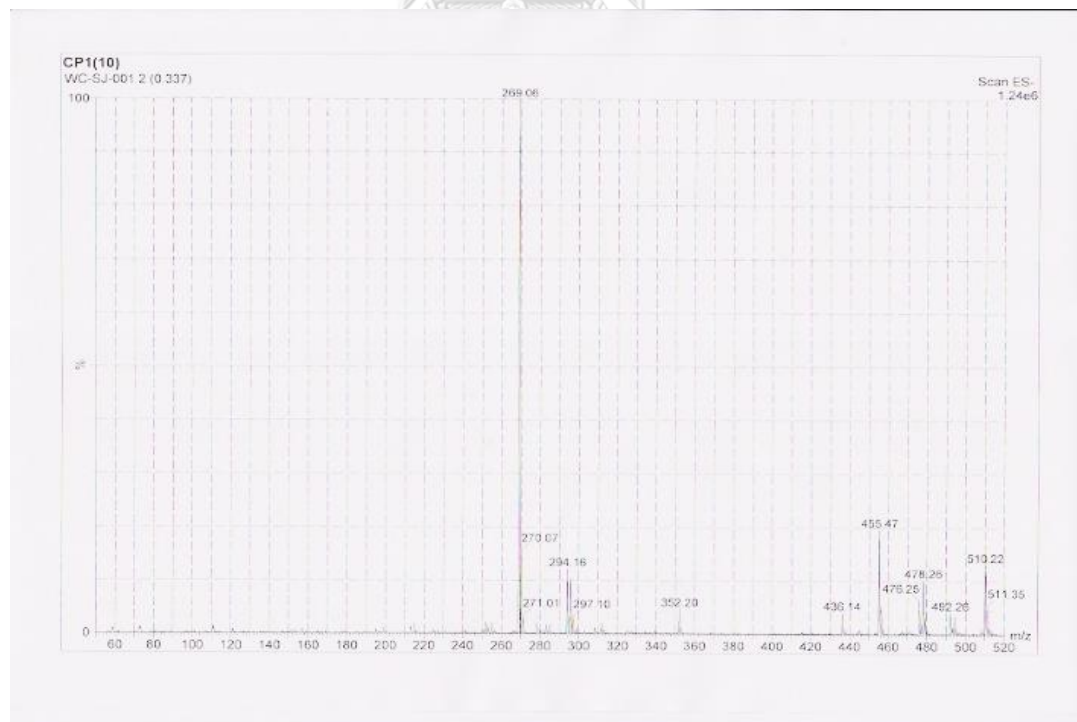
1	CM192		
2	DCD3		
3	DCD4		
4	DCD7		
5	DKT30		
6	DKT36		



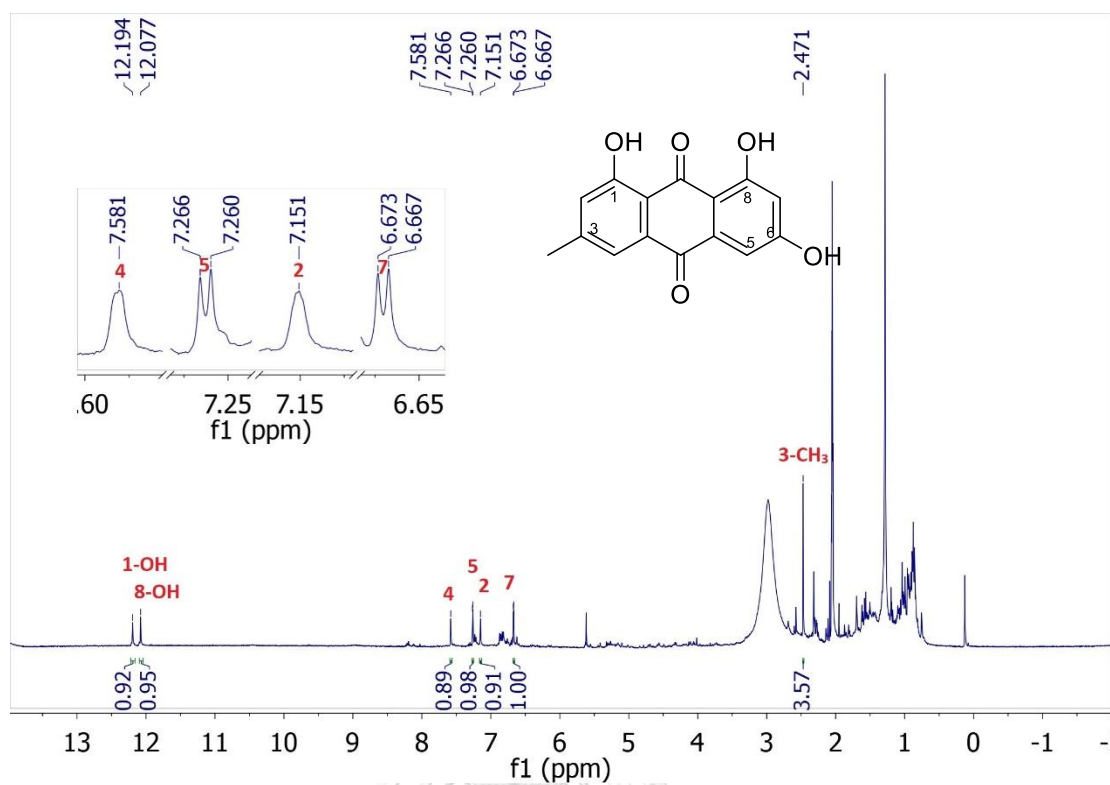
13	PL126		
14	RAT43		
15	RAT50		
16	RAT57		
<p>จุฬาลงกรณ์มหาวิทยาลัย</p>			
17	RAT60		
18	RAT65		

19	RAT66		
20	RAT70		
21	RAT200		
22	RAT248		
23	RAT263		
24	RAT270		

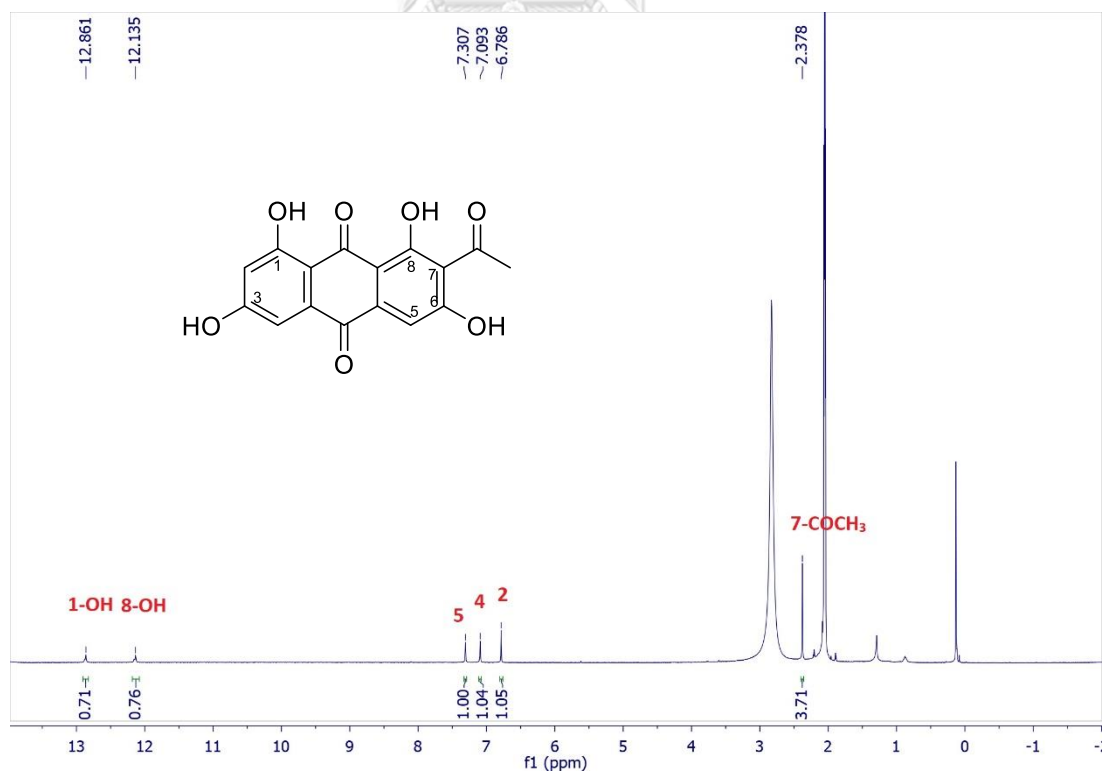
25	RAT346		
26	RAT359		
27	RN104		
28	SMS		
<p>จุฬาลงกรณ์มหาวิทยาลัย</p>			
29	SNK8		
30	SNK36		

S2.3 ¹H NMR spectrum of 2.2 in CDCl₃

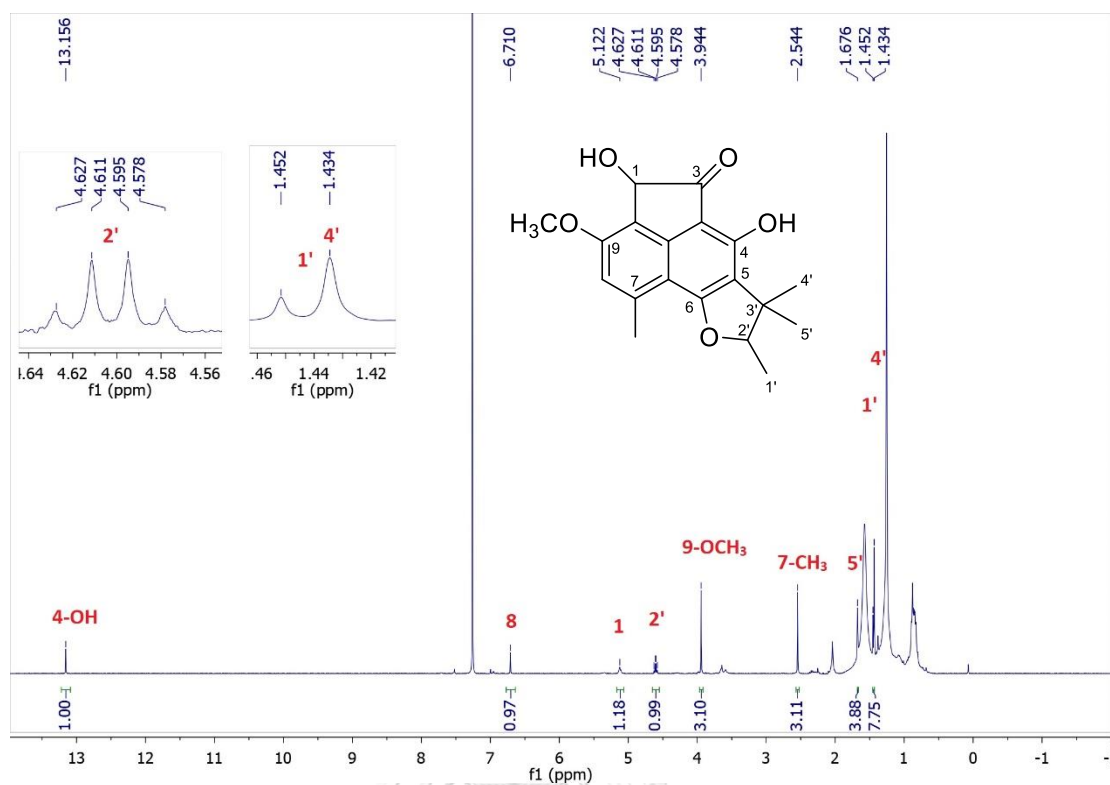
S2.4 Mass spectrum of 2.4 (ESI)



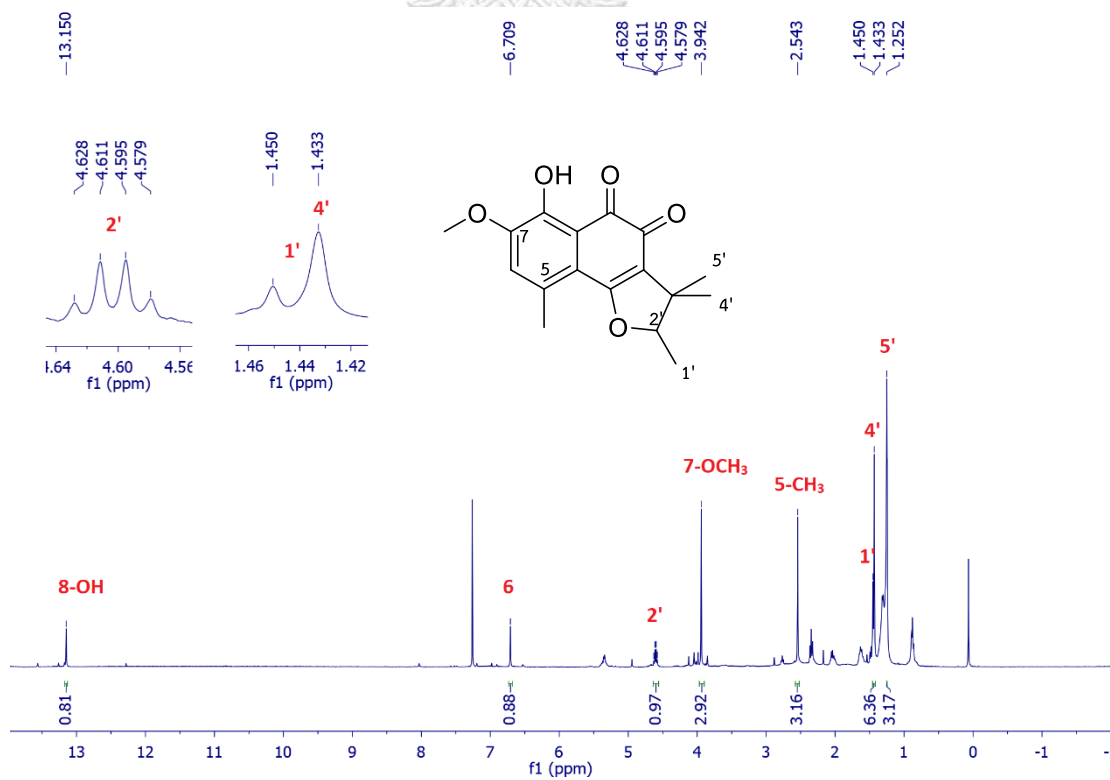
S2.5 ^1H NMR spectrum of 2.4 in Acetone- d_6



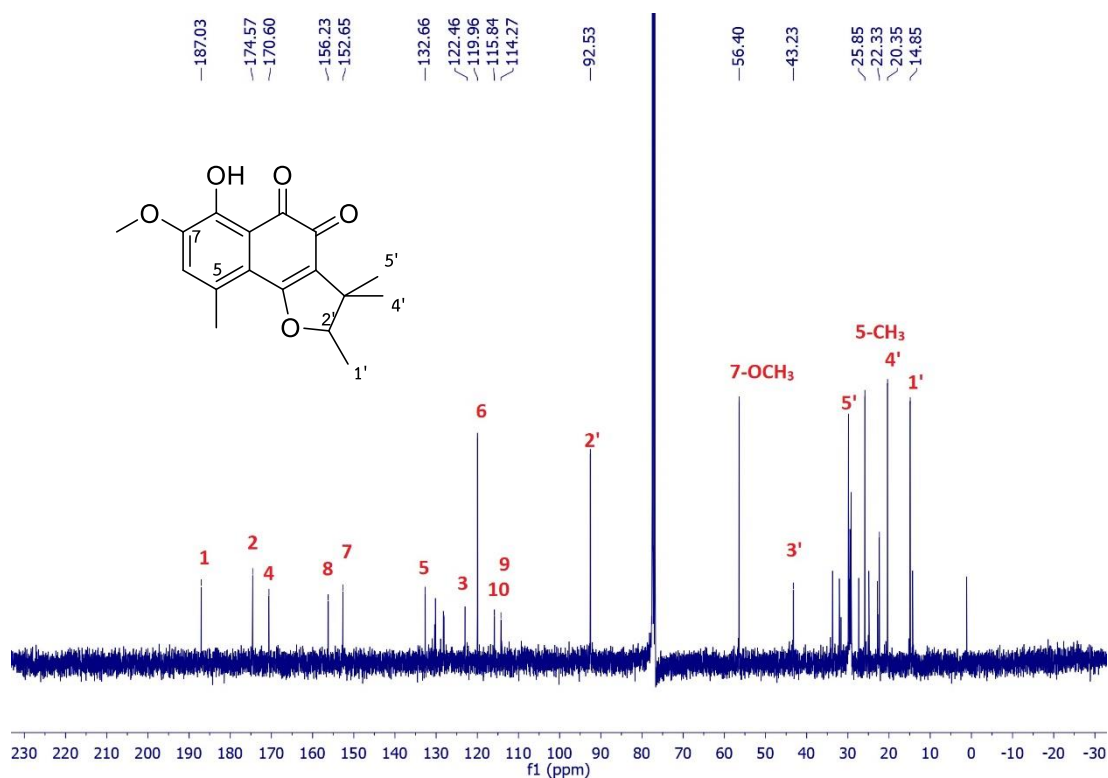
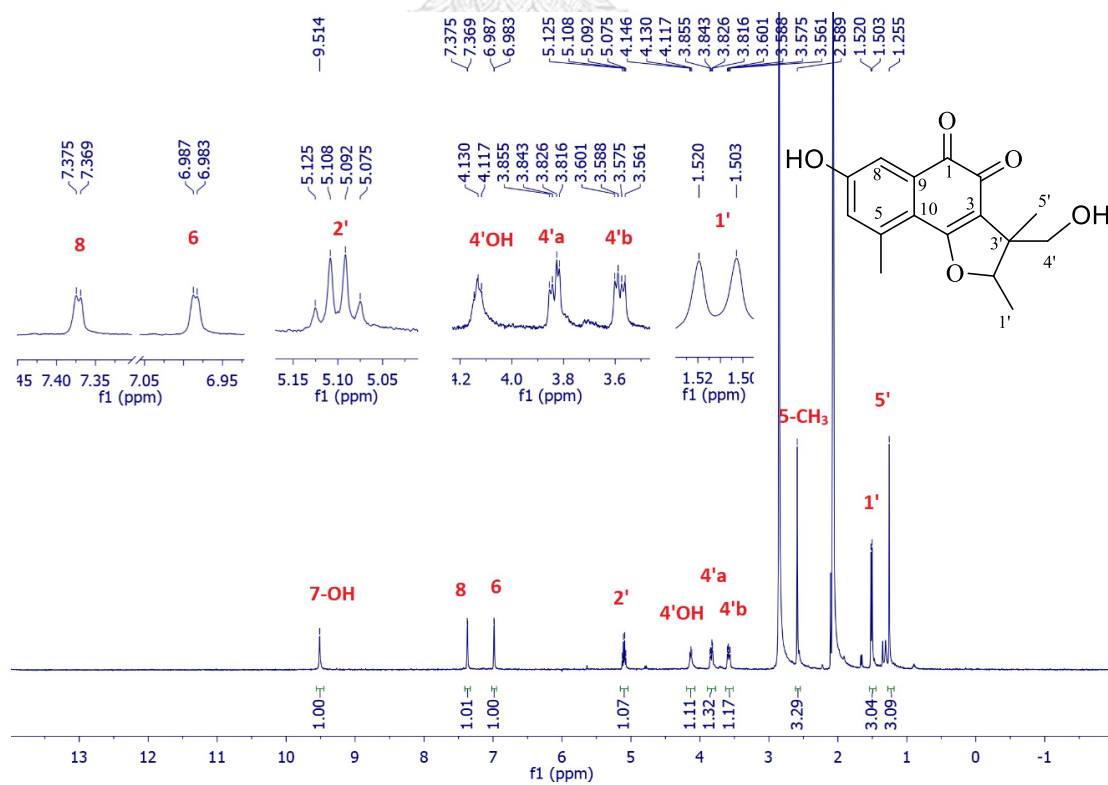
S2.6 ^1H NMR spectrum of 2.5 in Acetone- d_6



S2.7 ^1H NMR spectrum of **2.6** in CDCl_3



S2.8 ^1H NMR spectrum of **2.7** in CDCl_3

S2.9 ¹³C NMR spectrum of 2.7 in CDCl₃S2.10 ¹H NMR spectrum of 2.8 in Acetone-d₆

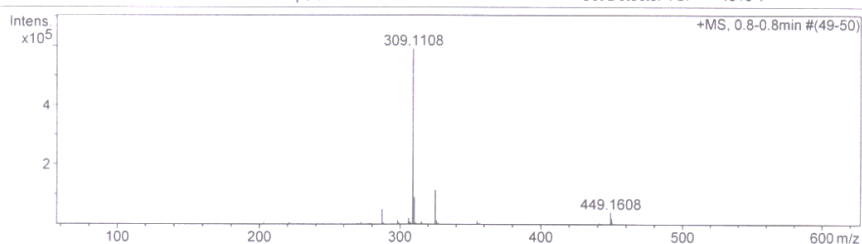
Mass Spectrum List Report

Analysis Info

Analysis Name	OSCUSY580701001.d	Acquisition Date	7/1/2015 10:00:20 AM
Method	MKE_tune_low_positive_20130204.m	Operator	Administrator
Sample Name	Thee1	Instrument	micrOTOF 72
	Thee1		

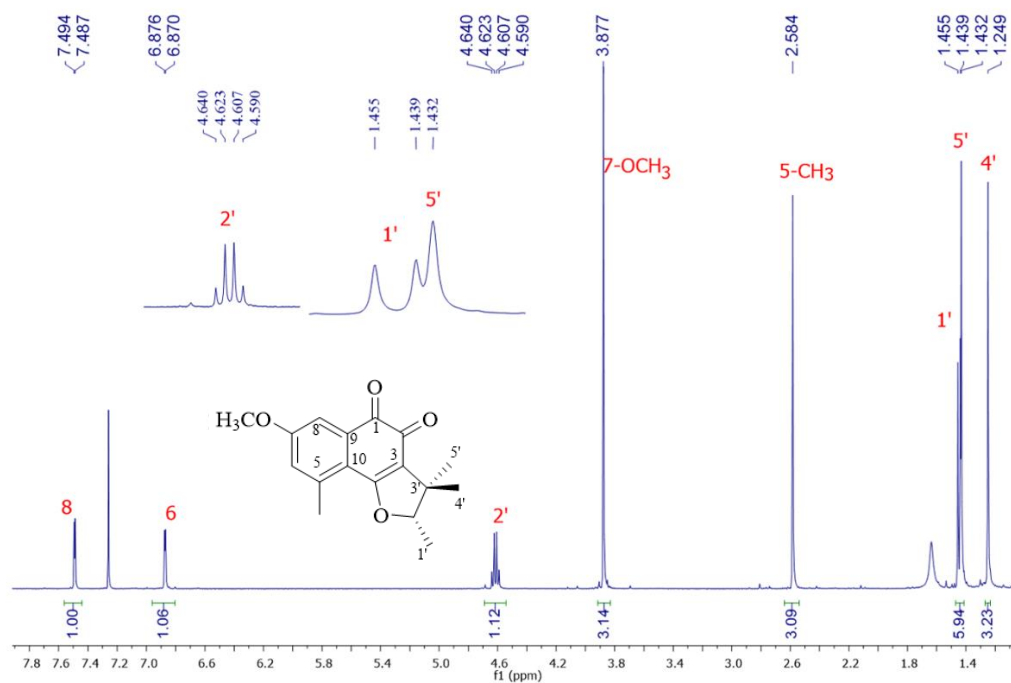
Acquisition Parameter

Source Type	ESI	Ion Polarity	Positive	Set Corrector Fill	79 V
Scan Range	n/a	Capillary Exit	180.0 V	Set Pulsar Pull	406 V
Scan Begin	50 m/z	Hexapole RF	90.0 V	Set Pulsar Push	388 V
Scan End	3000 m/z	Skimmer 1	45.5 V	Set Reflector	1300 V
		Hexapole 1	25.0 V	Set Flight Tube	9000 V
				Set Detector TOF	1910 V

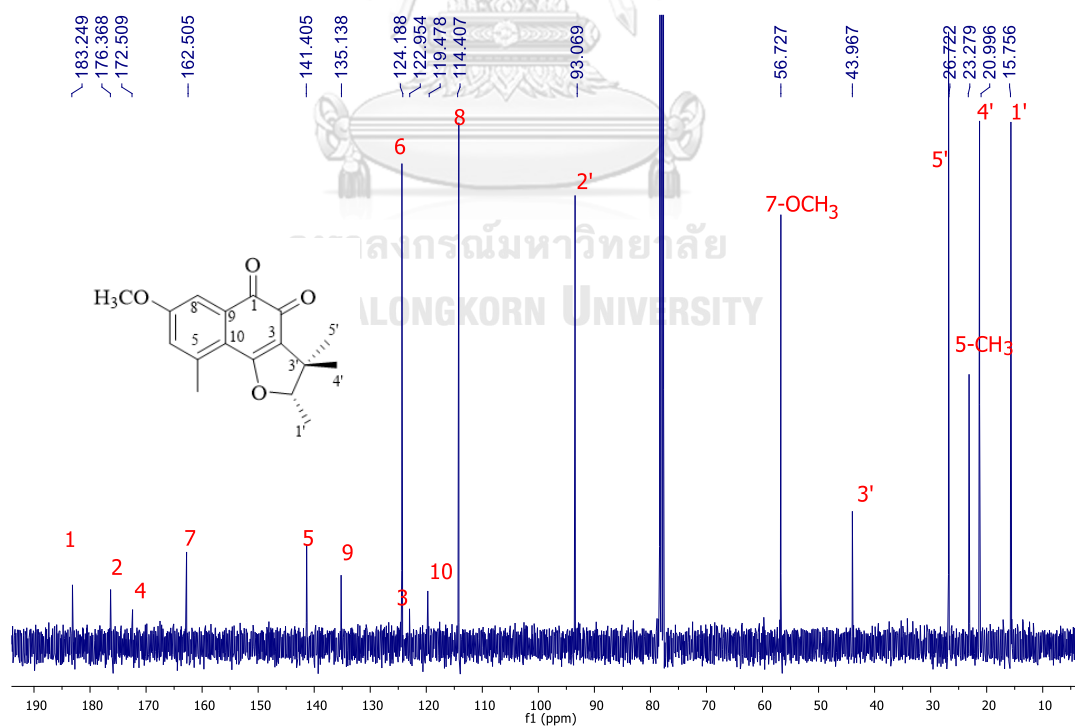


#	m/z	I	I %	S/N	FWHM	Res.
1	203.0683	4759	0.8	142.5	0.0309	6579
2	221.1838	6308	1.1	173.2	0.0343	6454
3	231.0629	3297	0.6	86.5	0.0343	6727
4	269.1125	2634	0.4	59.2	0.0387	6955
5	270.0823	3164	0.5	70.9	0.0458	5900
6	272.1030	8031	1.4	178.9	0.0353	7704
7	279.0833	3653	0.6	79.2	0.0384	7272
8	287.1268	50841	8.6	1073.6	0.0450	6375
9	288.1295	5108	0.9	107.3	0.0423	6810
10	298.1108	14416	2.4	292.9	0.0388	7685
11	298.6121	6443	1.1	130.6	0.0428	6976
12	299.1117	3763	0.6	76.1	0.0392	7635
13	306.0998	20450	3.5	404.7	0.0429	7129
14	306.6009	6900	1.2	136.2	0.0409	7499
15	307.1145	7460	1.3	147.0	0.0429	7164
16	307.6175	2878	0.5	56.5	0.0409	7519
17	309.1108	591021	100.0	11587.2	0.0534	5785
18	310.1143	89933	15.2	1757.2	0.0467	6635
19	311.1154	4921	0.8	95.6	0.0474	6568
20	315.1050	8785	1.5	168.7	0.0401	7853
21	315.6068	2826	0.5	54.1	0.0381	8288
22	325.0842	115271	19.5	2147.8	0.0499	6516
23	326.0876	12402	2.1	230.2	0.0437	7464
24	327.0858	4712	0.8	87.1	0.0532	6154
25	355.1029	11637	2.0	215.7	0.0485	7318
26	441.1718	4037	0.7	101.7	0.0621	7104
27	441.6737	3021	0.5	76.2	0.0498	8869
28	449.1608	40324	6.8	1054.8	0.0595	7555
29	449.6624	19693	3.3	516.1	0.0591	7612
30	450.1649	5109	0.9	133.9	0.0563	7994

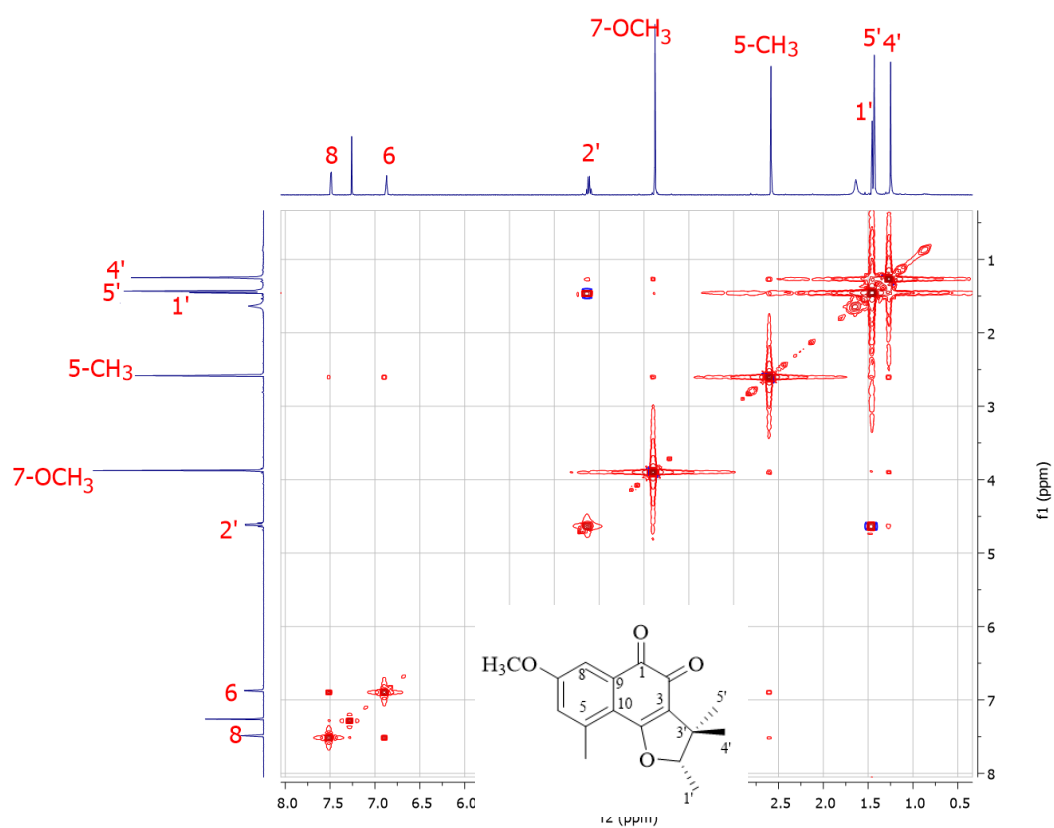
S3.1 HRESIMS spectrum of 3.1



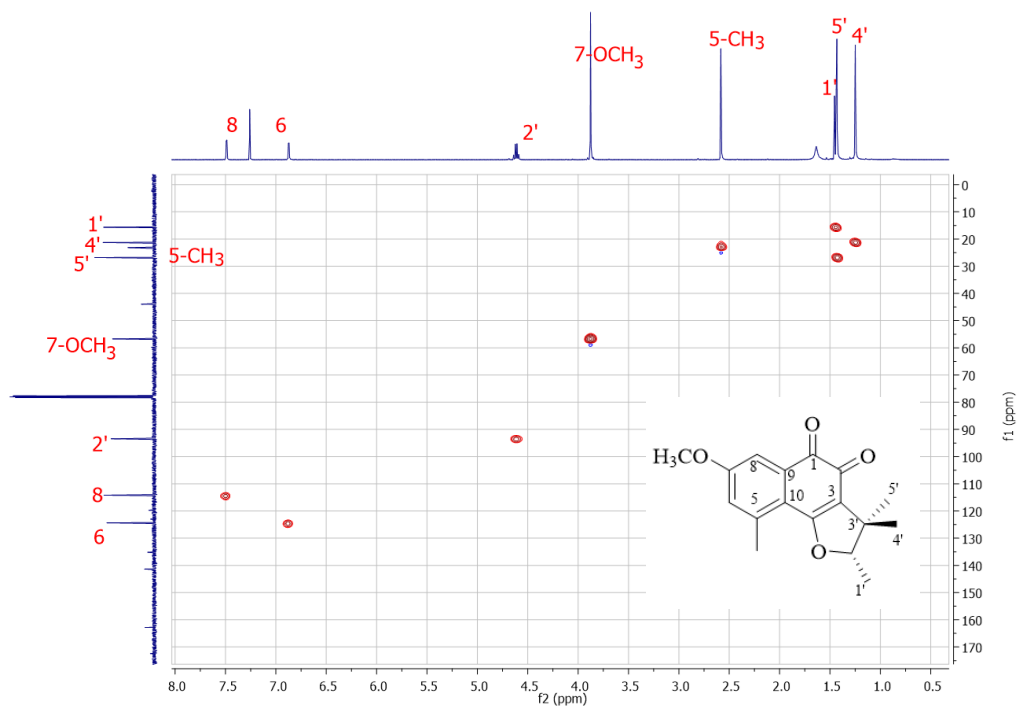
S3.2 ¹H NMR spectrum of 3.1 in CDCl₃



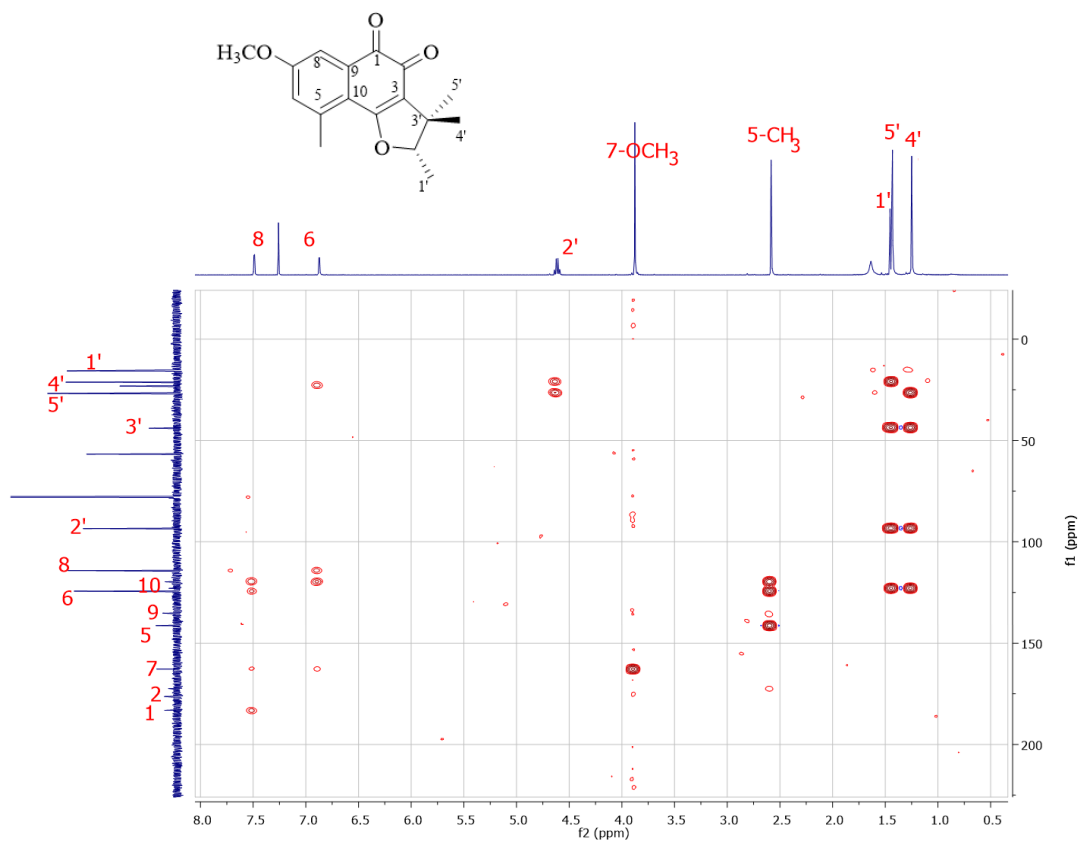
S3.3 ¹³C NMR spectrum of 3.1 in CDCl₃



S3.4 COSY spectrum of **3.1** in CDCl_3



S3.5 HSQC spectrum of **3.1** in CDCl_3



S3.6 HMBC spectrum of **3.1** in CDCl₃

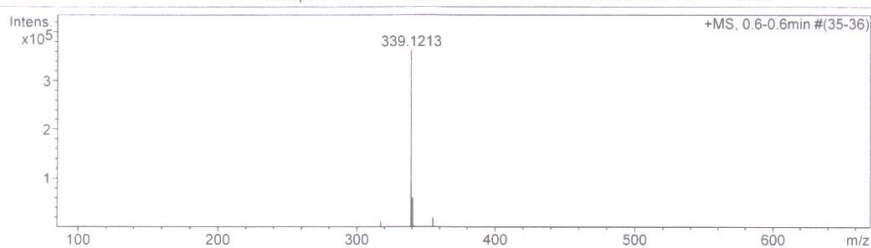
Mass Spectrum List Report

Analysis Info

Analysis Name	OSCUSY580701003.d	Acquisition Date	7/1/2015 10:15:03 AM
Method	MKE_tune_low_positive_20130204.m	Operator	Administrator
Sample Name	Thee3	Instrument	micrOTOF 72
	Thee3		

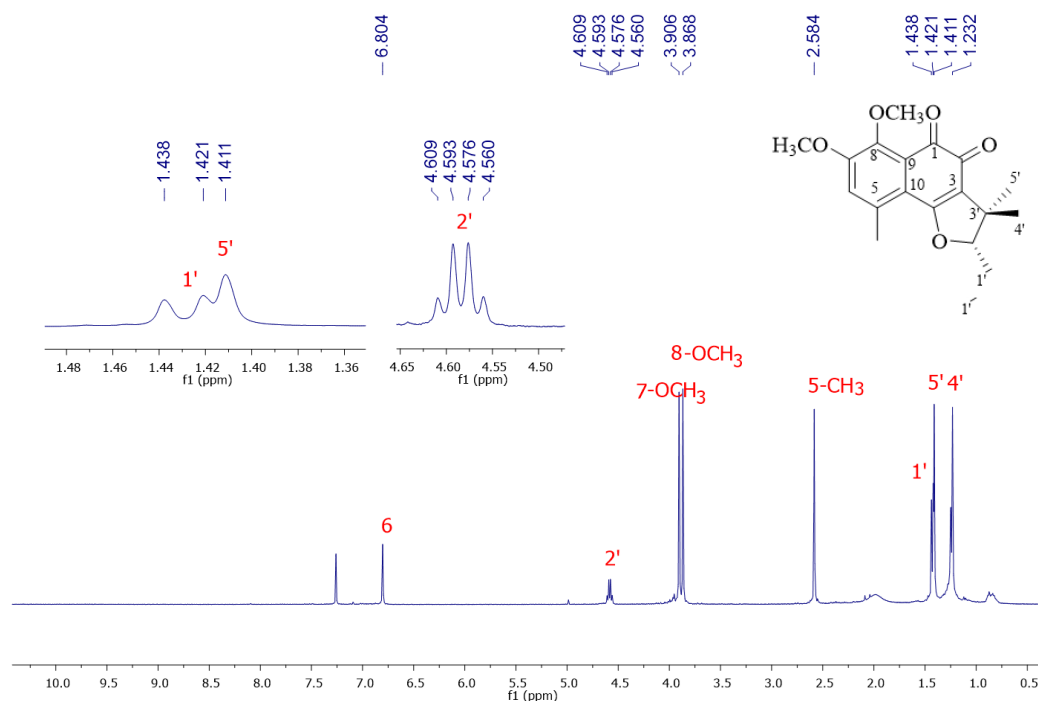
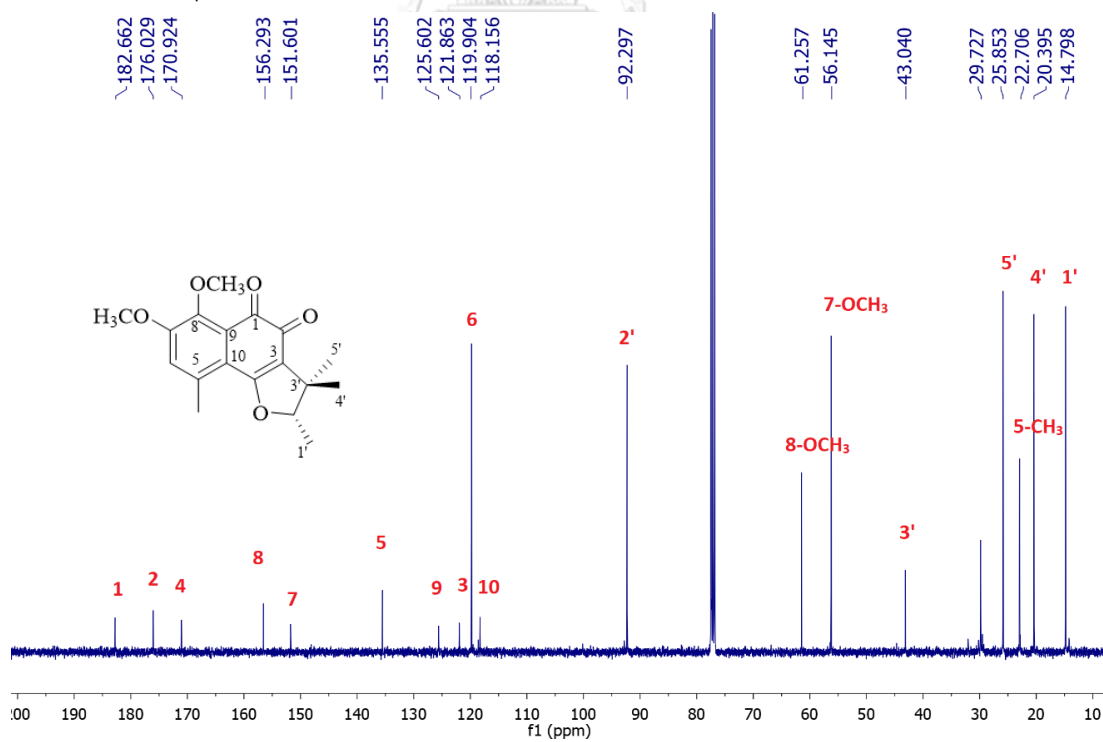
Acquisition Parameter

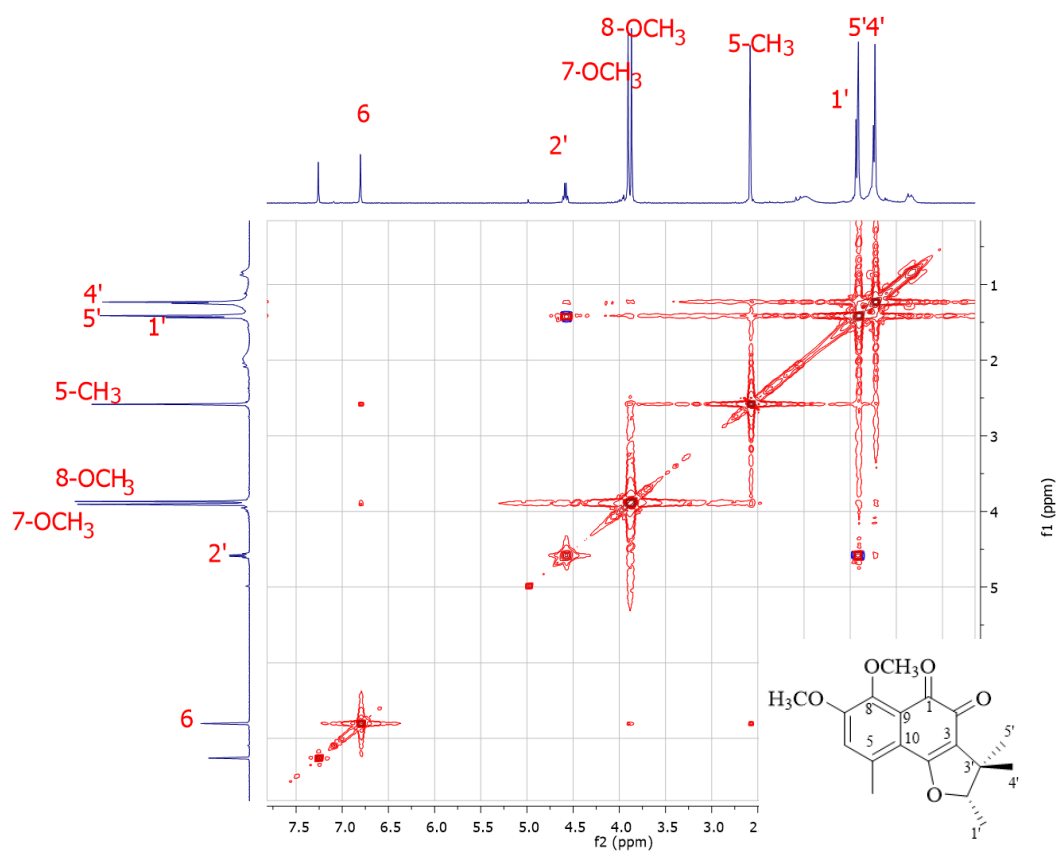
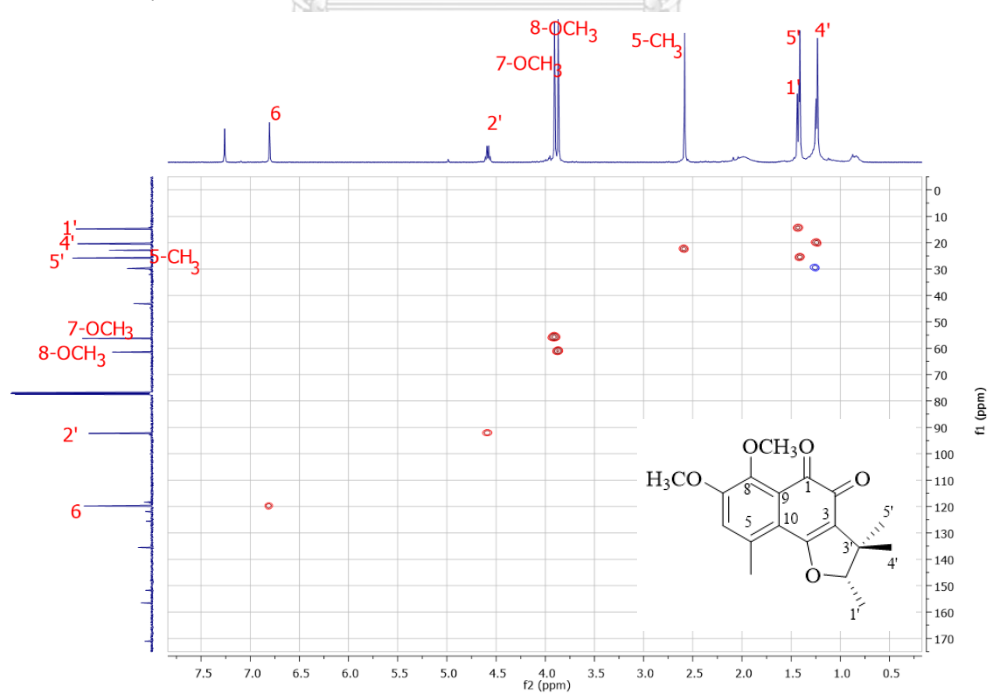
Source Type	ESI	Ion Polarity	Positive	Set Corrector Fill	79 V
Scan Range	n/a	Capillary Exit	150.0 V	Set Pulsar Pull	406 V
Scan Begin	50 m/z	Hexapole RF	90.0 V	Set Pulsar Push	388 V
Scan End	3000 m/z	Skimmer 1	45.5 V	Set Reflector	1300 V
		Hexapole 1	25.0 V	Set Flight Tube	9000 V
				Set Detector TOF	1910 V

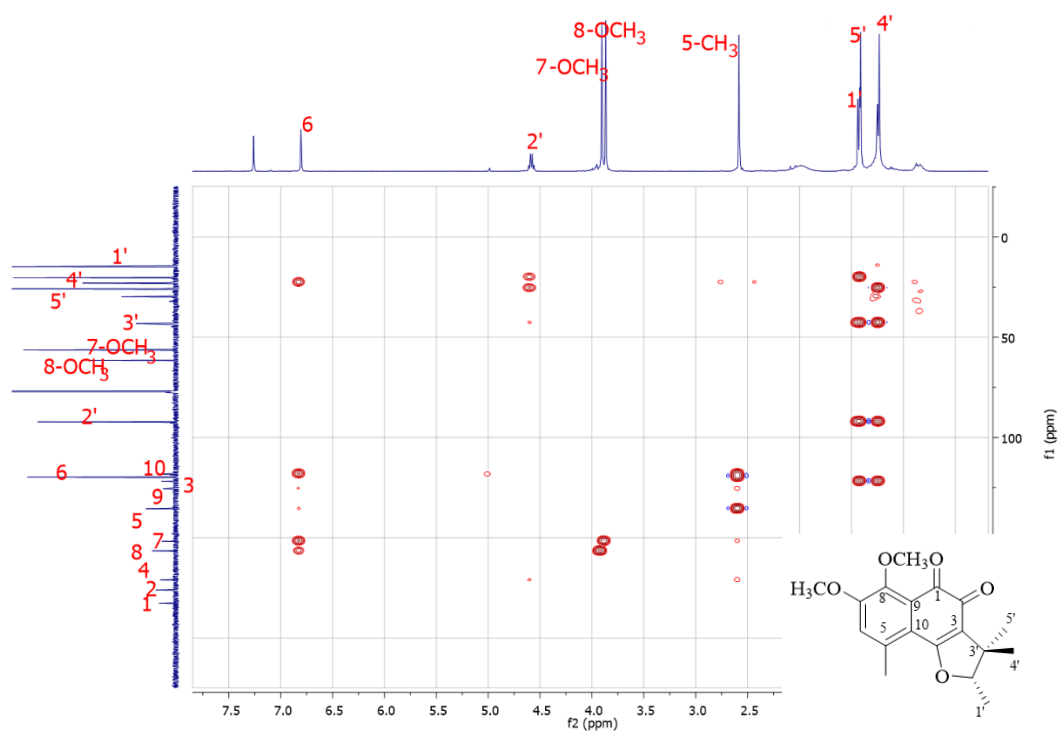
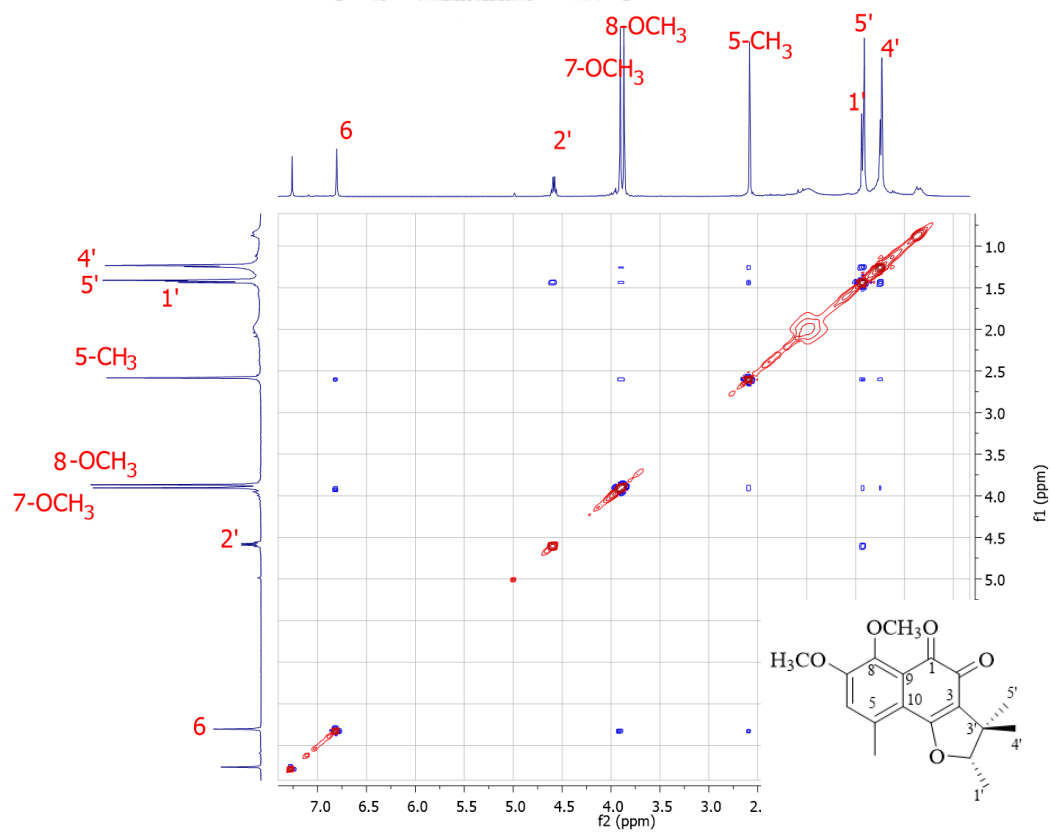


#	m/z	I	I %	S/N	FWHM	Res.
1	58.6092	709	0.2	40.1	0.0063	9373
2	129.8916	615	0.2	34.7	0.0155	8367
3	145.0844	613	0.2	34.5	0.0088	16508
4	287.0903	1712	0.5	73.3	0.0416	6903
5	297.6521	648	0.2	27.1	0.0117	25340
6	302.1132	588	0.2	24.4	0.0415	7280
7	309.1073	522	0.1	21.4	0.0582	5311
8	317.1372	13292	3.7	542.2	0.0447	7097
9	318.1421	1531	0.4	62.2	0.0463	6870
10	336.1104	842	0.2	33.1	0.0421	7993
11	339.1213	363663	100.0	14328.1	0.0599	5665
12	340.1247	60621	16.7	2384.5	0.0523	6498
13	341.1251	4161	1.1	163.5	0.0439	7766
14	355.0946	20595	5.7	833.8	0.0517	6864
15	356.0955	2149	0.6	87.0	0.0452	7881
16	357.0943	874	0.2	35.4	0.0443	8053
17	371.1435	1796	0.5	75.1	0.0527	7037
18	373.0915	1036	0.3	43.4	0.0637	5859
19	413.2648	2387	0.7	110.0	0.0561	7367
20	414.2677	577	0.2	26.5	0.0435	9519
21	494.1780	2747	0.8	157.6	0.0636	7772
22	494.6781	1345	0.4	77.1	0.0689	7185
23	655.2565	1088	0.3	79.6	0.1191	5502
24	1450.2681	665	0.2	55.4	0.0277	52433
25	1450.5335	709	0.2	59.1	0.0297	48865
26	1873.9018	531	0.1	44.8	0.0283	66106
27	1873.9802	582	0.2	49.1	0.0291	64384
28	2351.8464	708	0.2	59.7	0.0315	74552
29	2352.1952	1270	0.3	107.2	0.0328	71630
30	2352.2974	1104	0.3	93.2	0.0319	73627

S3.7 HRESIMS spectrum of 3.2

S3.8 ¹H NMR spectrum of 3.2 in CDCl₃S3.9 ¹³C NMR spectrum of 3.2 in CDCl₃

S3.10 COSY spectrum of **3.2** in CDCl_3 S3.11 HSQC spectrum of **3.2** in CDCl_3

S3.12 HMBC spectrum of **3.2** in CDCl_3 S3.13 NOESY spectrum of **3.2** in CDCl_3

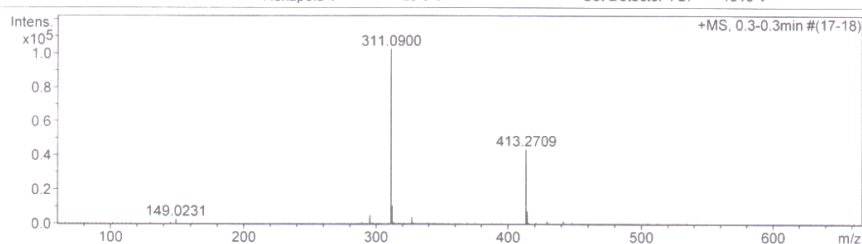
Mass Spectrum List Report

Analysis Info

Analysis Name	OSCUSY580701005.d	Acquisition Date	7/1/2015 10:25:19 AM
Method	MKE_tune_low_positive_20130204.m	Operator	Administrator
Sample Name	Thee5	Instrument	micrOTOF 72
	Thee5		

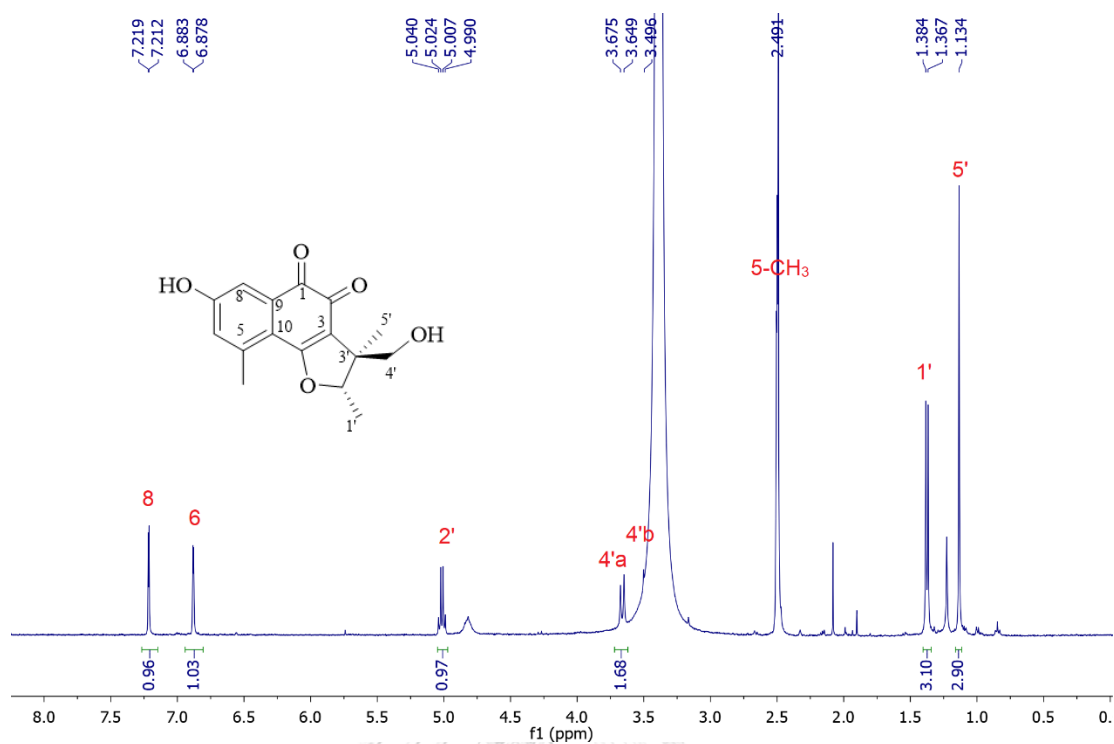
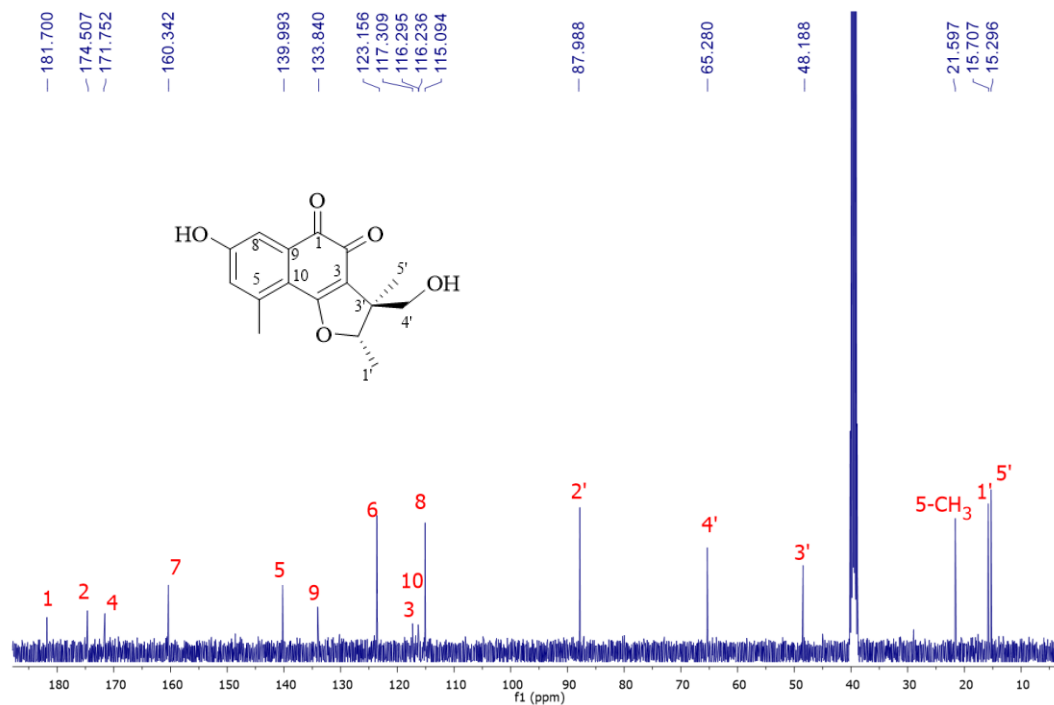
Acquisition Parameter

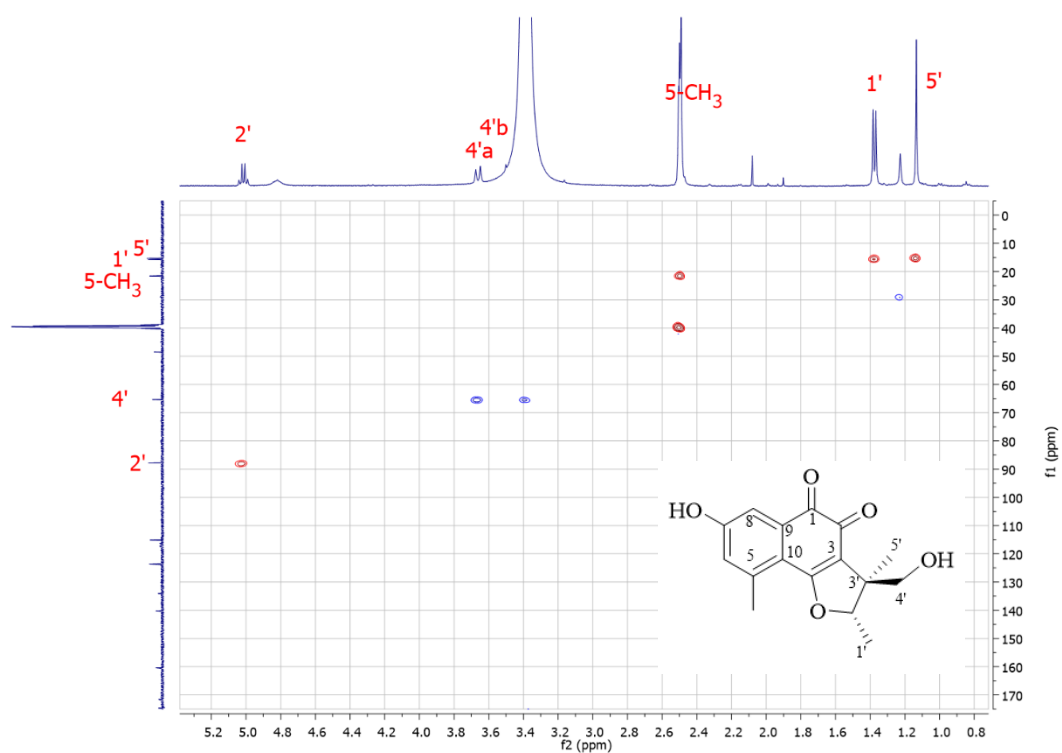
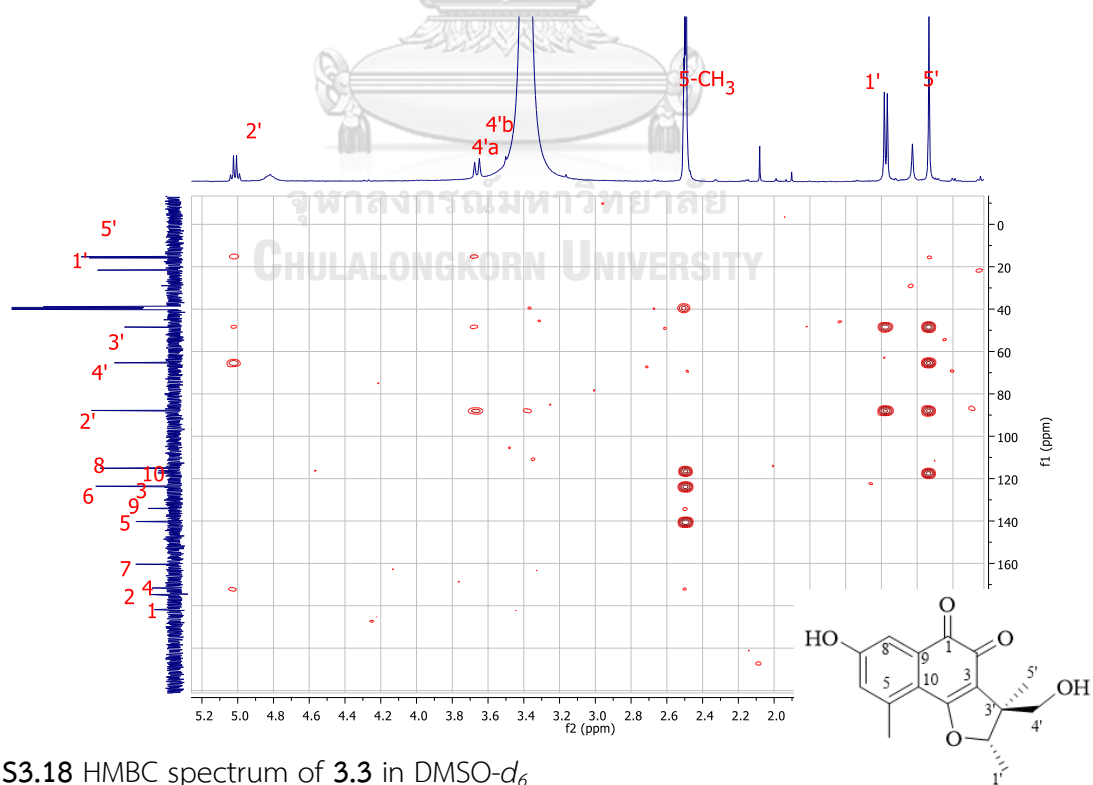
Source Type	ESI	Ion Polarity	Positive	Set Corrector Fill	79 V
Scan Range	n/a	Capillary Exit	180.0 V	Set Pulsar Pull	406 V
Scan Begin	50 m/z	Hexapole RF	90.0 V	Set Pulsar Push	388 V
Scan End	3000 m/z	Skimmer 1	45.5 V	Set Reflector	1300 V
		Hexapole 1	25.0 V	Set Flight Tube	9000 V
				Set Detector TOF	1910 V

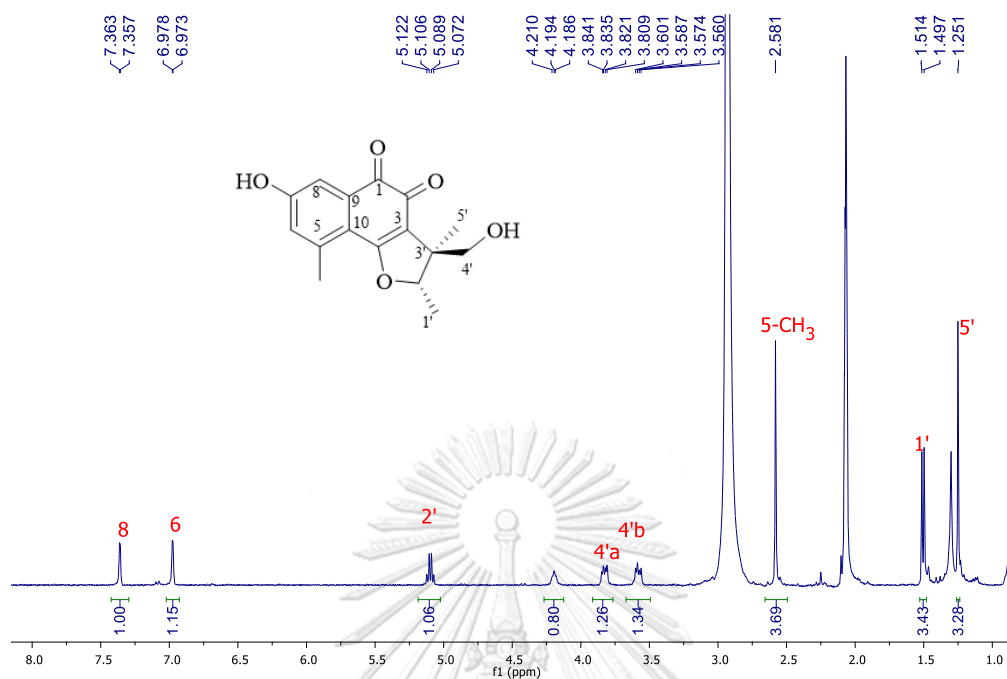


#	m/z	I	I %	S/N	FWHM	Res.
1	58.6085	615	0.6	34.5	0.0069	8466
2	66.3109	545	0.5	30.5	0.0065	10166
3	129.8936	581	0.6	32.5	0.0138	9402
4	145.0839	751	0.7	42.1	0.0089	16299
5	149.0231	2651	2.6	148.4	0.0270	5524
6	289.1069	1068	1.0	50.9	0.0432	6688
7	295.0939	5315	5.2	252.7	0.0416	7096
8	296.0987	616	0.6	29.0	0.0444	6666
9	297.6502	569	0.6	26.8	0.0117	25545
10	301.1393	550	0.5	25.8	0.0542	5554
11	311.0900	102420	100.0	4795.4	0.0493	6315
12	312.0925	10575	10.3	494.4	0.0415	7520
13	313.0928	935	0.9	43.5	0.0362	8640
14	327.0640	3868	3.8	178.0	0.0450	7271
15	339.1201	633	0.6	28.6	0.0564	6008
16	369.1322	573	0.6	27.3	0.0618	5977
17	413.2709	43603	42.6	2301.7	0.0696	5935
18	414.2726	7223	7.1	381.9	0.0632	6554
19	429.2484	1708	1.7	93.3	0.0745	5759
20	441.3017	1772	1.7	99.6	0.0642	6879
21	447.7567	715	0.7	40.7	0.0158	28379
22	504.4519	639	0.6	42.1	0.0151	33482
23	765.4830	590	0.6	50.3	0.0184	41507
24	765.6833	662	0.6	56.4	0.0182	42136
25	1450.2724	640	0.6	55.9	0.0739	19624
26	1450.4205	545	0.5	47.6	0.0325	44677
27	2166.6096	620	0.6	52.9	0.0326	66440
28	2351.8391	674	0.7	58.9	0.0314	74870
29	2352.1848	1237	1.2	108.1	0.0326	72050
30	2352.2880	1046	1.0	91.4	0.0317	74170

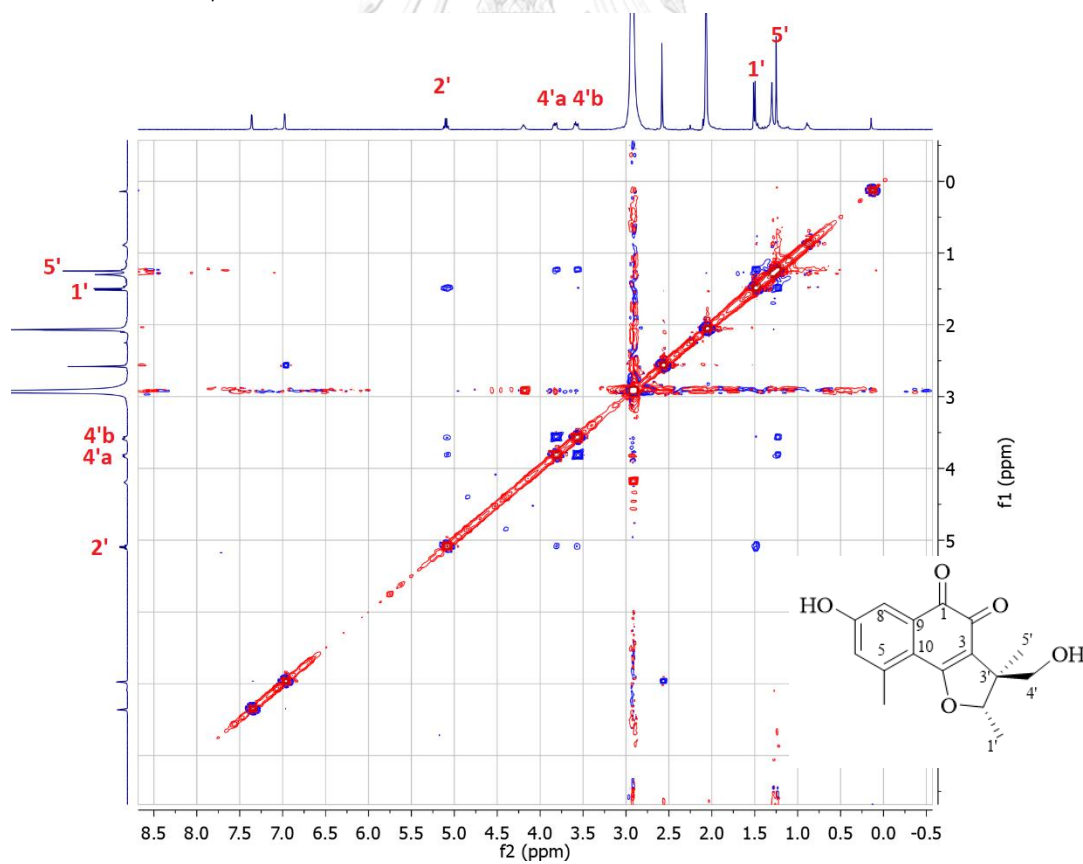
S3.14 HRESIMS spectrum of 3.3

S3.15 ^1H NMR spectrum of **3.3** in DMSO- d_6 S3.16 ^{13}C NMR spectrum of **3.3** in DMSO- d_6

S3.17 HSQC spectrum of 3.3 in DMSO- d_6 S3.18 HMBC spectrum of 3.3 in DMSO- d_6



S3.19 ¹H NMR spectrum of **3.3** in Acetone-d₆



S3.20 NOESY spectrum of **3.3** in Acetone-d₆

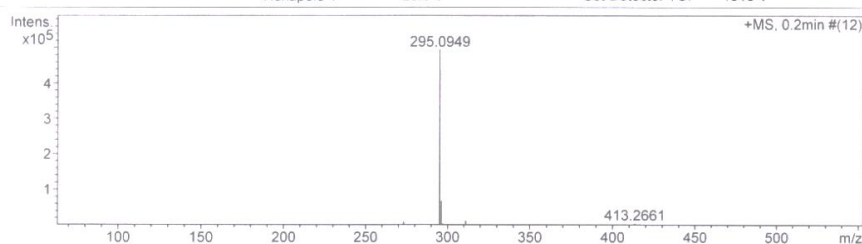
Mass Spectrum List Report

Analysis Info

Analysis Name	OSCUSY580701004.d	Acquisition Date	7/1/2015 10:22:25 AM
Method	MKE_tune_low_positive_20130204.m	Operator	Administrator
Sample Name	Thee4	Instrument	micrOTOF 72
	Thee4		

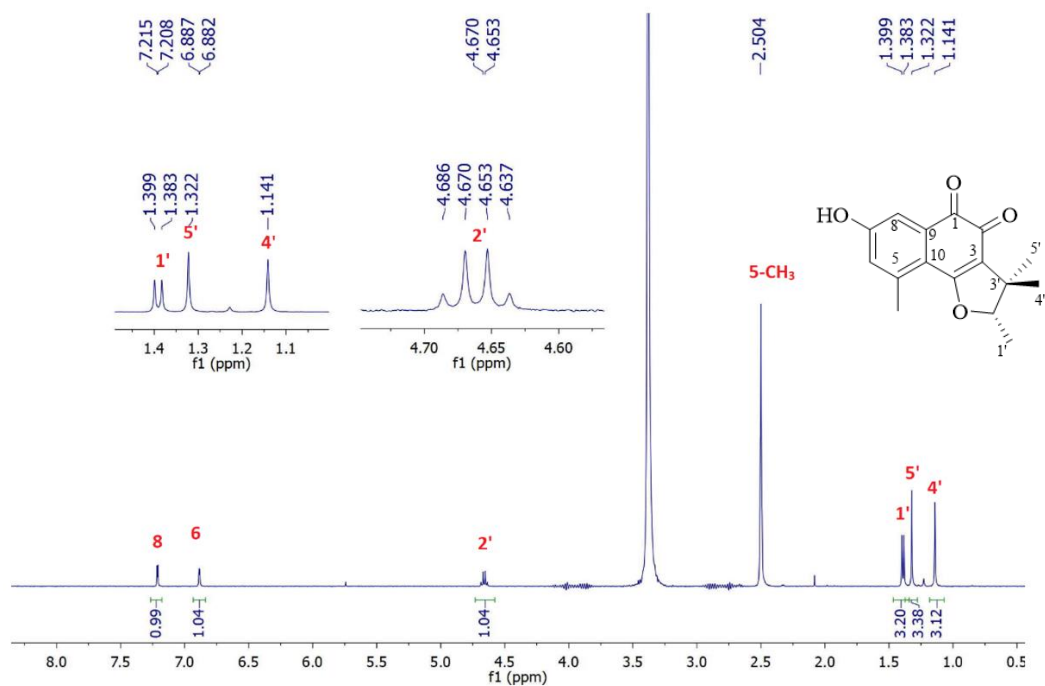
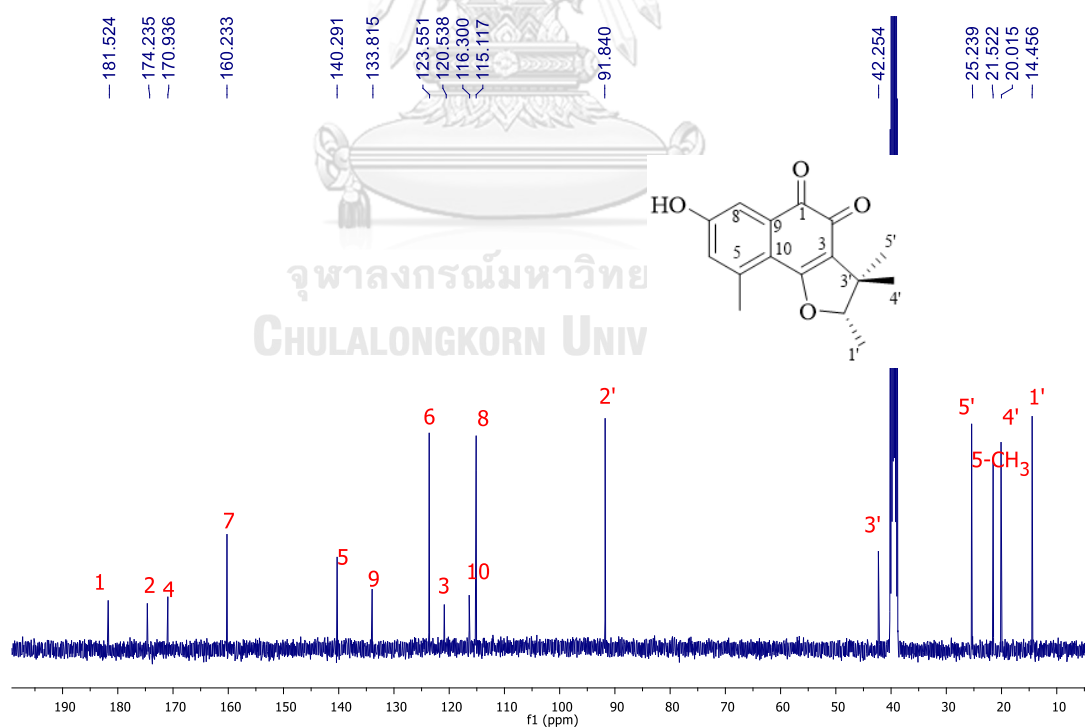
Acquisition Parameter

Source Type	ESI	Ion Polarity	Positive	Set Corrector Fill	79 V
Scan Range	n/a	Capillary Exit	180.0 V	Set Pulsar Pull	406 V
Scan Begin	50 m/z	Hexapole RF	90.0 V	Set Pulsar Push	388 V
Scan End	3000 m/z	Skimmer 1	45.5 V	Set Reflector	1300 V
		Hexapole 1	25.0 V	Set Flight Tube	9000 V
				Set Detector TOF	1910 V



#	m/z	I	I %	S/N	FWHM	Res.
1	58.6089	607	0.1	31.6	0.0065	8991
2	189.0524	1729	0.4	79.0	0.0286	6622
3	203.0688	697	0.1	30.6	0.0315	6440
4	217.0479	938	0.2	39.7	0.0355	6108
5	258.0866	2201	0.4	84.5	0.0396	6518
6	273.1106	9502	1.9	353.0	0.0396	6895
7	274.1165	1075	0.2	39.7	0.0412	6655
8	292.0835	936	0.2	33.2	0.0343	8516
9	295.0949	493977	100.0	17498.0	0.0504	5859
10	296.0981	68821	13.9	2432.4	0.0440	6729
11	297.0994	3678	0.7	129.5	0.0403	7367
12	300.5871	796	0.2	27.7	0.0127	23723
13	301.0957	1521	0.3	53.0	0.0514	5856
14	311.0688	13304	2.7	455.5	0.0429	7256
15	312.0724	1365	0.3	46.5	0.0419	7450
16	313.0733	650	0.1	22.0	0.0480	6525
17	339.1204	3041	0.6	98.2	0.0513	6607
18	413.2661	6332	1.3	238.9	0.0570	7245
19	414.2691	1537	0.3	57.9	0.0432	9581
20	428.1379	2283	0.5	89.1	0.0659	6495
21	428.6391	1374	0.3	53.6	0.0599	7153
22	437.1965	1471	0.3	58.6	0.0735	5950
23	441.2982	858	0.2	34.4	0.0616	7159
24	447.7519	751	0.2	30.6	0.0149	30060
25	567.2037	10436	2.1	579.1	0.0900	6305
26	568.2089	2470	0.5	136.9	0.0753	7543
27	1080.6837	605	0.1	49.3	0.0219	49287
28	2351.8390	596	0.1	49.3	0.0314	74920
29	2352.1824	964	0.2	79.9	0.0326	72170
30	2352.2913	806	0.2	66.8	0.0315	74730

S3.21 HRESIMS spectrum of 3.4

S3.22 ^1H NMR spectrum of 3.4 in DMSO- d_6 S3.23 ^{13}C NMR spectrum of 3.4 in DMSO- d_6

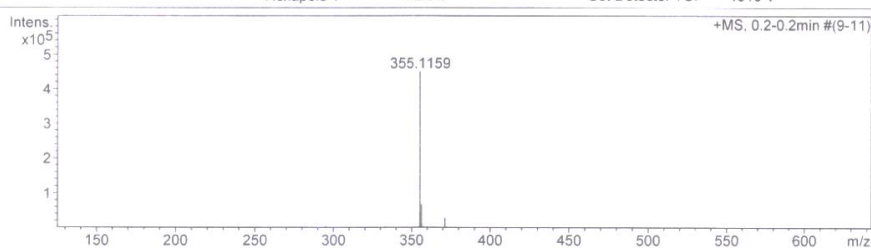
Mass Spectrum List Report

Analysis Info

Analysis Name	OSCUSY580701006.d	Acquisition Date	7/1/2015 10:28:30 AM
Method	MKE_tune_low_positive_20130204.m	Operator	Administrator
Sample Name	Thee3a	Instrument	micrOTOF 72
	Thee3a		

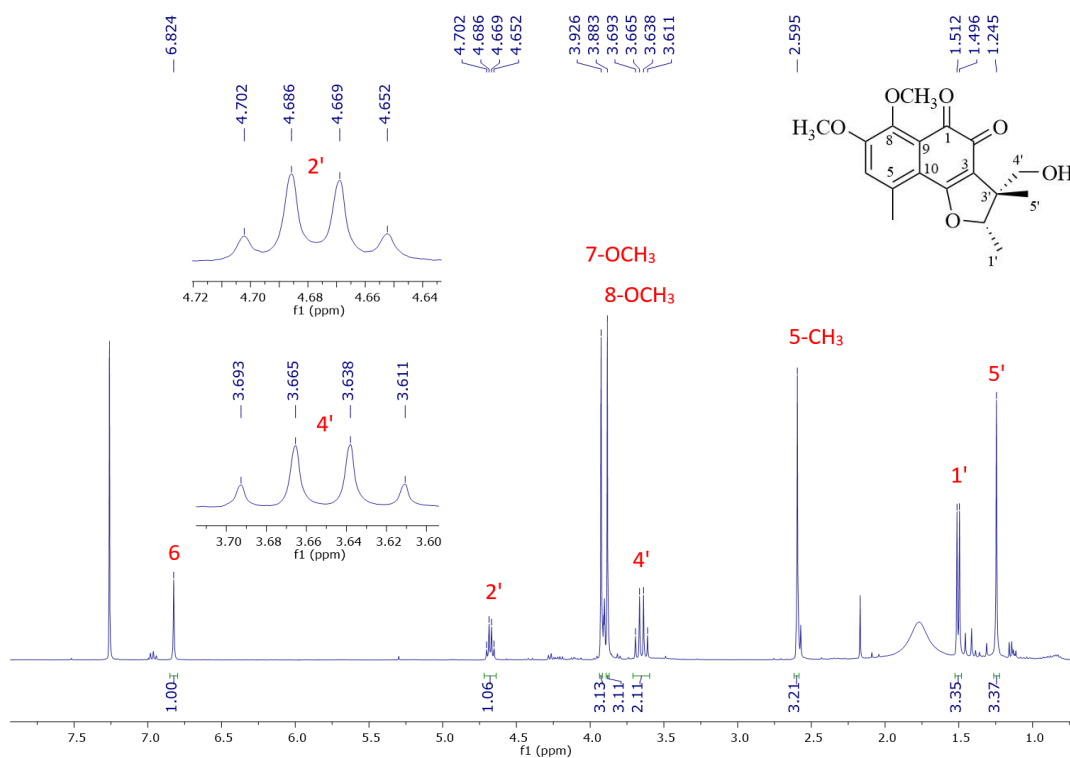
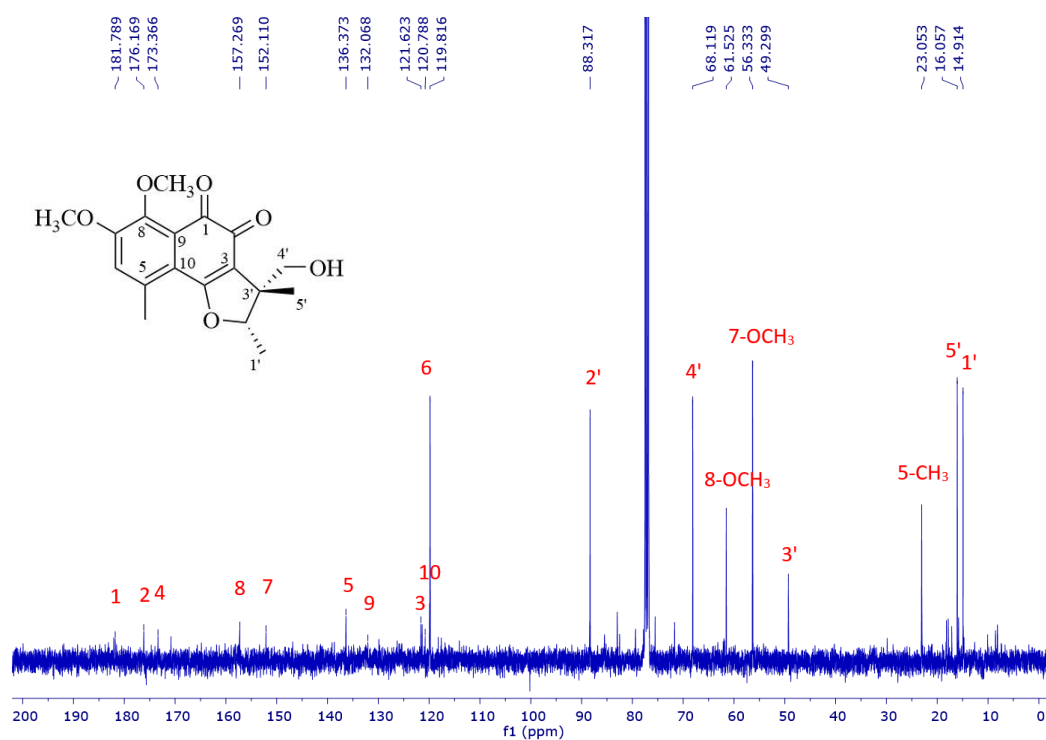
Acquisition Parameter

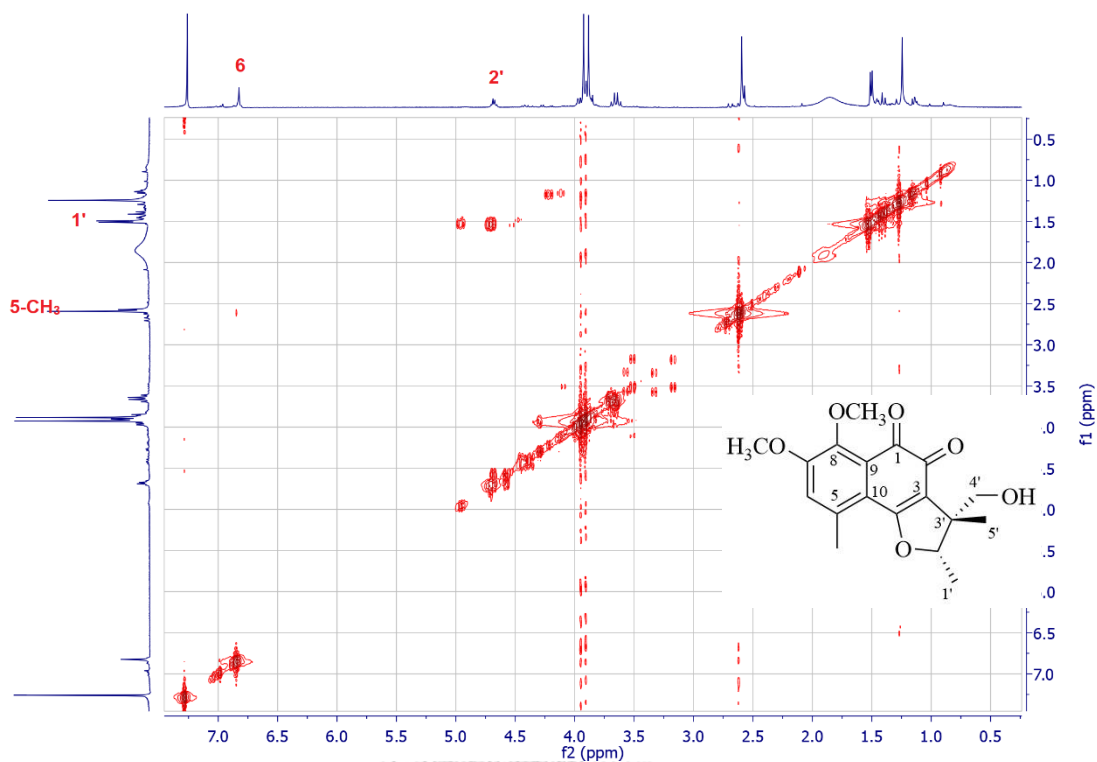
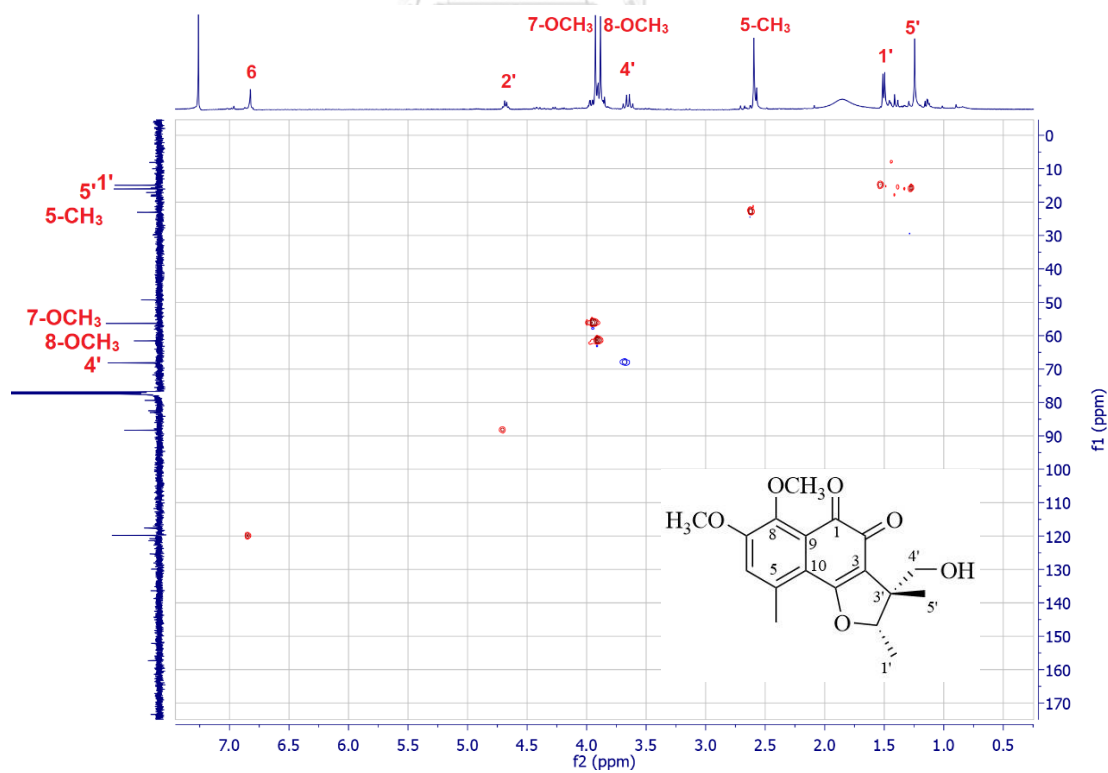
Source Type	ESI	Ion Polarity	Positive	Set Corrector Fill	79 V
Scan Range	n/a	Capillary Exit	180.0 V	Set Pulsar Pull	406 V
Scan Begin	50 m/z	Hexapole RF	90.0 V	Set Pulsar Push	388 V
Scan End	3000 m/z	Skimmer 1	45.5 V	Set Reflector	1300 V
		Hexapole 1	25.0 V	Set Flight Tube	9000 V
				Set Detector TOF	1910 V

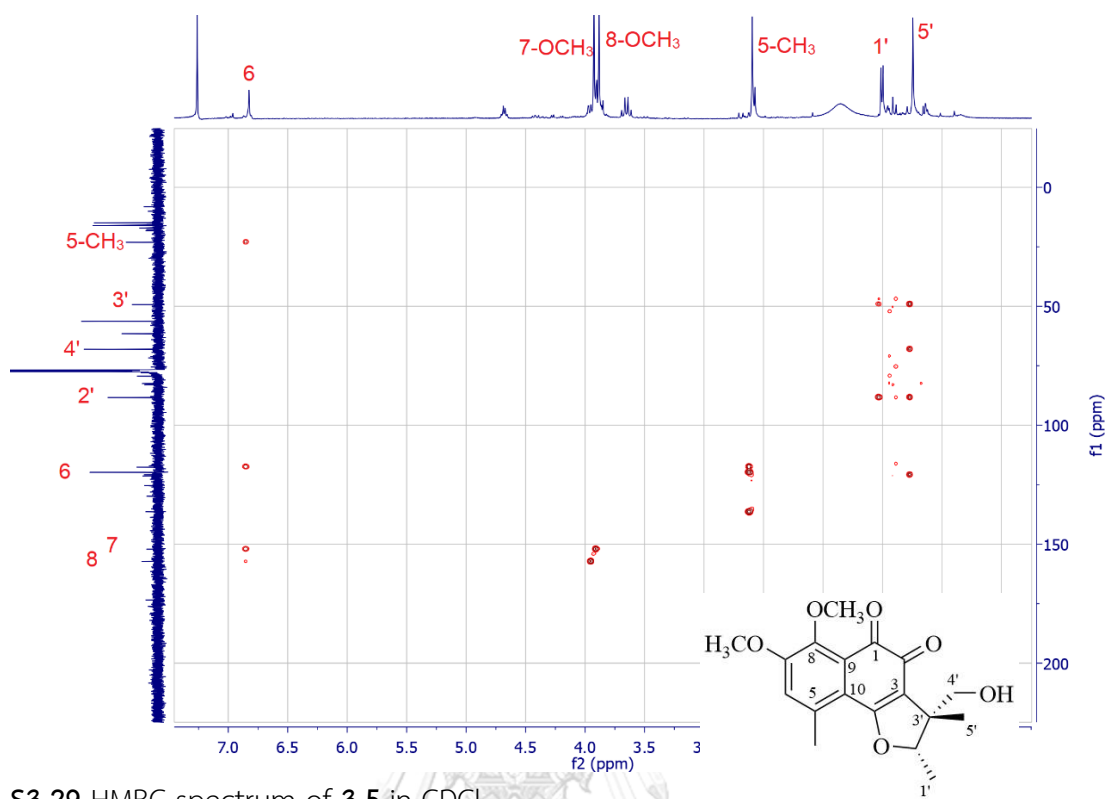
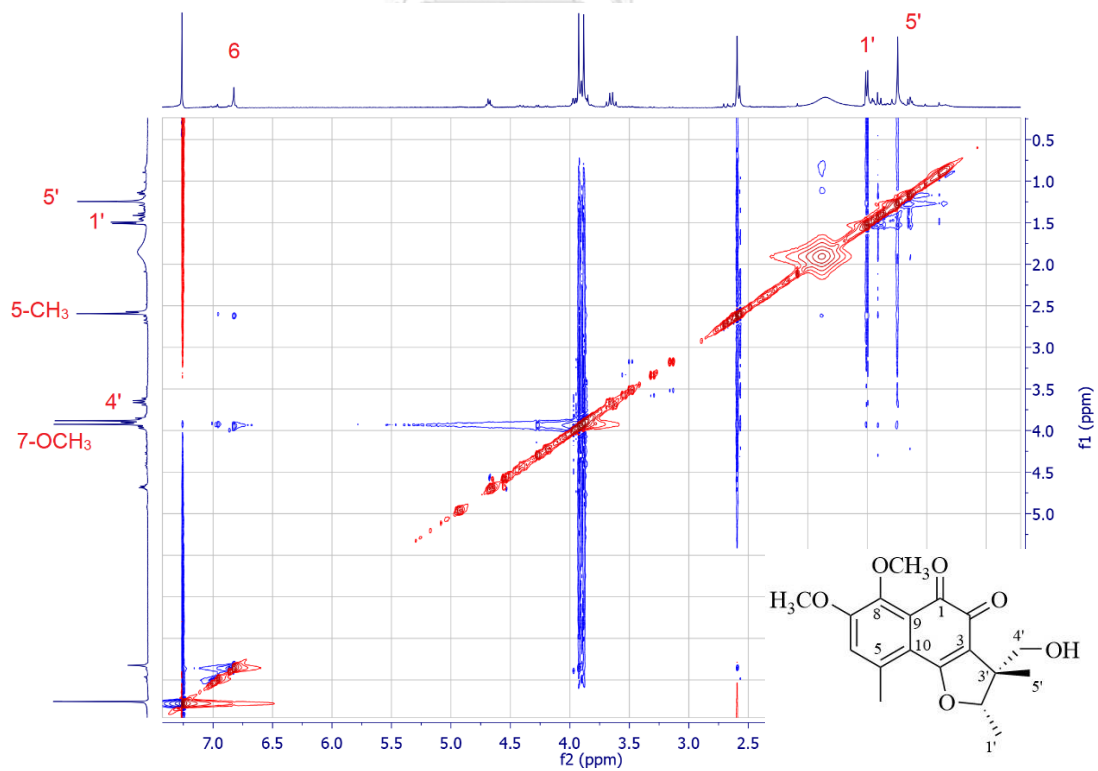


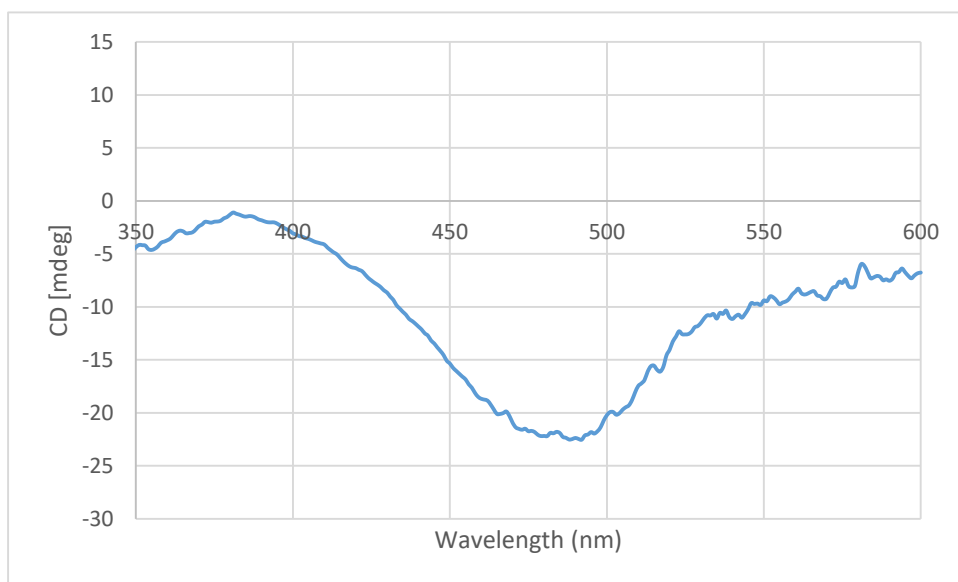
#	m/z	I	I %	S/N	FWHM	Res.
1	287.1221	1183	0.3	34.5	0.0540	5316
2	295.0917	4710	1.0	134.6	0.0421	7016
3	297.6510	946	0.2	26.7	0.0114	26033
4	301.1379	1478	0.3	41.3	0.0534	5643
5	315.1190	1610	0.4	43.3	0.0473	6657
6	333.1333	4471	1.0	114.6	0.0482	6910
7	337.1040	937	0.2	23.6	0.0577	5845
8	353.1007	959	0.2	24.6	0.0482	7325
9	355.1159	450648	100.0	11710.4	0.0607	5849
10	356.1180	67271	14.9	1751.9	0.0534	6666
11	357.1206	4385	1.0	114.3	0.0527	6771
12	371.0918	28403	6.3	766.0	0.0579	6408
13	372.0939	3194	0.7	86.2	0.0610	6098
14	373.0874	1563	0.3	42.2	0.0500	7466
15	375.2501	979	0.2	26.4	0.0737	5090
16	387.1324	1484	0.3	41.4	0.0571	6785
17	396.1386	1061	0.2	30.2	0.0501	7909
18	407.0852	1967	0.4	57.8	0.0552	7370
19	413.1528	1851	0.4	55.2	0.0571	7230
20	413.2479	840	0.2	24.9	0.0612	6749
21	419.2777	2139	0.5	64.9	0.0733	5717
22	463.2998	2854	0.6	98.4	0.0508	9122
23	507.3260	1422	0.3	56.4	0.0781	6498
24	518.1685	1311	0.3	54.1	0.0638	8118
25	551.3554	1018	0.2	45.9	0.0697	7910
26	687.2391	5977	1.3	317.4	0.1084	6338
27	688.2450	1349	0.3	71.5	0.1253	5492
28	695.2531	783	0.2	41.7	0.0223	31203
29	2352.1789	1274	0.3	107.4	0.0328	71746
30	2352.2844	1226	0.3	103.4	0.0315	74777

S3.24 HRESIMS spectrum of 3.5

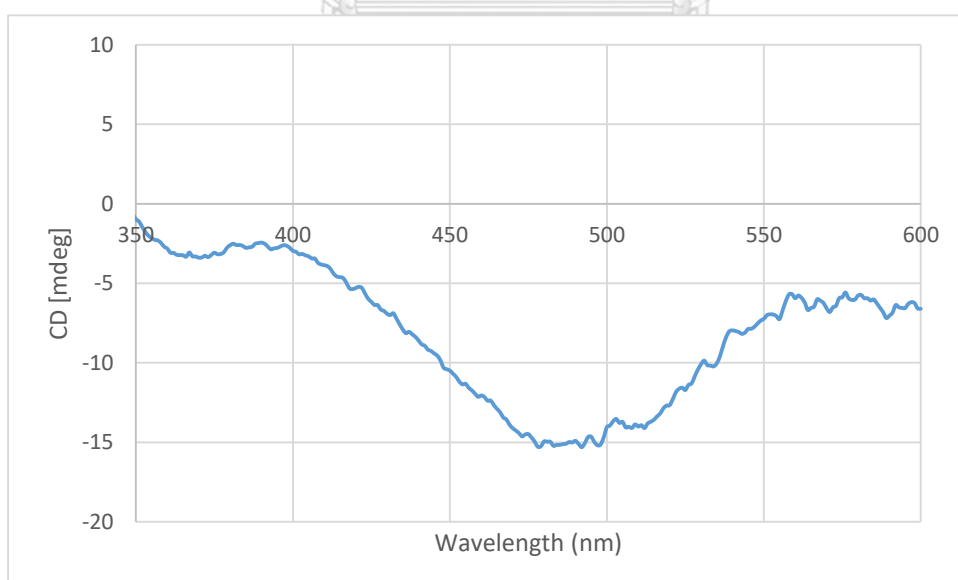
S3.25 ¹H NMR spectrum of 3.5 in CDCl₃S3.26 ¹³C NMR spectrum of 3.5 in CDCl₃

S3.27 COSY spectrum of 3.5 in CDCl₃S3.28 HSQC spectrum of 3.5 in CDCl₃

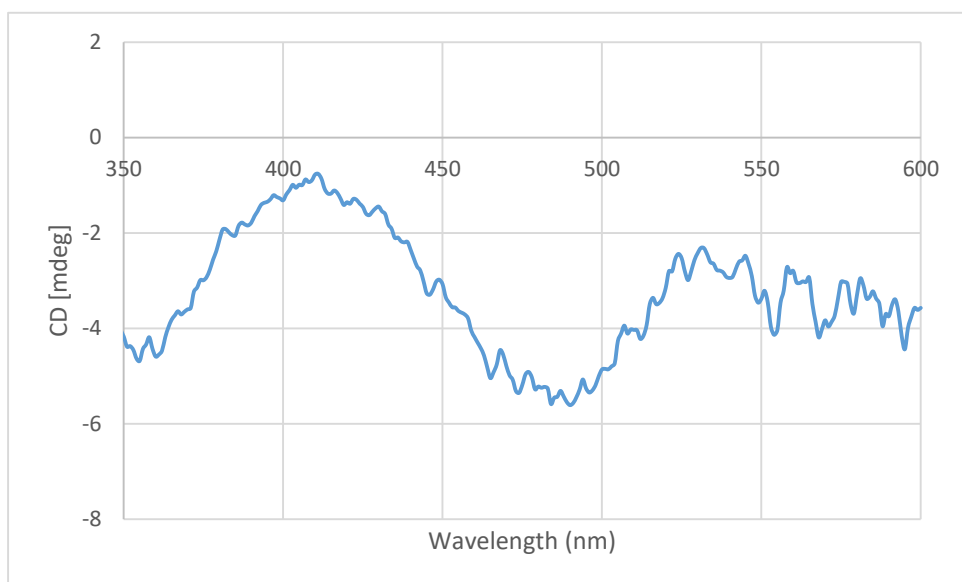
S3.29 HMBC spectrum of 3.5 in CDCl₃S3.30 NOESY spectrum of 3.5 in CDCl₃



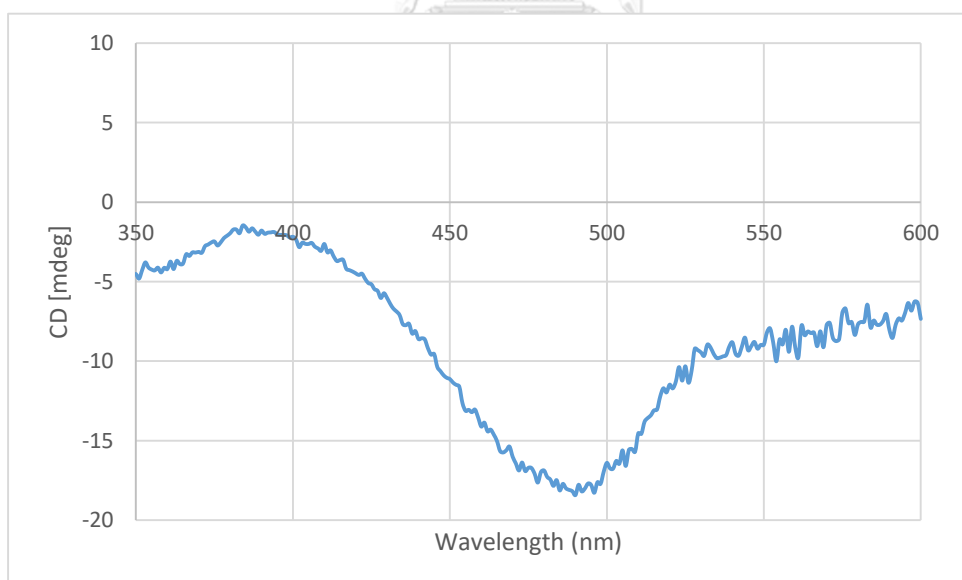
S3.31 CD spectrum (methanol) of 3.1



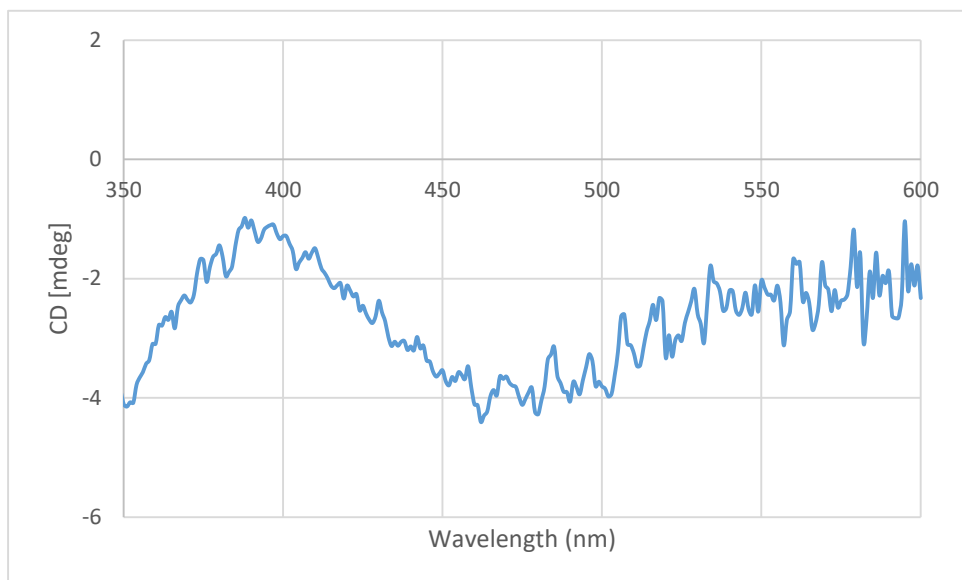
S3.32 CD spectrum (methanol) of 3.2



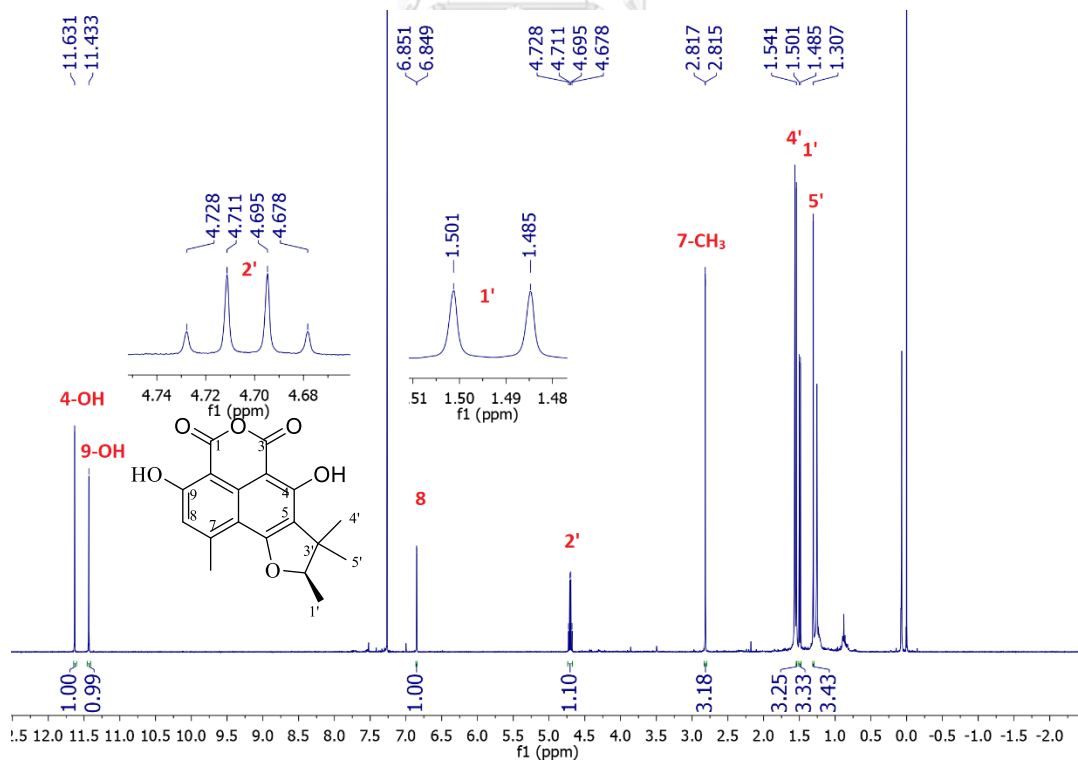
S3.33 CD spectrum (methanol) of 3.3



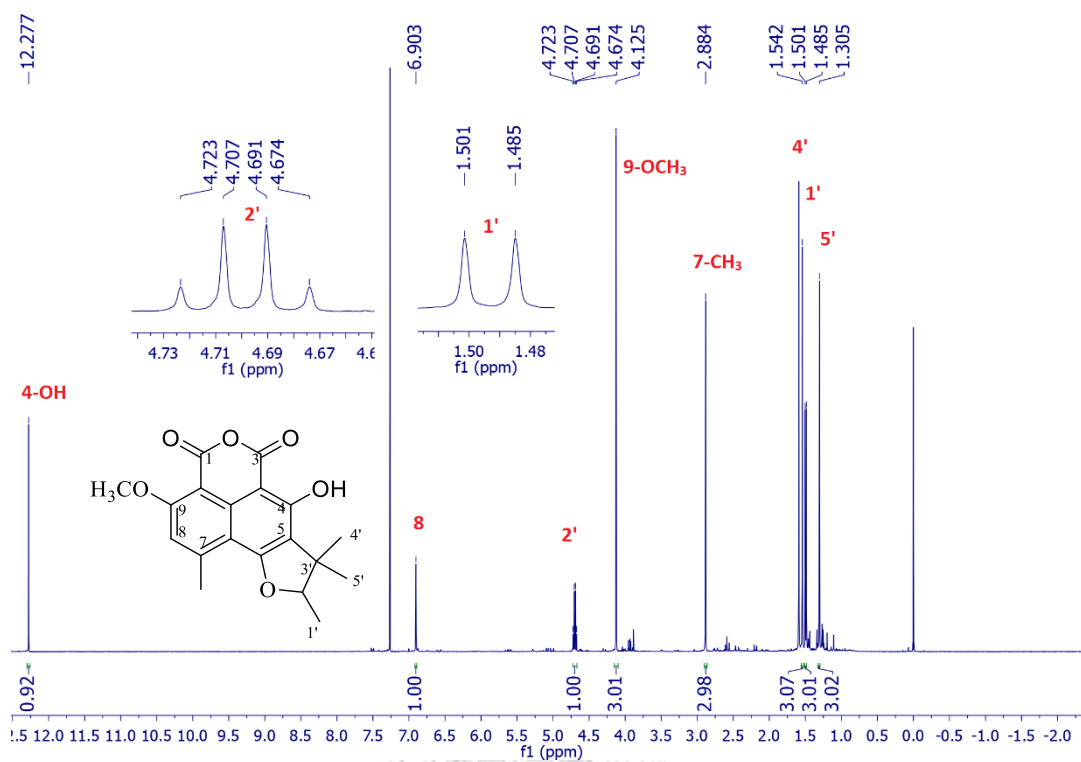
S3.34 CD spectrum (methanol) of 3.4



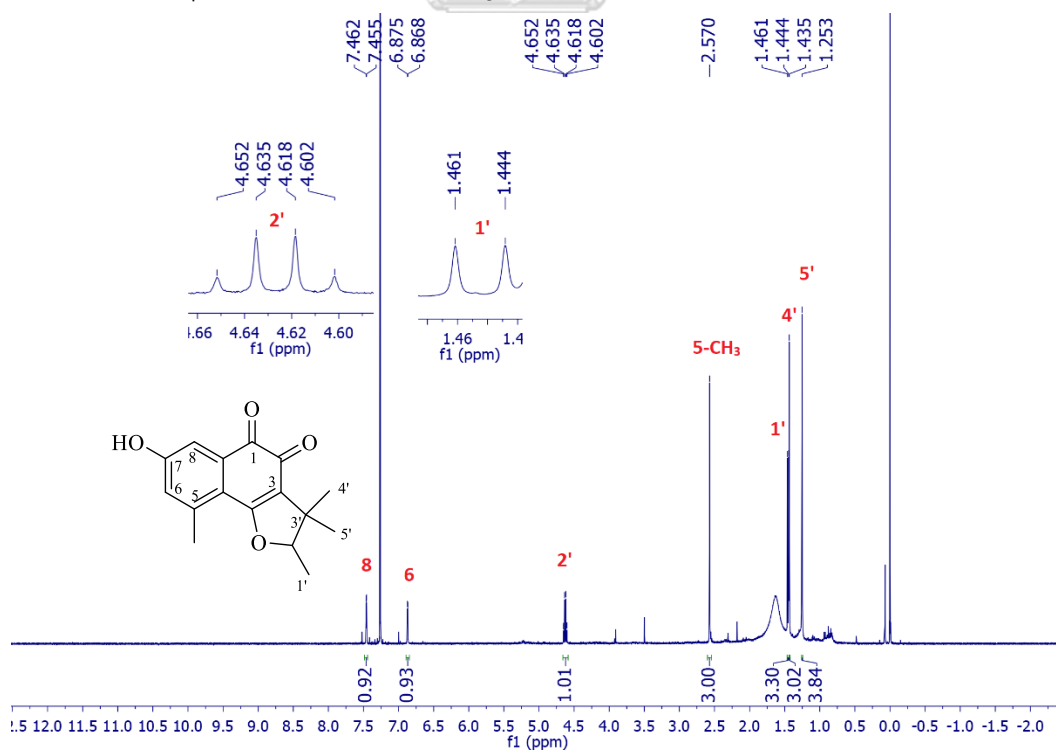
S3.35 CD spectrum (methanol) of **3.5**



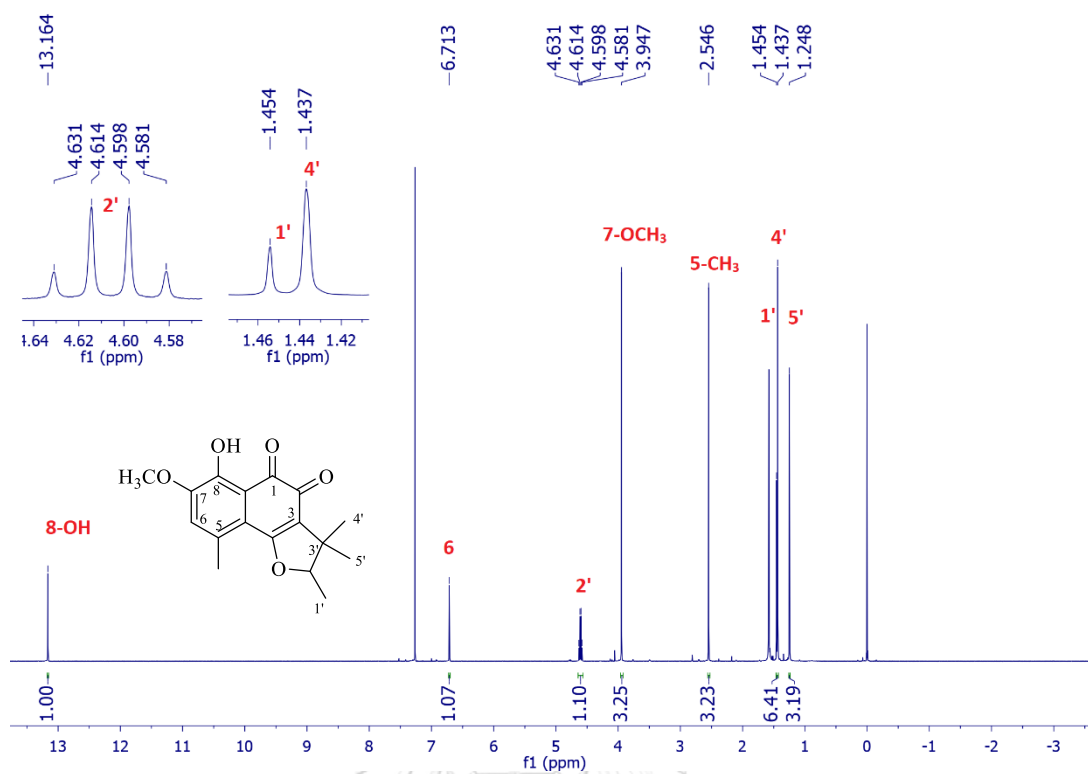
S4.1 ¹H NMR spectrum of **4.1** in CDCl₃



S4.2 ^1H NMR spectrum of **4.2** in CDCl_3



S4.3 ^1H NMR spectrum of **4.3** in CDCl_3



S4.4 ^1H NMR spectrum of 4.4 in CDCl_3

VITA

Ms. Suekanya Jarupinthusophon was born on September 7, 1980 in Bangkok, Thailand. She graduated with Bachelor's Degree of Science, major in Chemistry from Faculty of Science, Mahidol University, in 2002 and graduated with Master Degree of Science, major in Petrochemistry and Polymer Science from Faculty of Science, Chulalongkorn University, in 2005. During the time she was studying in the Doctor of Philosophy of Science program at the Department of Chemistry, Chulalongkorn University.

Her present address is 338, Klongchan, Bangkok, Thailand 10240.
Email: suekanya@gmail.com, Tel: 097-239-2450.

